Inorganic and Hybrid Nanofibrous Materials Templated with Organogelators†

Mario Llusar‡ and Clément Sanchez*,§

Dpto. de Química Inorgánica y Orgánica, Universitat Jaume I, 12071-Castellón, Spain, and Laboratoire de Chimie de la Matière Condensée de Paris, Université Pierre et Marie Curie-Paris and Centre National de la Recherche Scientifique (CNRS), 4, place Jussieu, 75252 Paris cedes O5, France

Received August 1, 2007. Revised Manuscript Received November 13, 2007

This article presents a general overview about the designed synthesis of one-dimensional (1-D) inorganic and organic–inorganic hybrid fibrous nanostructures templated through the use of organogelator-based supramolecular assemblies. The growing number of structural families and derivatives of low-molecular-weight organogelators (LMOGs) already used as templates for materials transcription are first presented, including a detailed compilation with relevant information about the gelation properties and the morphologies of their resulting self-assembled fibrillar networks (SAFINs). The main types of intermolecular interactions responsible for the gel-phase formation and some of the principal variables governing the gelation process and controlling the obtained fibrous morphologies (fibers, rods, ribbons, helices, tubes, etc.) are also discussed. After highlighting the most important processing methodologies that are available for materials transcription through organogel templates (coassembly, post-transcription, or self-templating procedures), the manuscript presents an updated description of the different inorganic (silica-based, other metal oxides, nonoxides) and organic–inorganic hybrid fibrous materials so far templated by using these approaches. The key mechanistic aspects and different templating pathways involved in the transcription process are also discussed, concluding with a final discussion about challenging aspects or future prospects in this field.

1. Introduction

The design and synthesis of highly anisotropic one-dimensional (1-D) nanostructured materials (such as fibers, rods, tubes, helices, belts, ribbons, and so on) is becoming a hot topic of research since these materials may exhibit distinct or very subtle electronic, optical, catalytic, chemical, and thermal properties, being in many cases superior to their bulk counterparts. These improved or sometimes new properties associated with one-dimensional nanostructured materials allow them to become potential candidates for application in many advanced fields such as optoelectronics, nanoelectronics, and asymmetric catalysis.[1–3] The synthesis and potential applications of a broad number of 1-D inorganic (or hybrid) materials have been recently reported in general and comprehensive review or feature articles.[2–4] Although these articles report on the use of a wide plethora of physical (top-down) or chemical (bottom-up) strategies (template- or nontemplate-based) to prepare nanofibrous materials (such as nanocasting with anodized alumina or mesoporous silicas, electrodeposition, vapor phase growth, solvothermal synthesis, and so on), most of them fail to include in the description the tremendous versatility and potentiality of templating methods based on fibrous organogels (or hydrogels).

Low-molecular-weight organogelators (LMOGs) are molecules capable of forming thermoreversible physical (supramolecular) gels at very low concentrations (ca. 10^{-3} mol dm^{-3}, typically lower than 2% w/w) in a wide variety of organic solvents. Upon gelation, the organized self-assembly of these molecules results in the formation of highly anisotropic 3-D structures, mostly in the shape of fibers, but also as ribbons, platelets, tubular structures, or cylinders. Since the first report of the Shinkai group in 1998,[5] supramolecular organogels (or hydrogels) have been successfully used as templates to direct the growth of a wealth of inorganic (commonly oxide-based, but also some metals and semiconductor chalcogenides) and also hybrid (organic–inorganic) nanofibrous materials exhibiting very different morphologies (such as fibers, rods, ribbons, belts, helices, and tubes).

In this review, we summarize and discuss in an organized, comprehensive manner the most important data reported on inorganic and hybrid organic–inorganic nanofibrous materials prepared through organogelator-templated approaches. This extensive list of data, with the corresponding references, is compiled in detail in Tables 1−4. Table 1 (section 2.1) gathers the main families of LMOG-based templates, their gelation parameters (solvents, gelation concentrations, temperatures, gelation additives, etc.) and the morphology of their self-assembled fibrous nanostructures (SAFINs). Tables 2−4 summarize, respectively, the nanofibrous morphologies of *silica-based oxides* (section 3.1.A), *nonsiliceous oxide*-(section 3.1.B) and *nonoxide*-based materials (section 4), and

* Corresponding author. Phone: 33 1 44275534. Fax: 33 1 44274769. E-mail: clems@ccr.jussieu.fr.
† Part of the "Templated Materials Special Issue".
‡ Universitat Jaume I.
§ Université Pierre et Marie Curie-Paris and CNRS.

10.1021/cm702141e CCC: $40.75
Published on Web 01/17/2008

hybrid (organic–inorganic) replica materials (section 5) resulting from organogel templating. These latter tables include relevant information on morphology and dimensions, the type of organogelator and solvent, the synthesis conditions and the employed *templating processing strategy* (*in situ* coassembly and sol–gel polycondensation, organogel self-assembly followed by post-transcription, impregnation or diffusion subsequent to organogelation, and self-templating).

In the text, a special emphasis is given to the different synthesis strategies and to the description of the general mechanisms proposed for efficient organogelator templated transcription.

2. Nanofibrous Self-Assembled Organogels As Materials Templates

In comparison with other cross-linked polymeric gels, where the network is formed and maintained through covalent interactions, most gels of LMOGs are thermoreversible physical gels. Thus, they are usually prepared by heating the gelator in an organic solvent until the mixture becomes a transparent solution, and the subsequent cooling below the characteristic gelation temperature (TG) brings out the transition to the gel phase. The gel consists of a three-dimensional (3-D) fibrillar network which entraps by virtue of supramolecular noncovalent forces a huge amount of solvent molecules. On average, typically several hundred to a thousand solvent molecules are trapped for one LMOG molecule (see section 2.1). A subsequent heating restores the original solution of nonaggregated molecules, and this process can be reverted by repeated heating–cooling cycles.

Some excellent reviews[6] or monographies[7] can be found in the literature that report about the main families of LMOGs. LMOGs have been traditionally used for many different purposes or applications such as separation technologies, drug delivery, contact lenses, cosmetics, and in the oil and food industries. An emerging "second generation" of LMOGs having smart responses to external stimuli (i.e., photo-, thermal- or redox-responsive)[8,9] has further expanded their potential application as advanced functional materials for solar or electrochemical cells, solid electrolytes, photonics, light-emitting diodes, or as reactive supports for more sophisticated materials.[8b,10,11] However, one of the most productive and fascinating research fields focused in LMOGs is based on the use of their SAFINs as templates for the transcription of nanofibrous materials.[12]

In this section, this review reports concisely about the main families or structural motifs of organogelator molecules already used as templates for the transcription of 1-D inorganic or organic–inorganic hybrid materials.[13] It also describes the morphologies obtained for the self-assembled organogel networks in the gelled solvents. Then, some mechanistic aspects of organogel formation will be we presented, discussing the different types of supramolecular interactions and aggregation modes driving the formation of organized 3-D nanofibrous networks. The chemical, structural, and processing key factors which must be controlled in order to design a desired specific morphology are also highlighted. Finally, an overall picture of the general strategies and the key aspects that must be considered for an efficient templated synthesis of inorganic or hybrid (organic–inorganic) nanofibrous materials through the use of organogels will be presented.

2.1. Description of organogelator Families and Their Self-Assembled Fibrous Networks (SAFINs). There is a huge and steadily growing number of gelator molecules already synthesized and characterized in the literature,[6,7] and therefore we will be only concerned about the main organogelator systems already used as templates for the transcription of nanofibrous materials (including also hybrid organic–inorganic gelator systems). Templating through more universal gelator molecules, also capable of gelating water or aqueous solutions (known therefore as "hydrogelators"), will be only considered occasionally. Indeed, most of hydrogelators leading to SAFINs may be classified as "pseudo-amphiphilic gelators", since they form highly viscous solutions of cylindrical micellar aggregates of pseudo-amphiphilic molecules (many of them are not conventional surfactants), rather than real solidlike fiber networks.[14]

Organogelator molecules could be classified, for instance, according to six main different criteria:

(*i*) their chemical nature or main structural scaffold (i.e., cholesterol-, amide-, urea-, amino acid or peptide-, ciclohexane-, and sugar-based organogelators)

(*ii*) the level of complexitiy of their structures (LMOGs containing one, two, three, or more heteroatoms, two-component and hybrid organogelators, etc.)

(*iii*) the type of supramolecular forces (mainly H-bonding, van der Waals, hydrophobic/solvophobic, aromatic or pi−pi stacking, electrostatic/ionic, charge transfer coordinating bonding, or usually a combination of some of them) leading to their self-assembly into fibrous networks

(*iv*) the fibrous morphologies of their SAFINs (fibrous, twisted or helical, ribbonlike, hollow fibers or tubular, lamelar, vesicular, and so forth

(*v*) the structural element or motif enabling an efficient transcription for template synthesis (with covalently or noncovalently attached positive charges, H-donating groups, coordinating or binding groups, and so on)

(*vi*) their properties and applications (polymerizable, liquid-crystalline or birrefringent, luminescent or fluorescent organogels, photoresponsive, metal-sensitive, etc.)

In the following discussion, we have used a classification scheme based on the main chemical (or structural) motif enabling their organogelation properties, and going from more simple to more sophisticated LMOGs (increased level of complexity of their structures), similarly to Weiss et al.[7b]

The categories of LMOGS below described are therefore (A) structurally simple gelators, (B) amide-, amino-acid-, or peptide-based gelators, (C) cyclohexane-based gelators, (D) sugar-based gelators, (E) cholesterol-based gelators, and (F) miscellaneous gelators. A figure with the structures or chemical names of the listed LMOGs are shown in Figure 1, while Table 1 summarizes some structural, textural, morphological, and other relevant organogelation information corresponding to the LMOGs families and derivatives used

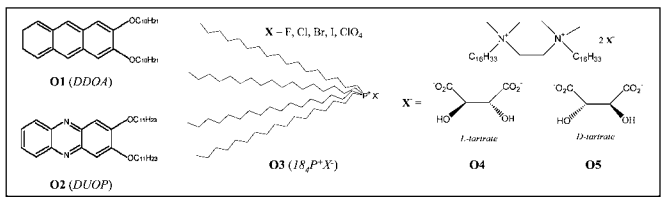

A) SIMPLE LMOGs

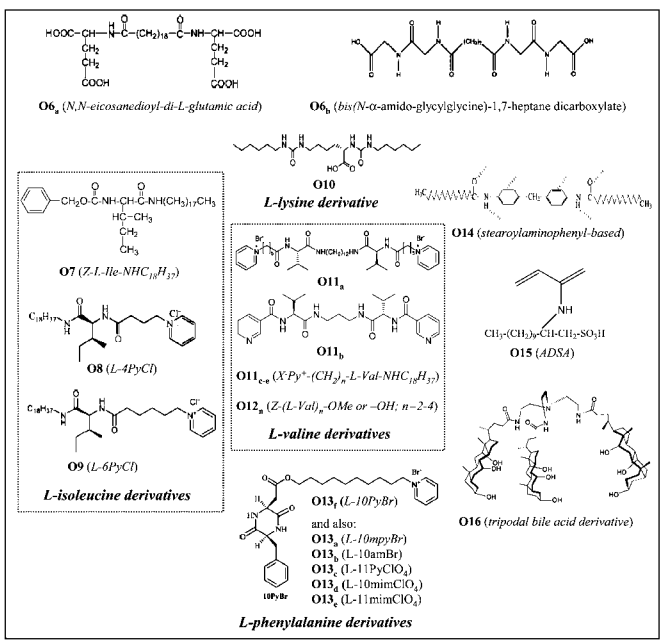

B) AMIDE-, AMINO ACID-, OR PEPTIDE-BASED

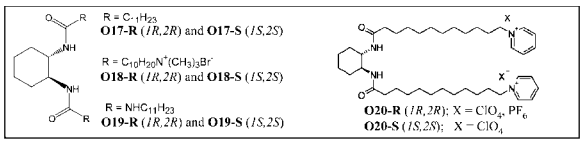

C) CYCLOHEXANE DIAMIDES OR BISUREA DERIVATIVES

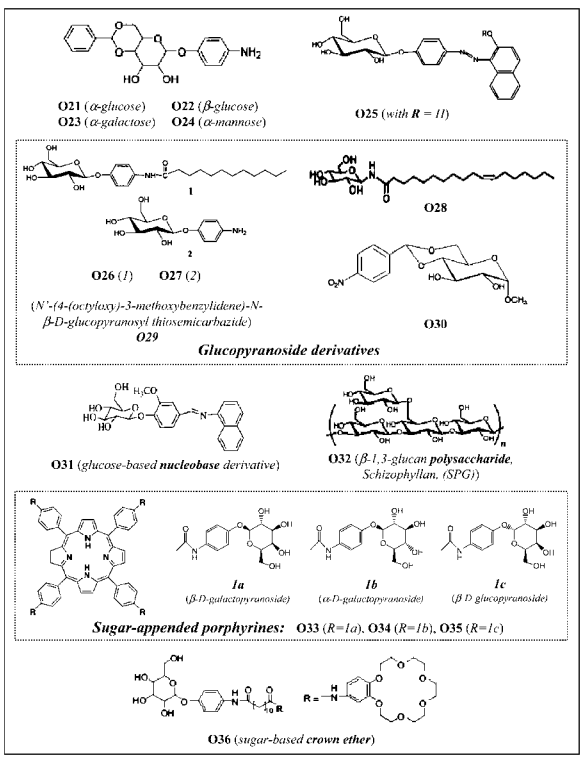

D) SUGAR-BASED DERIVATIVES

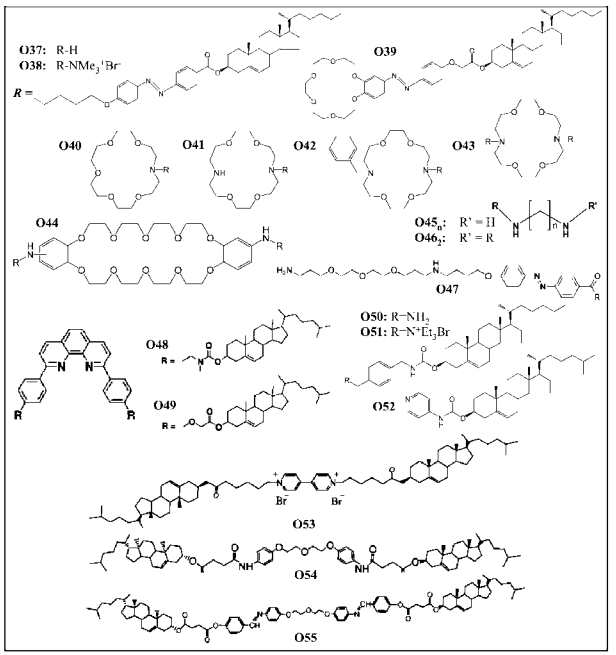

E) CHOLESTEROL-BASED DERIVATIVES

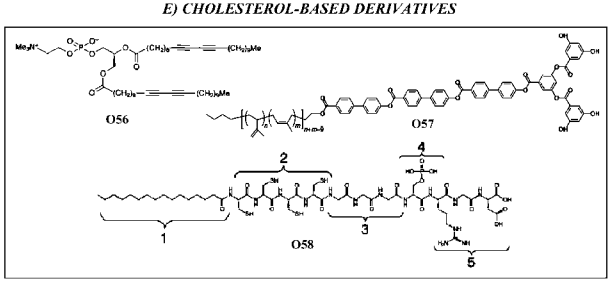

F) MISCELLANEOUS DERIVATIVES

Figure 1. Selected LMOGs used as templates for materials transcription.

Table 1. Main Families (and Derivatives) of LMOGs Used As Templates, with Selected References and Information of Their Gelation Properties (Solvents, Gelation Concentrations and/or Temperatures, Gelation Additives, etc.) and the Morphology of Their Self-Assembled Fibrous Nanostructures (SAFINs)

LMOGs family	derivative (examples)	refs.	gelated solvents (C_g at room T)[a]	gelation T °C (Conc. mM)[b]	additives or cosolvents	fibrous morphology[c] of SAFINs	templated materials (sections 3–5)
alkoxy-anthracenes	ex.:**O1**	15, 17, 105	in mmol dm^3 (mM): alcohols (0.6–10), alkanes (2.8–10), CH_3CN (0.75), DMSO (1.4), propylene carbonate (10)			long, rigid or flexible fibrils (φ = 30 nm), or fibrous bundles	Al_2O_3, SiO_2, R-SiO_2 (R = phenyl, amine)
alkoxy-phenazines	ex.:**O2**	15, 17, 105	alcohols, CH_3CN, DMF, acetone, *n*-heptane	31–33 (20), 44 (20), 9 (20), 9 (20), 3 (20)	CF_3COOH (TFA)	CH_3CN: intertwinned thin, straight fibers (several micrometers in length; ca. 150-nm-thick); longer elongated fibers	SiO_2, R-SiO_2 (R = phenyl, amine, mercapto, methacrylate, diamine, dinitro-phenyl)
phosphonium salts (tetra-*n*-alkoxy-phosphonium salts)	ex.:**O3** (18_4PX, with X = Cl, Br, I, ClO_4)	23, 24	in mM: hexadecane, benzene, 1-octanol, EtOH (10), benzene (10–30), THF (10), DMSO (10–50)	40 (20)–75 (10), 32–44 (10), 56–59 (10)	TEOS/catalyst	fibrous strands (several-micrometers-thick); platelike fibers or fibrous bundles (tubules)	SiO_2
ammonium salts (gemini surfactants)	ex.:**O4**, **O5**	25–26	chlorinated solvents (around 10 mM) and other polarizable solvents such as CCl_4, toluene, xylenes, chloro-benzene, pyridine (20–30 mM)		water (traces)	twisted flat ribbons (φ = 10–50 nm; helical pitch: 400–800 nm)	SiO_2
amide-, amino acid-, or peptide-based (noncontaining cyclohexane)	L-isoleucine derivatives; ex.: **O7**	33b	DMF, DMSO, PC, PEG, acetonitrile (0.9−2.1 wt %); alcohols (1−2.1 wt %); 1,4-dioxane, toluene (4–4.2 wt %) cyclohexane, benzene (1 wt %), CCl_4 (2.1 wt %). . .		optional: ($LiClO_4$ or $(n\text{-R})_4NClO_4$	DMSO: gathered nanofiber (16–24 nm thick)	TiO_2
	O8	36a,b	H_2O/EtOH (--)			huge fibrous aggregates	SiO_2
	O9	36a	cyclohexanone (12 g/L), THF (19 g/L), 1,4-dioxane (25 g/L), DMSO (24 g/L), acetonitrile (11 g/L), CCl_4 (10 g/L)			3-D entangled fibrous aggregates	SiO_2
	L-lysine-derivatives; ex.: **O10**	34, 37	EtOH, BuOH, dioxane/$Ti(OiPr)_4$ (85/15 v/v) (61 g/L)		$C_3H_7NH_2$	entangled nanofibers: 100–250 nm (EtOH), 50–100 nm (BuOH), 10–50 nm (dioxane)	TiO_2
	L-valine- derivatives; ex.: $\mathbf{O11_a}$	33c	H_2O (25 g/L), saline (14 g/L), 1 M salts: HCl (3 g/L), HOAc (36), NaCl (2), $MgCl_2$ (2), $CaCl_2$ (2)		inorganic salts and acids	entangled nanofibers (ca. 20-nm-thick) also with some helical fibers (intertwined)	SiO_2
	$\mathbf{O11_b}$	39	in mM: CH_2Cl_2 (3.1), acetone (5.2), DMF (10.4), dioxane (10.4), CH_3CN (8.3)			3D-entangled fibers (ca. 100-nm-thick) formed by thinner fibrils (ca. 20-nm-thick, several micrometers in length), and some helical fibers (not generalized)	SiO_2, FeO_xCl_y, Pd-gelator hybrid (composite)
	$\mathbf{O11_{c-e}}$	38b,c	in g/L for $O11_d$: 1-propanol (12), 1-butanol (7); in g/L for $O11_e$: EtOH (10), 1-propanol (12), 2-propanol (8), 1-butanol (8)			Intertwined fibrous bundles (formed by the aggregation of slender helical fibers)	SiO_2, TiO_2, Ta_2O_5
	$\mathbf{O12_n}$	40b	For methyl esters *Z*-(L-Val)$_n$-OMe and n = 2/3/4 (g/L): heptane (12)/toluene (14), *n*-alcohols (9–20), TEOS (10)/methylene chloride (33), *n*-alcohols (20–33)			butanol: 3-D network of micrometer-long fibers (ca. 40–60-nm-thick; random helicity) with β-sheet structure	TiO_2
	L-phenyl-alanine derivatives; ex.: $\mathbf{O13_{a-b}}$	42	water			water: 3-D fibrous network (fibers 10–20-nm-thick)	SiO_2
	$\mathbf{O13_{c-e}}$	43	gelates acetone, THF, methanol, ethanol, 1-propanol, *t*-butyl alcohol, and water (<0.5 wt %)			*t*-butyl alcohol: huge nanofibers (400–600-nm-thick) and fine nanofibers (50 nm)	SiO_2

Table 1. Continued

LMOGs family	derivative (examples)	refs.	gelated solvents (C_g at room T)[a]	gelation T °C (Conc. mM)[b]	additives or cosolvents	fibrous morphology[c] of SAFINs	templated materials (sections 3–5)
	O13$_f$	44	water (30 g/L)			in the presence of TEOS/HCl: helical single-stranded fibers (φ < 50 nm)	SiO_2, $_x$OSi-R-SiO_x (R = methylene, ethane, ethane, octane, and phenylene)
	stearoyl-aminophenyl-derivative; ex.: **O14**	45a	gelates (0.4–2.5 wt %) *n*-butanol, benzene, chloro-benzene, chloroform, cyclohexane, DMSO			randomly oriented fibrous bundles (φ = 50–200 nm)	SiO_2
		45b	gelates also (0.1–3 wt %) ethanol, THF, xylene, dioxane and diphenyl ether			rod-shaped (DMF), rolled-lamellar (DMSO), spherical-like pearl necklace (xylene), tubular (1-butanol)	SiO_2
	acryloyl-amide sulfonic-acid-based (ADSA; **O15**)	46	chloroform (180 g/L), THF (120 g/L)			chloroform: right- and left-handed helical ribbons (φ from tens to hundreds of nm)	Ag
	bile acid derivative; ex.: **O16**	47, 48	AcOH/H_2O (ca. 0.30 mM) and other aqueous acids (HCl + cosolvents. . .)		cosolvents (optionally): acetone, EtOH, MetOH, DMSO	CH_3COOH/H_2O (EtOH): nanofibers (φ = 8–10 nm, a few hundreds of nm in length)	SiO_2, TiO_2, ZrO_2, WO_3, ZnO, $ZnSO_4$, $BaSO_4$
cyclohexane-based	diamides: ex. **O17**, **O18**; bisureas: ex. **O19**	49–51	at 5 wt %: **O17** and **O19** gelate alcohols, protic/aprotic solvents; **O18** gelates only protic solvents (acetone, acetonitrile, THF, DMF, cyclohexane)			**O17** + **O18**/acetonit.: left-handed (*R*,*R*) or right-handed (*S*,*S*) helical fibers (20–60 nm width); **19** + **O18**/ethanol: left- or right-handed fibers (50–100 nm)	SiO_2
	pyridinium derivatives; ex.: **O20-R**	52a	with PF_6^-: *n*-butanol (20 mM)			extended fibrous rods (50–300 nm width) formed by thinner fibrils	TiO_2
	O20-R, **O20-S**	52b	with ClO_4^- (in mM): ethanol (17), 1-propanol (11), 2-propanol (12), 1-butanol (11), water (3)			ethanol: intertwined left- (**O20-R**) or right-handed (**O20-S**) helical fibers (30–160 nm)	Ti-, Ta-, and V-oxides
sugar-based	containing *p*-aminophenyl groups; exs: **O21-O24**	53–55	**O21**: chloroform, ethyl acetate, methanol, ethanol, propan-1-ol, butan-1-ol, H_2O (<3 wt %); toluene and diphenyl eter (<1 wt/ vol %); **O22**: ethanol, propan-1-ol, butan-1-ol (<3 wt %); *n*-octanol (<3 wt/ vol %); **O23**: methanol, ethanol, water (<3 wt %); **O24**: methanol, ethanol, HAc, water (<3 wt %)		$CoCl_2$, $CdCl_2$, $AgNO_3$ (improve gelation ability of **O21**)	**O21**/EtOH: small, frizzled fibrils (φ = 5–20 nm); **O22**/EtOH: straighter and larger fibrous bundles (φ = 50–150 nm) of thinner fibrils; **O23**/EtOH: larger fibrous structures (ca. 1400-nm-thick)	SiO_2, M-gelator (composite)
	azonaphthol derivative; ex.: **O25**	56, 57	H_2O or H_2O/EtOH mixtures			(3 wt % in H_2O): cryst. fibers (φ = 400–600 nm; few micrometers length); (0.1 wt % in H_2O): 3D network of fibrils (φ = 20–30 nm; length >1 μm)	SiO_2
	β-D-gluco-pyranoside derivatives; exs.: **O26**, **O27** (aminophenyl)	58	**O26**: at 0.1–3 wt % gelates, a variety of organic solvents (chloroform, THF, ethylacetate, 1-butanol); supergelator of H_2O/MetOH (1:1 v/v) mixtures (C_g < 0.1 wt %); **O27**: nongelator			**O26** (H_2O/MetOH= 10:1 v/v): bundles (20–500 nm) of partially twisted helical (left-handed) ribbons (φ = 20–100 nm witdth; pitch: 315 nm; several micrometers length)	
		59				**O26** + **O27** (1:1 w/w) (H_2O/MetOH= 10:1 v/v): double helical fibers (3–25 nm thick, several microns length)	SiO_2
	O28	60	water			hollow nanotubes (inner/outer diameter of ca. 80/200 nm)	Au-gelator composite
	O29 (thiosemi-carbazide)	61	H_2O (0.1–0.6 wt/vol %; with traces of EtOH)		EtOH (trace amount)	3D network of nanofibers (30–40-nm-thick, tens of micrometers in length)	CdS

Table 1. Continued

LMOGs family	derivative (examples)	refs.	gelated solvents (C_g at room T)[a]	gelation T °C (Conc. mM)[b]	additives or cosolvents	fibrous morphology[c] of SAFINs	templated materials (sections 3–5)
	α-D-gluco-pyranoside derivatives; ex.: **O30** (*p*-nitro-benzylidene)	62	gelates (1–3 wt/vol %) nonpolar (benzene, CCl_4, CS_2), and polar solvents (alcohols), and also water			H_2O: 3D-network of intertwined fibers (φ ca. 50–100 nm); H_2O/benzylamine (1:1 mol): much straighter fibers; CCl_4: frizzled fibrils (φ ca. 50–100 nm)	SiO_2
	nucleobase derivative; ex.: **O31**	64	gelates (<2 wt/vol %) benzene and H_2O/EtOH (20:1)			H_2O/EtOH (20:1 v/v): 1D short nanofibers (φ of 30–80 nm); benzene: 3D frizzled nanofibers (φ of 30–100 nm)	CdS, NiS
	sugar-appended porphyrines; ex.:**O33-O35**	66, 67	at 30 g/L (room T) gelate DMF/alcohol mixtures (1:3 v/v): **O33** and **O35** (MetOH, EtOH, 2-PrOH, 1-ButOH, bzlOH), **O34** (methanol and bzlOH); **O33**/DMF-bzlOH (1:3 v/v): MGC ca. 0.4 wt %			**O33** and **O34**/DMF-bzlOH (1:3 and 1:2 v/v): left- and right-handed helical bundles (20–300-nm-thick), respectively; **O35**/DMF-bzlOH (1:2 v/v): both left- handed helical and flat sheetlike structures	SiO_2
	sugar-appended crown ether; ex.: **O36**	69	at 5 wt % gelates organic solvents (1-butanol, 1-hexanol, benzene, toluene, *p*- and *m*-xylene) and H_2O	65 (5 wt %); 7 7–78 (5 wt %)	---; 1.0 wt % alkyl-diammonium ions	H_2O: right-handed helical fibers (φ ca. 10–38 nm; several hundred micrometers in length)	M-SiO_2 (M = Ag; uncharacterized)
cholesterol-based (steroid)	*(1) simple azobenzenes;* ex.:**O37**,**O38**	71, 5	**O37** gelates many organic solvents (hydrocarbons, alcohols, halogens, ethers) at 5 wt % or even <1 wt %; **O38** gelates MeOH, EtOH, and $MeCO_2H$ (HOAc) at 5 wt %			**O37**/HAc: granular **O38**/HAc: network of fibrils (50–200-nm-thick)	SiO_2
	O37 + **O38**	72b			CH_2Cl_2 (cosolvent, removed after gelation)	**O38**/(**O37** + **O38**) (5–15 mol % in HOAc): fibrous bundles (ca. 100-nm-thick) of thinner (10–20-nm-thick) helical stripes (pitch: 100–150 nm)	SiO_2
	(2) azobenzene + crown ethers	73–80	versatile gelators of many organic solvents				
	(a) monomeric, ex.: **O39**	73, 74	gelates (under 5 wt %) some alcohols, DMF, cyclo-hexane, *n*-hexane, aniline			**O39**/cyclohexane: partially twisted (helical) nanofibers (25–62-nm-thick)	
					$KClO_4/CH_2Cl_2$ (cosolvent)	**O39**/1-BuOH: fibrous organogel	SiO_2
	O40, **O41**	74, 75, 78	excellent gelators (under 5 wt %) of alcohols, CH_3CN, and DMF; gelate cyclo-hexane (under 10 wt %)		$KClO_4$ or $CsClO_4$	**O40**/cyclohexane: curved lamellar (filmlike) structure (30–40-nm-thick); **O41**/cyclohexane: tubules (inner φ: 170–390 nm; wall: 45–75 nm)	SiO_2, Ag-SiO_2, R-SiO_2 (R = coumarin or anthracene dyes)
	O42	76	under 5 wt %, excellent gelation ability for alcohols and also for DMSO, acetic anhydride and diamines		$AgNO_3$ or $CsClO_4$	*tert*-butyl alcohol: lamellar (without metals) or fibrous + lamellar structures (with metals)	M-SiO_2 (M = Ag, Cs, Na, K)
		77				acetic acid: rolled filmlike structure	SiO_2
	$\mathbf{O44_m}$	79b	similar to $\mathbf{O44_{24}}$ (see below)			similar to $\mathbf{O44_{24}}$	SiO_2
	(b) dimeric, ex.: **O43**	77	under 5 wt %: excellent gelator of long-chain alchols and amines			acetic acid: spherical vesicules (ca. 200-nm-thick) + larger spheres (φ of ca. 2500 nm)	SiO_2
					$Pd(NO_3)_2$	**O43**.Pd/aniline: metal-deposited fluffy globular aggregates (φ: 6 μm), with "canna-flower-like" coated surfaces (50-nm-thick)	Pd-SiO_2
	$\mathbf{O44_{30}}$	79, 80	gelates under 1 wt % (supergelator), many organic solvents (alcohols, acetic and propionic acid, acetonitrile, acetone, DMSO, DMF)			acetic acid: tubular structures (520-nm-thick) + linear and helical (right-handed) ribbons (1300 nm width)	SiO_2, TiO_2
	$\mathbf{O44_{24}}$	79b	gelate (<1 wt %) 1-hexanol, DMSO, DMF, and propionic acid			propionic acid: tubular structures (170–390 nm inner φ; 45–75 nm wall)	SiO_2
	(3) azobenzene diamines; ex.: $\mathbf{O45_n}$	81	for n = 1–4, versatile gelators of many organic (specially polar) solvents (alcohols, DMSO, DMF, aniline, benzene) under 5 wt %			$\mathbf{O45_n}$/aniline or 1-butOH: fibrous structures for n = 3 (20–50 nm) and n = 5 (10–70 nm); curved lamellar structures for n = 2 and n = 4	SiO_2 and M- SiO_2 hybrid composites (M = Ni, Pd)
	$\mathbf{O46_2}$	82	gelates1-hexanol, 1-octanol, toluene, and *m*- and *p*-xylenes (under 5 wt %)			1-octanol and *m*-xylene: fibrous helical bundles (50–100-nm-thick) of thinner helical fibrils (φ of 7.5 nm; long pitch)	SiO_2

Table 1. Continued

LMOGs family	derivative (examples)	refs.	gelated solvents (C_g at room T)[a]	gelation T °C (Conc. mM)[b]	additives or cosolvents	fibrous morphology[c] of SAFINs	templated materials (section 5)
	O47	83	gelates acetonitrile and acetone			acetonitrile: hollow tubules (560-nm-thick; inner φ of 460 nm; wall: 50 nm)	TiO_2, ZrO_2, TiO_2/ZrO_2, Ta_2O_5
	(4) without azobenzenes;	85, 86	CMG in mM: acetic acid (8), propionic acid (24), acetone (2.4),		TFA (optional)	acetic acid: fine (frizzled) nanofibers (5–30-nm-thick; several micrometers length);	SiO_2
	(a) phenantroline derivatives: **O48**		ethyl acetate (2.4), DMSO (4), DMF (24), 1- propanol (1.6), triethylamine (1.6), cyclohexane (8), methyl-cyclohexane (4)			1-propanol: entangled fibers (20–100-nm-thick)	SiO_2
	O49 (H^+)	85	acidic solvents (HAc) or adding acids (TFA) gelates (under 1–3 wt/vol %) DMF, acetone, acetonitrile, hexane, cyclohexane		added acid (TFA)	acetic acid: fibers similar to **O48**; acetone (TFA): uniform thin nanofibers (5-nm-thick)	SiO_2, TiO_2
	(b) benzylamine derivative:**O50**	87	gelates many alcoholic solvents (i.e., 1-BuOH under 5 wt %)			1-BuOH: fibrous network (φ ranging from 10 to 300 nm)	SiO_2
	(c) benzyl-ammonium salt **O51** + pyridine **O52**	87	an equimolecular mixture (**O51** + **O52**) gelates 1-BuOH			1-BuOH: analogous fibrous network to O50	SiO_2
	O52	88	versatile gelator (under 0.5 wt % gelates metanol, diphenyl ether, and acetonitrile), even in sublimable solid solvent (naphatalene)			fibrous network in benzene, xylene, toluene (2-D sheetlike if freeze-dried); naphtalene: whiskerlike	hybrid **O52**-Zn(II) porphyrine
	(d) viologen derivative:**O53**	89	supergelator of 1-butanol (<1 wt %)			1-BuOH: long and thick fibers (φ:100–500 nm) consisting of thin fibers (10 nm) based on two twisted 5 nm fibers	SiO_2
	(e) 3-oxopentane derivatives: **O54**	90	in wt/vol %: benzene (0.4), CCl_4 (0.28), EtOH (0.1), 1-BuOH (0.2), ethyl acetate (0.4), and acetic acid (0.4)			1-BuOH: long and thick fibers (φ: 100–500 nm) consisting of thin fibers (10 nm) based on two twisted 5 nm fibers	CdS
	O55	91	supergelator (<1 wt %) of cyclohexane, ethyl and butyl acetates, and mixed benzene−butanol (1:1–1:10 vol/vol)			fibrous network; fibers φ: 20–150 nm	CuS
other (miscellaneous)	diacetylenic phospholipid, ex.: **O56**	92–96	gelates water and other organic solvents			hollow tubules (diam.: 400–1000 nm, wall: 10–50 nm; 50–100 μm length)	lipid gelator-M (M = Ni, Cu, Au), or gelator-M_xO_y (M = Si, Al)
	"dendron rodcoil" (DRC); **O57**	98	gelates dichloromethane, ethyl methacrylate (EMA), and 2-ethylhexyl methacryl (EHMA)			ethyl methacrylate (EMA): twisted helical nanoribbons (pitch: 15–25 nm)	CdS
	peptide amphiphile (PA); **O58**	99	PH-responsive gels in water (2.5 mg/L) at a pH < 4			network of fibers (5–9-nm-thick; several micrometers in length	hydroxyapatite (HA, $Ca_{10}(PO_4)_6(OH)_2$)
SYLILATED GELATORS	ex.: **SO1**	115, 116	gelate cyclohexane, toluene, and THF (at 1–5 mg/L; 40 mg/L when racemic mixture)			see morphologies in Table 4 (for all SOX)	siloxane-containing hybrid organogels
	SO2$_n$	117	gelates toluene (at ca. 10 g/L)				
	SO3	118	gelates toluene and THF				
	SO4	119	can gel many polar solvents (more efficiently protic than aprotic), i.e., dioxane (10 g/L), chloroform (8 g/L), dioxane (10 g/L), DMSO (20 g/l), DMF (18 g/L), EtOH (40 g/L)				
	SO5 /**SO5**.Cu	121, 122	**SO5**.Cu gelates benzene (2 g/L), *p*-xylene (1 g/L), and anisole (1 g/L), whereas **SO5** only gelates benzene, and less efficiently (100 g/L)				
METALLOGELATORS	ex.: **MO1**	124	gelates $CHCl_3/CH_3CN$ mixtures (with Co/La, Zn/La, Co/Eu, and Zn/Eu)			see morphologies in Table 4 (for all MOX)	hybrid metalloorganogels
	MO2,**MO3**	125	Gel-like phase in $CHCl_3$; MGC is 0.007 wt % (**MO2**.Co) and ca. 10 wt % (**MO3**.Co)				

Table 1. Continued

LMOGs family	derivative (examples)	refs.	gelated solvents (C_g at room T)[a]	gelation T °C (Conc. mM)[b]	additives or cosolvents	fibrous morphology[c] of SAFINs	templated materials (sections 5)
	MO4	8a	(**MO4**)$_2$.Cu gelates benzonitrile, 1-butyro-nitrile, and THF/acetonitrile				
	MO5	126b	gelates hydrocarbons, i.e., methylcyclohexane				
	MO6	127	**MO6**.Zn gelates apolar organic solvents (i.e., cyclohexane, under ca. 1 wt %)				
	MO7	122	**MO7** and **MO7**.Cu gelate 11 solvents: CGC for **MO7** from 2.5 g/L (diphenyl ether) to 30 g/L /THF), and for **MO7**.Cu from 1 g/L (toluene) to 30 g/L (THF), while **MO7**.Zn only gelates 2 sovents: anisole (50 g/L) and 1,4 dioxane (15 g/L); **MO7**.Zn with 0.5 equiv of piperazine gelates benzene (3 g/L), toluene (3 g/L) and *p*-xylene (2 g/L)			
	MO8	129	**MO8** (monophosphonate ester).Fe(III): gelates (at 2 wt %) low-polarity liquids, such as hexane (Tg: 76–87) and *n*-octane (56–82)				
	MO9	130	(**MO9**)$_2$.Ag gelates toluene/EtOH (10:1 v/v): CGC can reach 2 g/L (T_g: 38.6 °C at CGC, and increases to 42 °C at 20 g/L); >also good gelation properties in various mixed solvents (mixtures of chloroform with acetone, ethanol, and other polar solvents)				

[a] C_g: When available, the critical gelation concentration (CGC), which is the minimum concentration for gelation at room temperature (25 °C) in the indicated concentration units (wt %, wt/vol %, g/L, or mM). [b] Critical gelation T (°C): highest temperature at which gelation occurs when cooling the gelator hot solution under fast or moderate cooling conditions (T_g is generally higher under very slow cooling conditions). [c] ϕ (or φ) = average diameter in the indicated units.

as materials templates (such as gelled solvents, the minimum gelation concentration at room temperature—MGC—or the critical gelation temperature at a given concentration, possible additives for gelation, etc.).

2.1.A. Structurally Simple Gelators. To begin with structurally more simple LMOGs families (containing only one heteroatom, such as ethers and thioethers, calixarene-based, substituted fatty acids, etc.), *2,3-bis-n-alkoxyanthracenes* have been used as organogel (or gelator-like) templates for materials transcription. In this family, the best gelation efficiency is obtained with $n = 10$ or 11.[15] Among them, DDOA (**O1**, bis-didecyloxyanthracene) can form fibrous organogels (due exclusively to non-H-bonding interactions such as $\pi-\pi$ stacking of the aromatic units and van der Waals interactions of the alkyl chains) in diverse solvents, mainly in alcohols and to a lesser extent in amines and alkanes (for instance, it is a supergelator in acetonitrile; CMC under 0.6–0.7 mM).[16] DDOA organogels exhibit generally rodlike fibrous morphologies, with long (hundreds of micrometers), flexible, and rather thin fibrils (around 30-nm-thick) forming a 3D network of fibers or fibrous bundles with extended interaction zones (confirming the important effect of the cooling rate during organogelation on the resulting fibrous morphologies). Organogels built with DDOA have been used for the templated growth of silica fibers[17–19] (for instance, a fibrous silica with a double porous network, at two different length scales),[17] and also alumina-based[20] and organosilica fibers (functionalized with phenyl and protonated amine moieties).[18,19]

Interestingly, the analogous phenazine derivatives (*2,3-di-n-alkoxyphenazines*), whose amphiphilic character is more pronounced, may also easily gelify polar solvents (EtOH, MetOH, acetonitrile, DMF, and acetone) and even *n*-heptane (at a low temperature, 3 °C). The organogels of the derivative with $n = 11$ (2,3-bis-*n*-undecyloxy-phenazine, DUOP, **O2**) in acetonitrile (Cg = 20 mM) consist of juxtaposed, fused, and intertwined thin straight fibers formed by the entanglement of long, thinner aggregates with a width of ca. 150 nm. Importantly, the gel-forming ability is significantly enhanced in the presence of trace amounts of a strong acid such as trifluoroacetic acid (TFA). Moreover, upon the addition of an equimolecular amount of TFA, the organogel molecules pack more efficiently, giving rise to longer elongated fibers without nodes. Remarkably, organogels of **O2** in acetonitrile have been used as templates for preparing fibrous and ribbonlike morphologies of silica[17] and organically modified organosilicas supporting accessible and functional organic moieties (see section 5.2) such as phenyl,[19] protonated amine,[19] and mercapto[21] and more recently also with methacrylate, ethylendiamine, and dinitrophenylamine functions (*private communication*).

Small and simple surfactant molecules such as some *tetra-n-alkylammonium salts* (with chloride, bromide, iodide, and perchlorate as anions and $n \leq 18$) may also behave as gelator-like molecules in various alkanes, alkenes, alkanols, or aromatic liquids. In general, gelation efficiency increases with increasing alkyl chain length, and among them, tetra-*n*-octadecylammonium salts ($18_4N^+X^-$) are the best gelators of the series.[22,23] However, attempts of using these gelators

as templates for silica transcription have not been satisfactory. Interestingly, the analogue phosphorous organogels (*tetra-n-alkylphosphonium salts*), for instance, 18_4PX (**O3X**, with X = Cl, Br, I, or ClO_4), may also gel similar organic solvents, although the resulting organogel fibrous networks are generally less stable than those with the ammonium cationic center.[23] However, the phosphonium salts have proven to be in some cases much more efficient templates for silica transcription. Indeed, different silica morphologies have been templated through the use of **O3** organogels in different solvents and under different acidic or basic catalyzed conditions, being analyzed the effect of key parameters on efficient silica transcription (see section 3).[24]

Related to the family of ammonium salts, some cationic ***gemini surfactants*** having *chiral tartrate* counterions [dimers of cetyltrimethyl ammonium ions with X^- = L-(**O4**) or D-(**O5**) tartrate (or L- + D- tartrate mixtures, **O4** + **O5**)] can assemble into twisted flat ribbons in both chlorinated and other aromatic organic solvents through headgroup connection.[25] These gelator-like molecules can be considered "two-component gelators", since the presence of a specific counterion—L- or D-tartrate—is needed for organogelation to occur. The handedness of the ribbons and their helical pitch can be tuned (400–800 nm) by changing the ratio between the L- and D-tartrates.[26] These double-helical morphologies with tunable pitch have been successfully transcribed into double-stranded helical or twisted silica.[27]

2.1.B. Amide-, Amino-Acid-, or Peptide-Based Organogelators. Many of the LMOG systems are constituted by molecules with two different types of heteroatoms (mainly O and N, as in gelator compound **O2**), and to this class belong many primary and secondary amides and related compounds such as amino acids, peptides, ureas, carbamates, and thioureas. The LMOGs containing these H-donating and -accepting moieties are ideal gelator molecules to produce highly oriented fibrillar networks due to their ability to self-aggregate through H-bond interactions that may be complemented by $\pi-\pi$ stacking and van der Waals interactions provided by the presence of long alkyl chains or aromatic units. Consequently, as described as follows, many of them (i.e., gelators **O6** to **O20**) have been used as templates for materials transcription.

For instance, several *bisamides* can gelate a wide variety of liquids due to enhanced directional H-bonding as well as van der Waals interactions. In these compounds, intermolecular H-bonding of linear α,ω-bisamides can be parallel or antiparallel depending on the number of separating methylene units. In particular, the gelation efficiency depends more on whether the number of methylene units is even or odd than on the length of the R group.[28] Interestingly, the L-glutamic-acid-based bolaamphiphile (tetracarboxylic bisamide) $\mathbf{O6_a}$ (*N,N-eicosanedioyl-di-L-glutamic acid*, referred to as EDGA) can gel water/ethanol mixtures forming helical nanotubes, which has enabled the template transcription of double- and multiple-wall Ag nanotubes.[29] In addition, aqueous solutions of the related bolaamphiphilic dicarboxylic (tetraamide) oligopeptide $\mathbf{O6_b}$ (*bis(N-α-amido-glycylglycine)-1,7-heptane dicarboxylate*) may also self-assemble into pH-sensitive 1-D morphologies (microtubules or helical ribbons),[30] which have been metal-coated with Cu and Ni, leading to Ni and Cu metal nanowires that might be interesting for nanoelectric circuits. However, both gelator systems should be considered as micellar rodlike aggregates rather than real solidlike hydrogels.[31]

Special research interest has been focused on the organogelation properties of some *amino acid derivatives*,[32] in which the nitrogen atom is part of an amide moiety. To this group belong the L-amino acid gelators studied by the Hanabusa's group based on *L-valine* and *L-isoleucine*,[33] as well as on *L-lysine*[34] amphiphiles. These are ambidextrous gelators and thus can form both hydrogels in aqueous solutions and organogels in organic solvents.

Examples of *L-isoleucine*-containing LMOGs used as templating agents are organogelators **O7** (N-benzyloxycarbonyl-1-isoleucyl-octadecylamide, referred to as *Z-L-Ile-NHC$_{18}$H$_{37}$*),[33b] which has been used in the preparation of TiO_2 fibers,[35] and two pyridine derivatives of L-isoleucylaminooctadecane, **O8** and **O9** (referred to as *L-4PyCl* and *L-6PyCl* in the literature, respectively), used in the transcription of helical silica nanostructures (twisted ribbons, fibers, and tubes).[36]

O7 is an excellent gelator which can harden a wide variety of organic fluids, from highly polar solvents to nonpolar aprotic ones, including also some alcohols. On the other hand, the structurally related amphiphilic compounds **O8** and **O9** may be chosen to exemplify the subtle frontier between *cationic surfactants* and *amphiphilic gelators*: **O8** can form an emulsion of vesicle-like aggregates in pure water (thus behaving as a cationic surfactant), but the emulsion changes into a 3-D network of huge fibrous aggregates (thus behaving as a gelator) upon the addition of a small amount of EtOH (or in situ generated from $Si(OEt)_4$ hydrolysis). **O9**, however, is able to form hydrogels in water and organogels in different organic solvents. Therefore, compounds **O8** and **O9** would belong to a novel type of templating agents in the frontier between surfactants and gelators, combining the superior properties of both types of organized molecular systems (surfactants and LMOGs).[36]

The *L-lysine-based* organogelator **O10** may form nanofibrous organogels at considerably high gelator concentrations and has been used as an efficient template for the synthesis of TiO_2 nanotubes with controllable size depending on the solvent.[37]

Finally, *L-valine-based* gelator derivatives $\mathbf{O11_a}$ (dodecamethylene-1,12-bis(N-(6-pyridiniumhexyl)-L-valine)dibromide, $\mathbf{O11_b}$ ($C_{25}H_{34}N_6O_4$, *N,N′*-bis-[N-nicotinoyl-L-valyl]-propylene diamine), $\mathbf{O11_{c-e}}$ (valylaminooctadecane derivatives), and $\mathbf{O12_n}$ (*Z*-(L-Val)$_n$-OMe or -OH (n = 2–4)) have been also satisfactorily used as templates ($\mathbf{O11_{a-e}}$ contain pyridine moieties, while $\mathbf{O12_n}$ are benzoylated derivatives). Gelator $\mathbf{O11_a}$ (or its homologue with PF_6^- as a counterion) functions as a "super-hydrogelator" (high gelation efficiency) in pure water, saline, and aqueous solutions containing various inorganic salts;[33c] it could also presumably form organogels in low-polarity organic solvents (as is the case with $\mathbf{O11_b}$), although their organogelation properties have still not been reported. Thus, only hydrogels of this compound have been

used as a template, leading to the transcription of inner helical mesoporous silica fibrous bundles.[38a]

The pyridine-containing amino acid derivative **O11$_b$**,[39] and their benzoylated (amidocarbamates) analogues[33a,40a] may form pH-responsive hydrogels and organogels. The benzoylated derivatives and mixtures of them[40a] are more flexible gelators, forming organogels in a wide variety of organic solvents, while the pyridine derivative **O11$_b$** remains soluble in conventional polar organic solvents, forming organogels in less polar ones. The latter have been found to be more appropriate templates for materials transcription. Indeed, acetonitrile organogels of **O11$_b$** have been efficiently used to template the growth of silica nanofibrous structures with different morphologies depending on pH/catalyst conditions.[41] Similarly, Hanabusa et al. have employed organogel templates of related L-valine pyridinium salts (X^- Py^+ $(CH_2)_n$-L-Val-$NHC_{18}H_{37}$, **O11$_c$** (n = 3, X = Cl), **O11$_d$** (n = 5, X = PF_6), and **O11$_e$** (n = 10, X = PF_6)) to transcribe SiO_2 nanohelices (O11$_c$)[38b] and also metal oxide (TiO_2[38b,c] and Ta_2O_5[38c]) nanotubes (with both O11$_d$ and O11$_e$). On the other hand, the benzoylated *L-valine*-based oligopeptides **O12$_n$** (*Z-(L-Val)$_n$-OMe* or *-OH*; n = 2–4) have been recently found to form stable organogels in a variety of solvents [the methyl esther form (-OMe) is a more efficient gelator thant the acid form (-OH)].[40b] These peptides form micrometer-long helical fibers with a β-sheet structure, and fibrous organogels (in butanol) of the methyl ester tripeptide (**O12$_3$**: *Z-(L-Val)$_3$-OMe*) have been efficiently used as templates for the transcription of TiO_2 nanostructures (spheres at low gelator concentrations, and 1-D shapes like fibers or hollow tubes at higher concentrations).[40b]

Recently, Hanabusa's group has developed a series of amino acid based cationic cyclo(dipeptide) gelators containing *L-phenylalanine* moieties (**O13$_{a-f}$**, structurally very similar to the ambidextrous **O9** gelator) and used them for the transcription of silica fibrous materials. Compound **O13$_a$** (L-10mpyBr) contains a protonated methylpyridinium (*mpy*) group, which is substituted in **O13$_b$** by a trialkylammonium (*am*) moiety; gelators **O13$_b$** (L-11pyClO_4) and **O13$_f$** (L-10pyBr) contain protonated pyridinium moieties (*py*), while the gelator derivatives **O13$_d$** (L-10mimClO_4) and **O13$_e$** (L-11mimClO_4) are N-methylimidazolium salts (*mim*).

In a first report, the fibrous hydrogels of gelators **O13$_a$** and **O13$_b$** enabled the preparation of cottonlike silica composed of right-handed helical bundles.[42] Later, the sol–gel transcription of the related compounds **O13$_{c-e}$** resulted in all cases in silica having simultaneously three different morphologies (see section 3).[43] More recently, helical fibrous hydrogels of the related derivative **O13$_f$** (10PyBr) were used to template the growth of helical mesoporous silica and also of hybrid organosilica nanofibers (see section 5).[44]

Other structurally different compounds such as **O14**, **O15**, and **O16** can be mentioned, also belonging to the group of gelators containing amine or amide functions (but without cyclohexane moieties). Gelator **O14** containing two aminophenyl moieties (*bis-(4-stearoylaminophenyl)methane*, referred to as *BSAPM*) can form organogels in many solvents at very low concentrations (as low as 0.1 wt %). Organogels of **O14** in *n*-butanol were first used as templates to produce silica nanowires with a nonentangled, straight rodlike morphology.[45a] More recently, different silica morphologies have been also transcribed with the same gelator template (also adding a small quantity of CTAB cationic surfactant) depending on the employed solvent (tubular in 1-butanol, rolledlike in DMSO, spherical in xylene, and rodlike in DMF).[45b] On the other hand, the racemic organogelator **O15** (*2-acryloylamide-dodecane-1-sulfonic acid*, referred to as ADSA), containing three different heteroatoms (N, O, and S), has been successfully transcribed into both right- and left-handed silver nanohelices.[46] Finally, gelator **O16** is a highly efficient gelator of aqueous acids at remarkably low concentrations (0.30 mM),[47] and in some cases, their gelation efficiency can be improved by adding small amounts (8−10% v/v) of an organic cosolvent (such as acetone, ethanol, methanol, or DMSO). What is noteworthy is that fibrous hydrogels and organogels of **O16** in CH_3COOH (aqueous or aqueous-alcoholic) mixtures have been used to prepare nanotubes of silica, and a number of metal oxides (TiO_2, ZrO_2, ZnO, and WO_3) and sulfates ($BaSO_4$ and $ZnSO_4$).[48]

2.1.C. Cyclohexane-Based Organogelators. As another particular class of LMOGs (of special relevance for the transcription of tubular or helical inorganic nanostructures), we must highlight the family of **cyclohexane chiral derivatives** containing **amide** (**O17** and **O18**) or **urea** moieties (**O19**). Similarly to other gelator molecules, the presence of charges in these gelators has a deleterious effect on the gelation ability. Thus, the neutral cyclohexanediamide (**O17-R** or **O17-S**) and cyclohexane-bisurea (**O19-R** or **O19-S**) derivatives are versatile gelators of a broad variety of organic solvents,[49] while the cationic diamide derivative (**O18R** and **O18S**) presents a more reduced gelation ability.[50] Interestingly, organogels of mixtures of neutral and charged diaminocyclohexane derivatives (**O17** + **O18**) in acetonitrile, or also of neutral urea- and cationic amide-based gelators (**O19** + **O18**) in ethanol, exhibit left-handed or right-handed helical morphologies, and these fibrous organogels have been used as templates in the transcription of hollow, helical silica fibers, for which chirality reflects the one present in the original organogel fibers.[51] Also related to this family of gelators are the cyclohexanediamide derivatives **O20** containing pyridinium hexafluorophospate (**O20-R**) or perchlorate (**O20-R** and **O20-S**) as the charged species.[52] Gelator **O20-R** with PF_6^- as the counterion [*trans*-(1*R*,2*R*)-1,2-cyclohexanedi(11-aminocarbonyl-undecylpyridinium) hexafluorophosphate] is able to form a rodlike fibrous organogel in *n*-butanol (MGC equal to 20 g/L), and it can also afford highly viscous fluids with sol–gel mixtures of titanium alkoxides and alcohols but without chiral fibrous morphologies. This has enabled the transcription of hollow achiral tubular TiO_2 nanofibers.[52a] In contrast, gelator **O20** (**R** and **S**) with ClO_4^- as the counterion presents a better gelation ability for polar solvents and forms organogels consisting of chiral left-handed (**O20-R**) or right-handed (**O20-S**) helical

fibrous bundles, which have been efficiently transcribed into a variety of inorganic materials as titanium-, tantalum-, and vanadium-based metallic oxides.[52b]

2.1.D. Sugar-Based Organogelators. Also noteworthy for templating applications are the families of *sugar-based* organogelators. As a first example, the fibrous (tubular) or spherical organogels of four monosaccaride versatile gelators (**O21**−**O24**)[53] have been efficiently transcribed into silica with different novel morphologies such as hollow tubes or "lotuslike" or spherical shapes.[53b,54,55] These gelators consist of a central sugar (**O21**, α-glucose; **O22**, β-glucose; **O23**, α-galactose; and **O24**, α-mannose) functionalized on opposite ends with two aromatic rings. One of them is a *p*-aminophenyl group, which contributes to an additional H-bonding effect to reinforce the gelation ability and also improves the transcription into silica. These organogels are stabilized through intermolecular H-bonding interactions, and noteworthy in the case of gelator **O21**, the gelation ability can be markedly improved via **metal coordination**, through a bridging effect between gelators and metal ions [particularly to Co(II), Cd(II), and Ag(I)].[53a]

On the other hand, the *sugar-appended azonaphtol* derivative **O25** can gelate water/ethanol mixtures,[56] and interestingly, the fibrous hydrogels of this compound were successfully used as templates in the transcription of hollow, tubular silica.[57]

A typical example of the use of a "**binary gel system**" for materials transcription is provided by the mixture of *β-D-glucopyranoside* derivatives **O26** (*p-dodecanoyl-aminophenyl-β-D-glucopyranoside*, which is a versatile organogelator and even a supergelator of water)[58] and **O27** (*p-aminophenyl-β-D-glucopyranoside*, without organogelation properties). Mixtures of both gelators have enabled the formation of double-helical fibrous silica.[59] On the other hand, it has been recently found that a newly optimized glycolipid [**O28**, *N*-(11-*cis*-octadecenoyl)-β-D-glucopyranosylamine, incorporating a cis double bond into the lipophilic part] self-assembles in water, leading to hollow nanotubular structures, which then allowed the confined organization of Au nanocrystals into their hollow cavities.[60] Similarly, the excellent hydrogelator **O29** (another β-D-glucopyranoside) has been satisfactorily used as a template to fabricate netlike CdS nanofibers.[61] On the other hand, the structurally related α-*D-glucopyranoside* derivative **O30** (methyl 4,6-O-(*p*-nitrobenzylidene)-α-D-glucopyranoside)[62] has directed the growth of hollow, tubular silica owing to the cooperative **gelator-catalyst** (benzylamine) interactions, which resulted in being indispensable for an efficient transcription.[63]

More recently, a hydrogel based on a *glucose-appended nucleobase* (Schiff base) derivative (compound **O31**) has been employed as the template to synthesize **CdS** and **NiS** nanostructures with different morphologies.[64]

As a striking example of transcription through **endogenous templating** (see mechanistic aspects in section 3.2), the naturally occurring β-1,3-glucan **polysaccharide** (*Schizophyllan commune*, herein **O32**), self-assembles into helical aggregates and has been used as a template to form novel organosilica nanofibers. [65]

Also belonging to the family of *sugar-based* gelators, a variety of *sugar-appended porphyrines*, with four monosaccharide groups at their periphery (compounds **O33**, **O34**, and **O35**), have been found to gel DMF−alcohol mixed solvents at relatively low concentrations.[66,67] Interestingly, the organogels of **O33** and **O34** in DMF/BzOH mixtures exhibit 1-D fibrous morphologies with left-handed (**O33**) and right-handed (**O34**) helices reflecting the chirality of the specific molecular structure of gelator compounds. On the contrary, the organogels of **O35** produce a different pattern (both a left-handed helical structure and a flat sheetlike structure).[67] Remarkably, **O33** has been transcribed into silica with different helical or nonhelical morphologies, depending on the polycondensation kinetics of silica (section 3.2).[68,69] In the case of organogels obtained from molecules **O34** and **O35**, the helical fibrous bundles were also satisfactorily transcribed into micrometer-scale silica helical bundles.[68]

Finally, the *sugar-based crown ether* derivative **O36** has proven to be a versatile gelator of various polar and nonpolar organic solvents, and also of water.[69] The right-handed helical fibrous hydrogel formed by **O36** in the presence of $AgNO_3$ acted as an efficient template in the formation of metal-coated nanotubular silica structures by sol–gel polymerization of TEOS.

2.1.E. Cholesterol-Based Organogelators. Among the different steroids, cholesterol has proven to be the more versatile in order to design functional LMOGs,[70] and cholesteric-based LMOGs (compounds **O37** to **O55** in Figure 1) must be considered among the most flexible templates for materials transcription. Indeed, the first class of LMOGs successfully used as a template for the formation of silica-based nanofibrous materials contained an azobenzene-appended cholesteric moiety as the main structural motif (compound **O38** or mixtures of **O37** with **O38**).[5] It was first discovered that the **azobenzene-appended cholesteric** gelator **O37** and other related gelators could gel a number of organic solvents as well as liquid silanol derivatives.[71] But, it was not possible to transcribe their fibrillar morphology into silica analogues. However, acetic acid solvated organogels made with the less versatile gelator **O38** resulted in the successful transcription of tubular silica,[5] becoming a crucial finding for the development of materials transcription through organogel templates. Moreover, the shape of the transcribed silica could be tuned by adding EtOH or using as templates mixtures of the neutral gelator **O37** with the charged gelator **O38** (section 3).[72]

After this first example, many different families of monomeric (*ALS* compounds **O39**−**O42**, **O45**$_n$, **O47**, and **O50**−**O52**) or dimeric ($A(LS)_2$ compounds **O43**, **O44**, **O46**$_2$, **O48**, **O49**, and **O53**−**O55**) **cholesterol-based** LMGs (with A = aromatic group, L = functional linker, and S = steroid, cholesteric group) have been employed as templates for materials transcription, resulting in the formation of a variety of nanostructures.a−c Similarly to gelator derivatives **O37** and **O38**, compounds **O39**−**O47** are all based in the azobenzene−cholesterol scaffold, while gelators **O48**−**O54** do not possess any azobenzene-appended moiety.

Versatile cholesteric gelators for materials transcription have been designed through the combination of the

azobenzene−cholesterol scaffold with a *crown or aza-crown ether* moiety [located at the periphery (**O39−O42**) or near the center of the molecule (**O43** and **O44**)]. In these gelators, the crown ether groups prevent the formation of a crystalline precipitate (thus enhancing the gelation ability) and can also act as guest binding sites of a variety of metal ions, amines, and so forth, thus allowing control of the gelation properties through **host–guest interactions**.[12b] Therefore, the gelation ability and the morphologies of the resulting organogels may be controlled through the addition of different metal salts ($KClO_4$, $CsClO_4$, $AgNO_3$, $Pd(NO_3)_2$, etc.), and at the same time, the cationic charges incorporated to the crown ethers have proven to be crucial for the transcription into inorganic materials. In this respect, Ono et al. have been able to prepare silica with diverse morphologies (curved lamellar, hollow fibers, tubular, and "rolled paperlike") or even metal−silica hybrid composite materials (i.e., with M = Ag or Cs) through the use of the monomeric derivatives **O39−O42** and $\mathbf{O44}_m$ as templates.[73–77] More recently, fibrous organogels of **O40** (in 1-butanol) have also enabled the synthesis of luminescent organosilica nanotubes loaded with functional dyes useful for optical sensors and luminescence diodes.[78]

In comparison to these "mono"-type cholesterols, the **dimeric** azobenzene-appended cholesterols **O43** and **O44** have proven to be even more efficient organogelators. The gelator derivative **O43** self-assembles in acetic acid to give multilayered vesicles with two different sizes, whose transcription into silica results in multiwalled silica spheres.[77] Interestingly, the dimeric cholesterol derivative $\mathbf{O44}_{30}$, with a larger (central) *30-crown-10-ether* moiety, presents an even greater gelation ability. Indeed, the organogel of $\mathbf{O44}_{30}$ in acetic acid consists mainly of a mixture of linear and right-handed helical ribbons, and also of tubular structures, suggesting that the structure of this organogel involves several metastable intermediate processes (linear ribbon → helical ribbon → tubule).[79] Transcription of an acetic acid organogel of $\mathbf{O44}_{30}$ into silica results in both helical ribbons and double-layered tubular structures.[79a] Similar structures were also transcribed into TiO_2 from acetic acid organogels of $\mathbf{O44}_{30}$.[80] In contrast, nonhelical silica morphologies were obtained using as templates organogels of the related monocholesteric compounds $\mathbf{O44}_m$, and dicholesteric $\mathbf{O44}_{24}$ in propionic acid. In both cases, similar silica structures having roll-paper-like walls were observed.[79b]

On the other hand, the transcription of fibrous organogels of other azobenzene−cholesterol gelators, without appended crown ether moieties but containing a pendant ($\mathbf{O45}_n$ and **O47**) or central ($\mathbf{O46}_2$) *neutral diamine moiety*, has afforded the formation of silica nanofibers, helical Ni-SiO_2 and Pd-SiO_2 hybrid nanocomposites, and also double-walled transition-metal oxide nanotubes (**O47**). In the case of 1-BuOH organogels of the pendant diamine compound $\mathbf{O45}_n$, with various chain lengths (n) between the amine group and the gelator scaffold, an interesting **odd–even relationship** occurs in the aggregation modes of these "gemini"-type cholesterol-based gelators (which is governed by the packing of the terminal groups).[81] Consequently, these "minor" changes in the molecular gelator structure were shown to have drastic effects on the overall morphology of the templated inorganic materials (see section 3). On the other hand, the homologous dimeric azobenzene-appended cholesterol $\mathbf{O46}_2$ may form helical fibrous organogels consisting of thinner helices arising from the 1-D molecular stacking due to interdigitated van der Waals interaction between cholesterol moieties. Consequently, its transcription into silica resulted in silica helical nanotubes with well-defined and monodisperse inner hollows.[82]

The azobenzene-appended cholesterol gelator **O47** [containing the azobenzene and cholesterol skeletons as solvophobic aggregate-forming groups, and a *1,13-diamino-4,7,10-trioxatridecanyl* unit as a solvophilic pendant (head) group] is another example of formation of self-assembled tubular organogels (similarly to **O40**, **O41**, and **O44** compounds).[83] Interestingly, the sol–gel transcription of the tubular morphologies of **O47** in acetonitrile resulted in the formation of double-walled transition-metal single (ZrO_2, TiO_2, and Ta_2O_5) and binary (ZrO_2/TiO_2) oxides.

In contrast to the above compounds (**O37–O47**), some other cholesterol-based gelators that do not contain azobenzene moieties (gelators **O48−O54**) have been used as templates for materials transcription. For instance, the dimeric cholesterol-based gelator derivatives **O48** and **O49** contain a *bis-aryl-phenantroline* moiety connecting the two cholesterol units, which may be useful for the introduction of a variety of metal ions. Compound **O48** is an efficient gelator of acetic acid[84] and many other organic solvents.[85,86] Moreover, the fluorescent properties of the organogel phase (in 1-propanol) are sensitive to protonation (proton-sensitive fluorescent organogel) of the phenantroline N atoms.[85] Interestingly, the transcription of **O48** in acetic acid allowed the formation of highly stable mesoporous hollow silica tubules because protonated amines can also function as efficient transcription directors. Hybrid gelator-silica fluorescent composite materials were also obtained in other solvents.[86] In the case of compound **O49**, the protonation of the phenantroline moiety ($\mathbf{O49H}^+$) appears to be indispensable for gelation, enabling at the same time an efficient transcription of well-defined SiO_2 hollow nanofibers with the size of its inner cavity corresponding to a unimolecular 1-D stacking of **O49** molecules.[85] Thicker fibrouslike aggregates of TiO_2 (ca. 100-nm-thick) were also transcribed using an **O49**/acetic acid organogel as the template (the thicker fibers with some granular titania arising from the faster sol–gel condensation of the titania alkoxide). Remarkably, in both cases, the organic–inorganic composites obtained before calcination conserve the fluorescent properties of the original xerogel templates (**O48** and **O49**) and therefore could find applications as optoelectronic devices. [85]

On the other hand, the versatile monocholestheric benzylamine gelator **O50** or mixtures of the related benzylammonium salt **O51** with the pyridinic derivative **O52** have also afforded the transcription of silica fibrous structures.[87] Very interestingly, a benzylamine moiety covalently linked to the gelator scaffold of compound **O50** enabled for the first time efficient transcription into fibrous silica in the absence of an externally added solution catalyst. Despite the fact that benzylammonium derivative **O51** has no organogelling properties, an equimolecular mixture of **O51** with

the pyridine-containing derivative **O52** can also form fibrous organogels. However, transcription into silica of a mixed **O51** + **O52** organogel in 1-BuOH was only possible in the presence of an added catalyst (benzylamine or hydrazine), resulting in the formation of hollow, fibrous silica.[87] Lastly, Shinkai and co-workers have further investigated the gelling properties of pyridine-containing cholesteric gelators such as **O52** and related derivatives. Indeed, **O52** emerged as a versatile supergelator of many organic solvents. It has even been used to give whiskerlike morphologies when applied to a sublimable solid solvent such as naphthalene.[88] As a striking example of the potentiality of postmodification of preformed fibrous organogels, they have postfunctionalized the gel fibers obtained from supergelator **O52** with fluorescent molecules like tetraphenyl porphyrine Zn(II), resulting in a hybrid organogel material with potential applications in photochemical and electrochemical devices.[88]

Finally, Wang's group has recently designed three dimeric cholesteric gelators (**O53** and **O54/O55**) and have used them as efficient templates for materials transcription. First, a fibrous xerogel of the cholesterol-based viologen gelator **O53** in 1-butanol with unimolecular stacking of fibers has been transcribed into fibrous silica with a very thin and monodispersed diameter.[89] On the other hand, through the use of fibrous xerogels of the more complex dicholesteric gelator **O54** (3-oxopentane derivative), it has been possible to transcribe novel "pearl-necklace", porous, hollow CdS nanofibers.[90] Similarly, two different organogel systems of the similar 3-oxopentane derivative **O55** have enabled the transcription of CuS nanofibers. Remarkably, the helical pitch can be tuned by controlling the binding sites, which depends on the solvation effects because the two different gelled solvents lead different interaction sites between Cu^{2+} ions and the binding sites of the gel fibers.[91]

2.1.F. Miscellaneous Gelators. Apart from the above-described families of LMGs, some other interesting gelator molecules have also been used as templates for material transcription, but they contain structural features difficult to classify in any of the previous groups. This is the case, for instance, of *miscellaneous* gelators **O56–O58**, which we describe below. The special class of hybrid organic–inorganic (self-assembling) gelators, in which the inorganic species is already incorporated in the self-assembling scaffolds through covalent or coordinative bonds (such as sylilated gelators and metallogelators) will be considered separately in section 5.3.

As a first example of these miscellaneous gelators, some **diacetylenic phospholipids** have been extensively used as templates for metallic coatings; for example, the polymerizable diacetylenic phospholipid molecule **O56** (*1,2-bis(10,12-tricosadiyonyl)-sn-glycero-3-phosphatidylcholine*, referred to as $DC_{8,9}PC$) has the ability to self-assemble, in aqueous solutions, into hollow tubule-shaped microstructures (diameters of 400–1000 nm, wall thicknesses of 10–50 nm, and lengths of 50–100 μm). These tubules and helical ribbons (formed in water/ethanol mixtures) have been used to template the patterning of thin coatings of metals (Ni and Cu),[92] silica,[93] and alumina[94] through a post-transcription methodology (coating on preformed $DC_{8,9}PC$ tubules), and also for the in situ deposition of spatially organized gold nanoparticles on phospholipid tubules.[95] Similarly, the in situ coassembly at the mesoscopical level of O56 **gels** with Si precursors has enabled the formation of silica−lipid hybrids having mesoscopical helical and tubular shapes and multilamellar polymerizable walls. Moreover, the silica−lipid tubules can be preserved after polymerization, but the helical surface patterning is lost.[96]

The so-called "*dendron rodcoil*" (DRC) compound **O57** (with a triblock architecture) is able to self-assemble into fibrous nanoribbons via H bonding, causing the gelation of various organic solvents. Although the resulting ribbonlike aggregates are flat in dichloromethane,[97] in some organic solvents (i.e., in ethyl methacrylate, EMA, or 2-ethylexyl methacrylate, EHMA), they adopt very thin helical morphologies (twisted helices). The in situ coassembly of a helical EMA organogel of **O57** with $Cd(NO_3)_2$, and subsequent exposure to H_2S (g), led to the formation of coiled nanohelices consisting of a polycrystalline CdS semiconductor which may be suitable for photovoltaic applications.[98]

An impressive example of the potential use of LMOGs as efficient templates for the transcription of more "sophisticated" inorganic materials is provided by the complex amphiphilic derivative **O58**, which consists of five distinct structural parts (A–E) and self-assembles into cylindrical micelles (pH-sensitive birefringent hydrogels in water at pH < 4). Taking advantage of the strong interactions between Ca ions and the phosphorylated serine part (D), it was possible to transcribe a xerogel of **O58** into hydroxyapatite (HA, $Ca_{10}(PO_4)_6(OH)_2$).[99]

2.2. The Organogelation Process: Supramolecular Interactions and Morphology Control. As previously mentioned, the process of organogel formation with LMOGs takes place typically upon cooling (below the critical gelation temperature) the corresponding hot solution of the organogelator molecules in an appropriate solvent, at relatively low concentrations (typically $<$1–2% w/w). Organogelation is therefore the result of very subtle and balanced (cooperative/competitive) interactions among the gelator and solvent molecules. Upon organogelation, the solvent molecules are immobilized, and strongly anisotropic structures are formed, mostly in the shape of fibers, but also as ribbons, platelets (sheetlike structures), tubules or cylinders, and so forth (see Table 1). The critical TG depends on many different variables such as the molecular structure of the gelator, which determines the type of supramolecular forces and aggregation modes responsible for organogelation; the gelator concentration, because TG rises exponentially with increasing concentration; the type of solvent through organogelator−solvent molecules interactions; the cooling protocol followed during organogelation; and the presence of additives or exogenous guests (metal salts, cosolvent, cogelator, etc.). LMOGs are said to have a higher *gelation efficiency* the higher their gelation temperatures, and/or the lower their concentration (minimum gelation concentration, MGC).

In the previous section, we have already described the main structural families of LMOGs and the rich variety of morphologies that may exhibit their self-assembled structures. Although a more detailed understanding of the mode of

aggregation of gelators and their structures is still needed, the self-assembly of the organogel fibrous networks is mainly governed by different supramolecular forces operating among gelator and solvent molecules. These forces may be London dispersion or other van der Waals interactions, hydrogen-bonding, aromatic or $\pi-\pi$ interactions, ionic or coordinating bonding, or usually a combination of them.

For instance, in the simple alkane gelators, the organogelation may be induced exclusively through London dispersion forces. In gelators containing amide, amino acide, urea, or peptide moieties, the aggregation is mainly due to H-bonding interactions (along with van der Waals interactions of aliphatic chains). H-bonding interactions are also the main interactions responsible for gelation in cyclohexane diamides or bisureas and in sugar-based gelators (combined with the van der Waals, stacking interactions of their ring units), whereas in the case of LMOGs bearing aromatic units (i.e., benzene, phenazine, anthracene, porphyrin, phenantroline, and cholesteric derivatives), the aggregation is mainly driven by $\pi-\pi$ or aromatic stacking (and/or solvophobic) effects. In the latter, the shape and size of the aromatic group becomes also a key structural factor toward gelation. Moreover, the introduction of moieties with chelating or binding sites (such as crown-ethers, or porphyrin moieties) allows modulation of the organogelation properties through host–guest interactions (adding exogenous guests such as metal ions, amines, nucleobases, etc.).

Therefore, it is possible to control the organogelation properties, functionality, and morphology of the resulting organogels (including chirality control) through an accurate design of the *molecular structure* of gelator molecules (even with very simple or subtle structural modifications), an appropriate choice of the solvent, and the introduction (when needed) of exogenous guests (metal salts, cosolvent, co-gelator, etc.). Remarkably, the *protocol* followed during the *organogelation* process (mechanistic and/or kinetics aspects) is of paramount importance and will be commented upon later (vide infra). *Solvent−gelator* interactions[100] are also crucial, the organogelation properties of gelator molecules being very dependent on the polar/nonpolar or protic/aprotic character of the solvent. This crucial role may be illustrated for instance in the case of gelator **O23** (the α-galactose derivative), which forms in EtOH fibrous structures but in water gives rise to spherical aggregates.[53] Many other examples of gelators forming organogels with different morphologies (or dimensions) depending on the gelated solvent may be found in Table 1 (i.e., gelators **O10**, **O14**, **O30**, **O31**, **O42**, **O43**, and **O48**).

Moreover, in some gelator derivatives, *pH conditions* also become a crucial factor to determine the solubility, organogelation, and morphology properties. This is the case of gelators containing amino acid groups or any other moiety that can be protonated in the presence of acids, becoming therefore "pH-responsive" organogels. In some cases, as with the pyridinic L-valine derivative $\mathbf{O11_b}$, the protonation of N atoms of the pyridine in acidic media enhances its solubility and prevents the organogelation, while at higher pH values (>ca. 3), the enhanced H-bonding interactions trigger the formation of a fibrous organogel (or hydrogel).[39] In contrast, in other cases, the protonation has an opposite effect, as occurs with gelator **O49**, in which the protonation of the phenantroline moiety ($\mathbf{O49H^+}$) is necessary for gelation.[85]

Also remarkably, the design of *two-component gelator* systems is becoming a topic of intense research, since they can result in highly tunable self-assembling systems and give rise to advanced functional materials.[101] For instance, in a dual-component gelator consisting of two glucopyranoside derivatives (the *p*-nitrobenzylidene derivative **O30** and its *p*-aminobenzylidene homologue), the organogelation process can be ascribed to *charge-transfer* interactions between electron-donor groups and results in the formation of a novel helical, fibrous-bundle structure while the single component gels consist of nonhelical fibrous networks.[102]

Apart from the above discussion, it must be highlighted that the ultimate morphology of the different organogel systems cannot be explained under only a purely chemical or structural analysis, centered on the effect of the molecular structure of the gelator and the type of solvent and on the different supramolecular forces operating among them. Effectively, an "additional" engineering of the supramolecular fibrous morphologies can be attained by careful control of the **thermodynamic** or **mechanistic aspects** involved in the *organogelation protocol* (the procedure followed during the evolution from the sol to the gel state). Through the use of different characterization techniques, organogel formation has been explained attending to three different mechanisms: (i) a phase separation process in the sol state, followed by fibril growth,[103] (ii) a generic heterogeneous nucleation model via the so-called "crystallographic mismatch branching",[104] and (iii) a precipitation process via the classical nucleation-growth mechanism.[105,106] In light of these proposed mechanisms, the degree of alignment or branching of the fibrous organogels may be tailor-controlled by adjusting thermodynamic aspects such as the initial supersaturation conditions and the cooling rate, as it was shown for instance for gelators **O1**[105] or **O3** ($18_4P^+X^-$).[23,24] Generally, more intrincate (intertwinned) networks result from faster cooling rates. This alignment effect can be very important for templating inorganic or hybrid replicas with potential application in fields where highly anisotropic materials are needed, such as in nanoelectronics or photonics. This alignment has already been attained through different ways. For instance, in the case of gelator **O1** (DDOA), a long-range alignment (orientation) of the fibrils of the organogel (in DMF) has been accomplished by simply applying mechanical shear stress during cooling of the isotropic hot sol.[107] Also interestingly, in the case of the gelator **O11A**, by performing gelation under vigorous stirring, the shear flow was observed to induce a considerable alignment of hydrogel nanofibers, which can also be duplicated in templated silica nanofibers.[38]

Closely related to the organogelation protocol is the process of *solvent removal*. In this respect, the transition from the wet gel to the corresponding dried xerogel (or aerogel) may also be accompanied by important textural and morphological rearrangements, depending on the time at which the entrapped solvent is extracted and on the employed methodology (free or controlled evaporation, use of vacuo

or supercritical conditions, etc.). For instance, in the case of **O52**, It was confirmed that the obtained fibrous morphologies strongly depend on the process of solvent removal, and their stability may be enhanced by using metal–ligand interactions (adding metal ions like Ag^+).[88] Similarly, Tan et al. have recently analyzed the nucleation and growth characteristics of a binary gel system of bis(2-ethylhexyl) sodium sulfosuccinate and 4-chlorophenol. They have found that, by reducing the evaporation of the pregel solution, it is possible to initiate gelation at the air–solution interface and to induce the alignment of multiple fibers with extremely long persistence lengths.[106]

In all of the above-mentioned discussion, organogelation is induced upon cooling the initial hot solution of the gelator. However, organogelation can also be realized isothermally at room temperature.[108] Moreover, for the emerging second generation of LMOGs, the gelation transition can be induced as a response to redox- or photostimuli, isothermally, or even by heating. This heating-induced organogelation is a very special case that has been recently reported (see section 5.3).

2.3. Main Strategies for Materials Templating with LMOGs. Herein, we highlight in general terms the different synthesis strategies (pathways), methodologies, or processes that can be used for the template synthesis of inorganic or hybrid (organic–inorganic) materials through the organogelator approach.

The three main synthesis pathways to form organogels and the resulting inorganic or hybrid nanofibrous replicas (types of materials A, B, C, and D) are schematically presented in Figure 2. LMOGs can be used as templates through either (a) an *in situ coassembly* (**IC**) process (**route 1**), (b) a *two-step simple post-transcription* (**PT**) (**routes 2 and 3**), or (c) a *self-assembly* (**SA**) process (**route 4**). For *PT*, organogel self-assembly (2) is associated with subsequent post-transcription (3), which occurs via impregnation or by the diffusion of mineral or hybrid precursors. The **SA** process (4) describes the case of **hybrid (**organic–inorganic) **organogelators**, in which the precursors of the inorganic species are already bonded to the organogelator molecules through covalent or coordinative bonds. Some examples and applications of this particular case of hybrid organogels will be treated with more detail as a special case of hybrid material (section 5.2).

Most of the nanofibrous inorganic or hybrid materials so far templated with organogelators have been prepared through the **in situ coassembly (IC)** process. However, there are also some synthesis examples where the organogelation was performed in the absence of inorganic or inorganic–organic sol–gel precursors (*PT* approach), though the authors fail in most cases to stress the crucial importance of using one or another templating procedure. In this case, the preformed organic xerogel is subsequently impregnated with, or subjected to, the **postdiffusion** of a solution of precursor salts (or also gas species; i.e., H_2S) with any other ingredient for sol–gel condensation (solvent, water, catalyst, etc.). The main differences between the *in situ* (IC) or *two-step* post-transcription (PT) methodologies will be commented upon later, along with other mechanistic aspects (section 3.2).

In the first two strategies (IC and PT), *nanofibrous hybrid composite materials* (**B**) can be obtained, which consist of organogelator fibrils coated with partially condensed inorganic/hybrid species. These latter ones can locate onto the external (*exotemplating*) and sometimes also internal (*endotemplating*) surfaces of the organogel nanofibrils (see section 3.2).

Because they can smartly combine different functionalities, these **hybrid nanofibrous materials** can be very interesting for many applications.[109,110] For instance, as previouly mentioned, the coassembly of the diacetylenic phospholipid **O56** with silica has enabled the formation of silica−lipid tubules that can be preserved after polymerization.[96] Similarly, the formation of hybrid nanocomposite materials consisting of metal (gold) nanoparticles stabilized by the supramolecular gel networks (in toluene) of two different dendritic-like gelators has been recently reported.[111] A hybrid gelator−silica material with fluorescent properties (interesting for optoelectronic applications) is shown in Figure 2.[86]

However, in most cases, the organogel template is subsequently removed (step **5**) to obtain an organogelator-extracted, *purely inorganic or hybrid (organic–inorganic) nanofibrous replica* (material **C**, which may or may not have an internal hollow). We show a template-extracted tubular organosilica in Figure 2.[78] The removal of the organogel nanofibrous scaffold is conventionally carried out through washing (with alcohol, water, or other appropriate solvents) or thermal procedures (the employment of UV-irradiation is another alternative).

In the third strategy (pathway **4**), which is a real supramolecular self-assembly approach (**SA**), the inorganic species is already bonded to the self-assembling (organic) species, and they can either be passive moieties or play an active (and essential) role in the self-aggregation of the fibrous organogel through polymerization reactions or coordinating interactions (see selected examples and references in section 5.2). The resulting material (**D**) is therefore a *hybrid organogel containing the inorganic species* in its own organogel nanofibrous scaffold (*self-templating*), and these systems are also being thoroughly investigated due to their many potential applications as functional advanced nanomateriales (in Figure 2, we show as an example a sylilated porphyrine-based organogel which becomes reinforced by sol–gel polymerization).[122b]

In any case, moreover, all of the resulting materials (A−D) could be eventually **postmodified** (pathway **6**) through any postfunctionalization reaction (reaction with chloroalkoxysilanes, polymerization, or any other derivatization reaction) leading to improved *multifunctional nanofibrous materials* (E).[109,110] Two examples are shown in Figure 6: a cholesterol-based gelator postmodified with porphyrine−Zn moieties[88] and a fibrous mercapto-silica which was subsequently grafted with gold nanoparticles.[21]

In the following sections, the different kinds of nanofibrous materials that have already been prepared through the organogel-template approach will be briefly reported on. They can be split into three different categories: (*i*) oxide-based materials (section 3), (*ii*) nonoxide-based materials (section 4), and finally (*iii*) hybrid (organic–inorganic) materials (section 5).

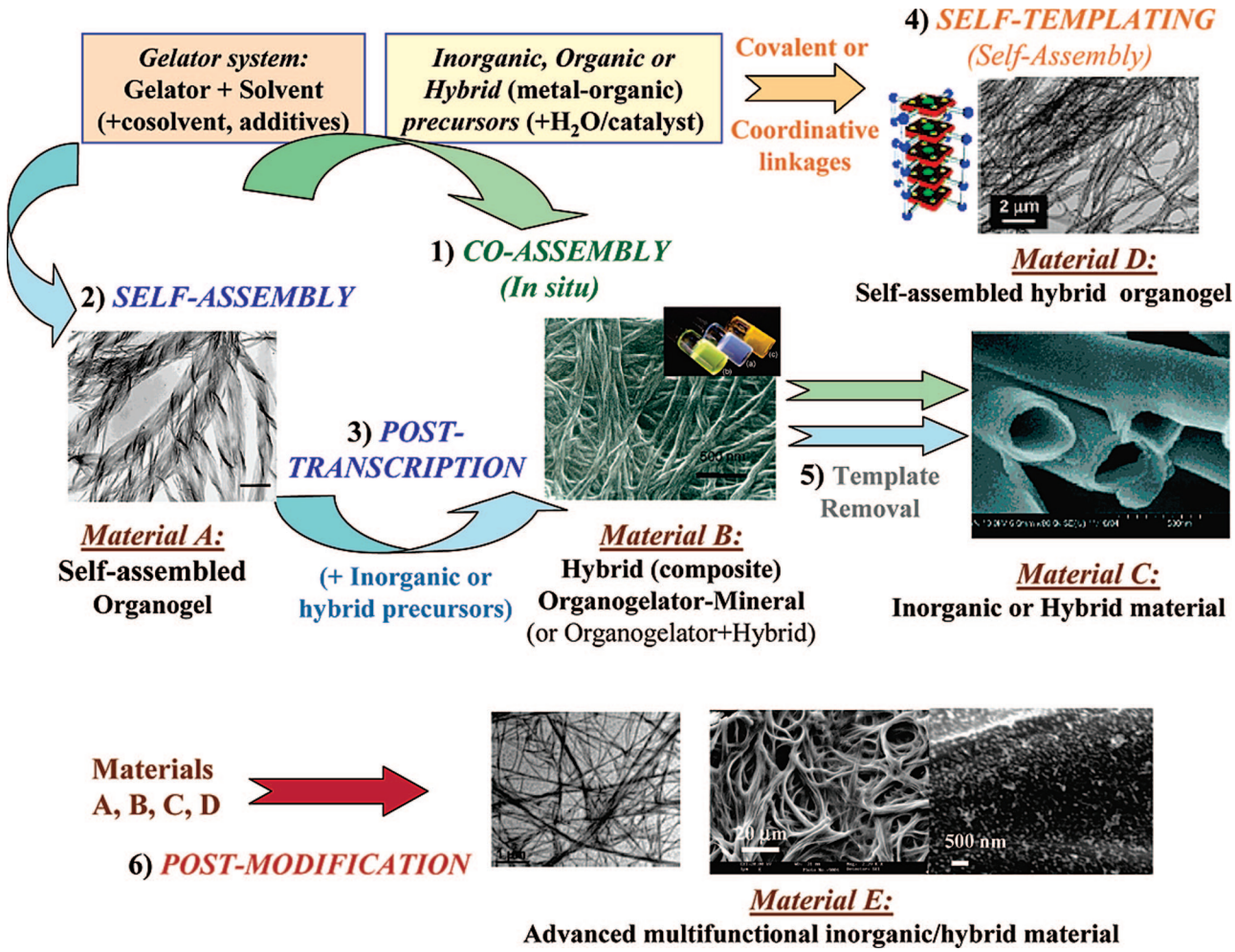

Figure 2. General pathways for the synthesis of nanofibrous (inorganic or hybrid) materials through the use of organogel templates, involving different (one-step or multistep) templating strategies (in situ coassembly, self-asembly + post-transcription, and self-templating). Postmodification of any material is possible (step 6). The selected materials (A−E) are the following: (A) dual-component sugar-based organogel O30 + *p*-aminobenzylidene derivative with charge-transfer phenomena, ref 102; (B) hybrid gelator-silica material templated with fluorescent phenantroline gelator O49/TFA/acetone, ref 86; (C) hybrid hollow tubes of fluorescent coumarin-dye organosilica after removal of O40 template, ref 78; (D) reinforced porphyrine-sylilated organogel SO5.Cu, ref 122b; (E) cholesteric organogel of O50 postmodified with porphyrine-Zn moieties (left, ref 88) useful for photo and/or electrochemical devices and hybrid mercapto-silica templated through gelator O2 (right, ref 21) before and after postgrafting with gold nanoparticles. Adapted with permission from refs 102, 78, and 122b (Copyright 2002, 2005, and 2005 American Chemical Society), ref 88 (Copyright 2007 Elsevier), and ref 21 (Copyright 2005 Wiley-VCH Verlag GmbH & Co. KgaA).

3. Oxide-Based Nanofibrous Materials

In this section, we summarize first (section 3.1) the different morphologies of both siliceous (A) and nonsiliceous (B) oxide-based nanofibrous materials that have been so far templated with organogelators and how these morphologies can be tailor-controlled through different synthesis parameters or preparation conditions. We then conclude (section 3.2) with a brief discussion about the key aspects for an efficient transcription and some proposed templating mechanisms.

3.1. Templated Morphologies and Preparation Methodology. *3.1.A. Silica and Metal−Silica Fibrous Materials.* The different *silica-based* nanofibrous materials (silica or metal−silica composites) templated through the organogel approach (including some relevant information about preparation conditions) are summarized in Table 2. For each morphology, the available corresponding dimensions, the synthesis conditions (type of organogelator, solvent, acid or basic conditions, catalyst, other additives or cosolvents, etc.), and the strategies for the templating process (in situ coassembly or post-transcription strategies) or for organogel removal are presented. Some selected SEM or TEM images are also shown in Figure 3. Herein, we discuss some general and important points related with the templating of silica-based nanofibrous materials.

Analyzing the reported templated synthesis, in most cases, the transcription of silica-based material has been carried out through the **coassembly route** (IC), which involves the in situ formation (upon cooling) of an organogel in the appropriate organic solvent and in the presence of the silicate oligomers (and controlled amounts of water and catalysts when necessary), which upon condensation give rise to an inorganic siloxane-based gel (strategy **IC(G)** in Table 2). Some cases of in situ templating through hydrogels in aqueous media are also included in Table 2, due to the relevance of the silica morphologies that have been obtained. Sometimes (i.e., with **O13**$_f$ or **O56**), the fast progress of the silica sol–gel

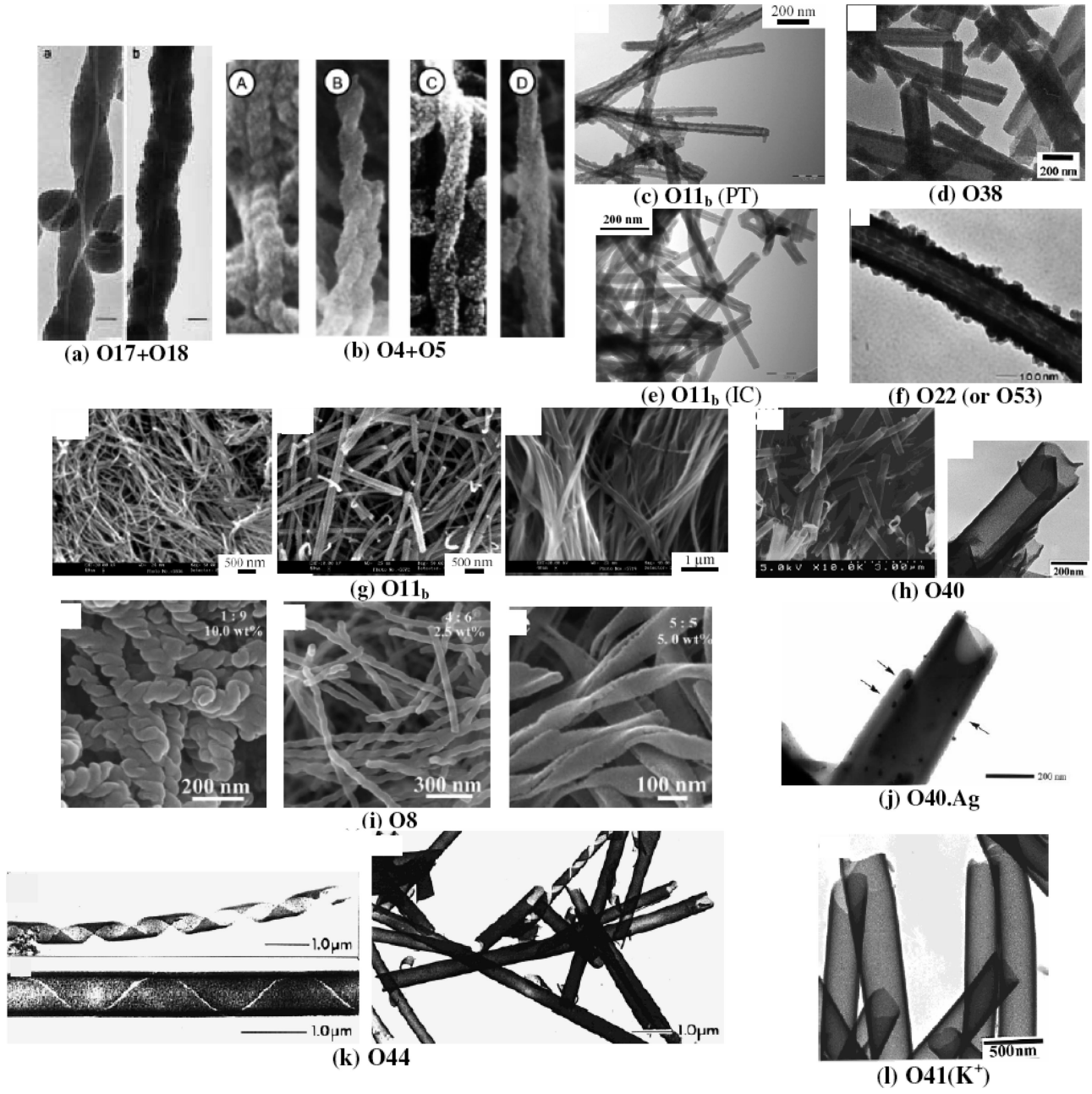

Figure 3. SEM or TEM images of selected silica nanofibrous morphologies templated through organogels. *Single and double-stranded helical fibers*: (**a**) left- and right-handed single helices with inner helical hollow (**O17** + **O18**, ref 51a), (**b**) rope-like, double-helical (right-handed) fibers with tunable pitch (**O4** + **O5**, ref 27). *Straight nanotubes (single hollow) of different aspect ratios*: elongated nanotubes prepared by *post-transcription* (**c**) or *in situ* coassembly (**e**) routes (**O11$_b$**, ref 41) and (**d**) shorter and thicker nanotubes being the first transcription example (**O38**, ref 72b). *Multihollow "lotus-shape" fibers*: (**f**) prepared with **O22**, ref 54; similar with **O53**, ref 89. *Morphology control through solvent/pH/catalyst conditions:* (**g**) gelator-silica xerogels with thin fibrils (left), flat ribbons (center), and thicker ribbonlike bundles (right) prepared with **O11$_b$** under strong acid, soft acid, or basic conditions (ref 41) and (**i**) left-hand double helices (left), single-stranded loosely coiled helices (center), and double-twisted ribbons (right) obtained with **O8** at different alcohol/water ratios and NH_3 wt % (ref 36b). *Rolled-paper-like (multiwalled) tubules*: obtained with (**h**) **O40** without metals (ref 74), (**j**) **O40** with Ag (ref 75), and (**l**) **O41** with K^+ (ref 74). *Helical ribbons and double-layered tubes*: (**k**) obtained with **O44** (ref 79a). Adapted with permission from refs 51a, 74, and 79a (Copyright 2000 and 2001 American Chemical Society) and refs 27, 41, 54, 72b, 36b, and 75 (Copyright 1999, 2000, 2001, 2002, and 2006 The Royal Society of Chemistry).

condensation reactions prevents the formation of the organogel and results in the formation of a precipitate (strategy **IC(P)** in Table 2). In these cases, the templating (if effective) takes place in the solution phase rather than through formation of a true organogel.

Alternatively, the transcription may be accomplished in a two-step post-transcription route (strategy **PT** in Table 2), in which the addition (diffusion, impregnation, etc.) of silicate species (catalysts, water, etc.) is performed after formation of the organogel fibers. For instance, in the case of the valine derivative **O11$_a$** the addition of TEOS must be subsequent to the formation of organogel nanofibers in order to transcribe well-aligned silica nanofibers, whereas the in situ procedure (**IC**) leads only to nontemplated silica particles.[38a] Similarly, the use of either an in situ or a post-transcription strategy with the homologue gelator **O11$_b$** was also decisive in

Table 2. Summary of Different *Silica-Based* Nanofibrous Morphologies Templated with Organogels (Or hydrogels), Including Relevant Information about Morphology and Dimensions, Type of organogelator and Solvent, Synthesis Conditions, and Templating Strategy, and Their Corresponding References

gelator	refs	solvent	synthesis conditions,[a] pH/catalyst/additives/washed−calcined	templating strategy[b]	silica morphology and dimensions[c]
O1 (DDOA)	17	MetOH	12.6/NH_4OH (HCl + NH_4OH)/--/W ($CHCl_3$)	IC (G)	Two-scale porous nanofibers (φ: 200 nm; mostly coaligned)
	18–19	EtOH	ca. 2–3/HCl (hydrolytic) or TFA (nonhydrolytic/--/C (350 °C)	IC (G)	Fibers and fibrous bundles (entangled or coaligned; φ: 200–300 nm to 1–2 μm)
O2 (DUOP)	17	EOH	12.6/NH_4OH (HCl + NH_4OH)/--/W ($CHCl_3$)	IC (G)	Intertwined ribbonlike fibrous bundles (2–10-μm-thick) of juxtaposed coaligned fibrils (ca. 200-nm-thick)
	18–19	EtOH	ca. 2/TFA/--/C (350 °C)	IC (G)	Intertwined fibrous bundles of thinner fibers or fibrils (φ: 200–400-nm-thick)
O3 (18_4PX)	24	EtOH	9.5–10/NH_4OH/X = I, Br/C (500 °C)	IC (G)	Platelike fibrous objects (φ < 100 nm)
		benzene	9.5–10/benzylamine/X = I, Br, Cl/C (500 °C) or W (MetOH)	IC (G)	Unbundled fibers (tubules of > 100 μm length, φ of several micrometers); also "necklacelike" fibers
				IC (G) aged	Thicker, straight and flat fibers
			A/acetic acid/X = I, Br, Cl/C (500 °C) or W (MetOH)	IC (G)	Thinner tubules (diameters from hundreds of nm to several μm)
			B or A/benzylamine or acetic acid/X = Br/C (500 °C) or W (MetOH)	IC (G)	Similar but with more granular (untemplated) silica
			A/$FeBr_3$/X = Br and TEOS-$SiCl_4$/C (500 °C) (nonhydrolythic)	IC (G)	Similar fibrous objects (tubules) to those under hydrolytic conditions
		THF	2–9/acetic acid, benzylamine, NH_4OH, and HCl/X = I, Br, Cl/C (500 °C) or W (MetOH)	IC (G)	Narrower fibers
O4 + **O5**	27	pyridine/water (1:1 v/v)	B/benzylamine/--/C (500 °C)	IC (G; 3 days)	Pure **O4** (100% ee): ropelike right-handed helical fibrils (presumably double-stranded); **O4** + **O5** (50 → 20% ee): double-stranded helices (pitch: 200 → 500 nm);
				IC (G; 7 days)	**O4** + **O5**: entangled and twisted tapes (helical pitch: ca. 400–800 nm)
O8	36a,b	H_2O or EtOH/H_2O (1:9 v/v)	B/NH_3/--/ W (MetOH) + C (550 °C)	IC (G)	1 wt % NH_3: left-handed helical and short (200–300 nm length) nanotubes (φ_{inn} = 15 nm); 11.3 wt % NH_3: nanoribbons + inner-helical nanotubes; 5 wt % NH_3: nanoribbons + nanotubes + nanofibers
		EtOH/H_2O (3:7 or 4:6 v/v)	B/NH_3/--/ W (MetOH) + C (550 °C))	IC (G)	2.5 wt % NH_3: left-handed double-helical mesoporous nanofibers (φ = 50 nm; pitch = 140 nm); 10 wt % NH_3: left-handed single-stranded twisted nanoribbons (80 nm width; pitch = 140 nm)
O8	36b	1-prOH or 2-prOH/H_2O (1:9 or 2:8 v/v)	B/NH_3/--/ W (MetOH) + C (550 °C)	IC (G)	Left-handed double-helical mesoporous (wormlike) nanofibers (φ = 50–100 nm; length = 300–600 nm; pitch = 100–140 nm); lower diameter and pitch by ↑ [NH_3]
		1-prOH/H_2O (5:5 v/v)	B/NH_3/--/ W (MetOH) + C (550 °C)	IC (G)	2.5 wt % NH_3: left-handed helical nanotubes (φ_{out} = 25 nm; 5 wt % NH_3: double- twisted nanoribbons; 10 wt % NH_3: twisted nanoribbons
		2-prOH/H_2O (3:7 or 4:6 v/v)	B/NH_3/--/ W (MetOH) + C (550 °C)	IC (G)	2.5 wt % NH_3: single-stranded loosely coiled (straight) nanofibers
O9	36a	H_2O	B/NH_3/--/ W (MetOH) + C (550 °C)	IC (G)	5 wt % NH_3: mesoporous (6 nm channels) twisted (tubular) ribbons (longer and less helical than with **O8**)
$\mathbf{O11_a}$	38a	H_2O	B/NH_3/--/ W (MetOH) + C (500 °C)	IC (G) + PT (shear flow)	Bundles of ultrafine, aligned nanofibers (around 60-nm thick) formed by the gathering of mesoporous nanotubes (inner helical channels of ca. 2.2 nm and helical pitch of 3.2 nm)
$\mathbf{O11_b}$	41	CH_3CN	A → B/CF_3COOH or HCl → NaOH/water/W (CH_3CH) or C (350, 500, 800, 1000 °C)	IC (G)	Acid cond.: nanotubes (φ_{ex} = 25–40 nm; φ_{in} = 3–10 nm; random inner helicity); basic cond.: 3D-network of ribbonlike bundles (0.25–2-μm-thick)
			A/CF_3COOH/water/C (500 °C)	PT	Thicker, straighter, and more elongated nanotubes (φ_{ex} = 40–80 nm; φ_{in} = 5–35 nm)
$\mathbf{O11_c}$	38b	ethanol	B/NH_3/water/W(CH_3CN) + C (500 °C)	IC (G)	Mesoporous (hollow) nanohelices (25–40 nm thick; inner ϕ of ca. 10 nm)
$\mathbf{O13_{a-b}}$	42	water	A/HCl (aq.)/--/W (methanol) + C (500 °C)	IC (G?)	Cottonlike aggregates of helical (right-handed) bundles (of intertwined fibers: nanoribbons and nanotubes with 3–4 nm inner diameter)
$\mathbf{O13_{c-e}}$	43	ethanol	B (soft)/propylamine/ water/W (methanol)	IC (G)	Helical nanotubes (φ_{in} = 10–40 nm; inner helical hollow) + right-handed helical nanobundles (100-nm-thick) of gathered nanotubes + right-handed helical nanosprings (300-nm-thick; inner φ of ca. 100 nm)
		t-butyl acohol	B/tetrabutylammonium fluoride, TBAF/water/W (methanol)	IC (G)	With $\mathbf{O13_c}$: right-handed helical nanotubes (inner φ of ca. 30 nm) coated with silica nanoballs (<10 nm)
$\mathbf{O13_f}$	44	water	A/HCl/--/W (HCl aq./MetOH)	IC (P)	Right-handed (twisted) and long (hundreds of μm) mesoporous nanofibers (ca. 300-nm-thick, inside uniform φ of 2 nm), consisting of bundles of thinner nanofibers (ca. 50-nm-thick)
		water	B/NH_3 (aq.)/--/W (HCl aq./MetOH) + C (500 °C)		Straight mesoporous nanofibers (300 nm width; tens of μm length; inside φ of ca. 2 nm) consisting of bundles of thinner nanofibers, ca. 60-nm-thick)
O14	45a	*n*-butanol	A/HCl/--/C (500 °C)	IC (G)	Straight rodlike nanowires (φ ca. 200–500 nm; few μm length
	45b	a variety of solvents	A/HCl (aq.)/CTAB/C (650 °C)	IC (G)	Different morphologies depending on the solvent: tubular (1-butanol), roll-like (DMSO), spherical (xylene), and rodlike (DMF)
O16	48	CH_3COOH/H_2O 1:4 v/v	A/CH_3COOH/--/W (EtOH) + C (500 °C)	IC (G)	Hollow nanotubes (30–40-nm-thick, inner φ of 4–5 nm; few hundred nm length)
O17 + **O18**	51a,b	acetonitrile	B/benzylamine/water/C (500 °C)	IC (G)	Left-handed (*R*,*R* mixtures) or right-handed (*S*,*S* mixtures) helical hollow fibers (100–150 nm width; inner tubule of 20–60 nm; helical pitch: 340–345 nm)

Table 2. Continued

gelator	refs	solvent	synthesis conditions, [a] pH/catalyst/additives/washed−calcined	templating strategy[b]	silica morphology and dimensions[c]
O18 + **O19**	51b	acetonitrile	B/benzylamine/water/C (500 °C)	IC (G)	Left-handed (*S*,*S* mixtures) or right-handed (*R*,*R* mixtures) helical hollow fibers (90–120 nm width; inner tubules: 50–70 nm, opposite handedness to silica fibers)
O21-O23	53b−55	EtOH	B (soft)/benzylamine/--/C (500 °C)	IC (G)	**O21**: single hollow fibers (tubules 20–30-nm-thick; inner φ of 5–10 nm; 350–700 nm length); **O22**: straighter, larger lotus-shaped tubes (150–200-nm-thick; inner tube of 50–100 nm with thinner tubules 5–10 nm; **O23**: straighter, larger fibers ($\varphi \approx 1400$ nm)
O25	57	EtOH/H_2O	B (soft)/benzylamine/ --/C (500 °C) or B (strong)/ NaOH/--/C (500 °C)	IC (G)	[**O25**] = 0.1 wt %: nanotubes (80–85-nm-thick; inner φ of 20–25 nm; few μm length); [**O25**] = 3 wt %: rigid and much larger nanotubes (900–1400-nm-thick; inner φ of 450–600 nm)
O26 + **O27**(1:1 w/w)	59	water/methanol (10:1 v/v)	B (soft)/benzylamine/ --/C (500 °C)	IC (G)	Double-helical (right-handed) nanotubes (50–80-nm-thick; 5.0 nm nanospace between strands; pitch of 50–60 nm)
O30	63	water	B (soft)/benzylamine/--/C (500 °C)	IC (G)	3-D network of hollow (tubular) fibers ca. 50–100-nm-thick)
O33	67, 68	DMF/bzlOH (1:3 v/v)	B (soft)/benzylamine/water (trace)/W (MetOH) + C (500 °C) (A: sol–gel with heating conditions, 80 °C)	IC (G)	Nonhelical fibrous structure (50-nm-thick; inner hollows of ca. 5 or 9 nm)
O33	67, 68	DMF/bzlOH (1:3 v/v)	B (soft)/benzylamine/water (trace)/W (MetOH) but noncalcined (B: sol–gel at room *T* conditions)	IC (G)	Left-handed, helical bundles (150–300-nm-thick)
O34, **O35**	67	DMF/bzlOH (1:2 v/v)	B (soft)/benzylamine/water (trace)/W (MetOH) but noncalcined (B: sol–gel at room *T* conditions)	IC (G)	Left-handed (**O35**) and right-handed (**O34**) helical bundles (μm-scale)
O36	69	water	B (soft)/benzylamine/$AgNO_3$ (1.5 equiv.)/C (500 °C)	IC (G)	3D network of Ag-containing silica nanotubes (25–30-nm-thick; inner φ of ca. 8.5 nm; few μm length)
O38	5	HAc	A or B (soft)/HOac (A); benzylamine (B)/CH_2Cl_2 (cosolvent)/(CH_2Cl_2 removal, vacuo) + C (500 °C)	IC (G)	Straight nanotubes (150–300-nm-thick, with inner diameters of 10–200 nm)
		HOAc/ EtOH (3/1 m/m)	A (soft)/HOac/CH_2Cl_2 (cosolvent)/(CH_2Cl_2 removal, vacuum) + C (500 °C)	IC (G)	Nanofibers without inner hollows
O37 + **O38**	72	HOAc	A (soft)/Hac/CH_2Cl_2 (cosolvent)/ (CH_2Cl_2 removal in vacuo) + C (500 °C)	IC (G)	At **O38**/(**O37** + **O38**) (R) = 0.25–1: straight hollow nanotubes (diameters gradually smaller at lower R); at R = 0.1–0.01: right-handed helical nanotubes (ca. 40–80-nm-thick; inner φ of ca. 10 nm; pitch of 100–200 nm); at R <0.01: conventional granular
O39	73	1-BuOH	B (soft)/bzlNH_2 (B)/CH_2Cl_2 (cosolvent), $KclO_4$/(CH_2Cl_2 vacuo evap.) + C (500 °C)	IC (G)	High [$KClO_4$] (40 mM): hollow nanofibers (inner/outer diameter Ca. 10/50 nm); medium [$KClO_4$] (20 mM): hollow nanofibers (inner/outer diameter ca. 50/100–200 nm)
O40, **O41**	74	1-BuOH	B/bzlNH_2 (soft) or Et_4NOH (strong)/ CH_2Cl_2 (cosolvent), $KClO_4$ or $CsClO_4$ (optional)/(CH_2Cl_2 vacuo evap.) + C (500 °C)	IC (G)	**O40** (with or without metals): "rolled-paper-like" multilayered tubules (ca. 200-nm-thick); **O41** (with/ without metals): "paper-roll-like" multilayered tubules (ca. 400/200-nm-thick; thinner walls); also tubules with Et_4NOH
O40.Ag (in THF)	75	1-BuOH	B (soft)/bzlNH_2 (B)/$AgNO_3$ (THF)/(THF evaporation + sol−gel in 1-BuOH) + C (500 °C)	IC (G)	Multilayered "rolled-paper-like" tubules (inner φ of 190–210 nm; wall thickness of 40–60 nm) with Ag nanoparticles (into the interlayer
O42	76	1-BuOH	B (soft)/bzlNH_2 (B)/$AgNO_3$ or $CsClO_4$ (or also $NaClO_4$ or $KClO_4$/C (500 °C)	IC (G)	With Ag^+ or Cs^+: right-handed spirals (inner φ of 25–50 nm; additional lamella with $CsClO_4$) containing metal nanoparticles; with Na^+ or K^+: hollow nanofibers
	77	HOAc (first THF)	B (soft)/bzlNH_2 (B)/THF/ (THF evaporat. + sol–gel in HOAc) + C (500 °C)	IC (G)	Rolled-paper-like tubules (inner/outer diameters of 150–170/450–500 nm)

Table 2. Continued

gelator	refs	solvent	synthesis conditions, [a] pH/catalyst/additives/washed−calcined	templating strategy[b]	silica morphology and dimensions[c]
O43	77	HOAc (first THF)	B (soft)/bzlNH$_2$ (B)/THF/ (THF evaporat. + sol–gel in HOAc) + C(500 °C)	IC (G)	Hollow vesicular structures with multilayered walls (5 nm spacing)
O44$_{30}$	79a,b	HOAc	A (soft)/bzlNH$_2$ (B; optional) /--/C (500 °C) (moderate heating during sol–gel)	IC (G)	Helical ribbons (450–1500-nm-thick; 1700–1800 nm pitch) + double-layered tubes (560-nm-thick; inner hollow of 460–480 nm; interlayer hollow of 8–9 nm)
			(in the absence of heating during sol–gel)	IC (G)	Double-layered tubules (outer/inner diameter of 600/340 nm; 90–100 nm interlayer hollow)
			(80 °C/2 days heating during sol–gel)	IC (G)	Vesicular structures
	79a	1-butanol	A or B (soft)/bzlNH$_2$ (soft B) or Et$_4$NOH (strong B)/--/C (500 °C)	IC (G)	Moderate heating conditions: similar helical ribbons and tubular structures
O44$_{28}$, **O44$_m$**	79b	propionic acid	A (soft)/propionic acid (soft A)/--/C (500 °C)	IC (G)	Tubular structures (400–500 nm) with "roll-paper-like" multilayered walls
O45$_n$	81	1-BuOH (or aniline)	B /benzylamine (soft) or Et$_4$NOH (strong)/--/C (500 °C)	IC (G)	n = 3 or 5: hollow (tubular) nanofibers with inner and outer φ of 15–40 nm (n = 3) or 50–150 nm (n = 5); (n = 2 or 4): "rolled-paper-like" structure (inner φ of 380–400 nm; wall thickness of 40–60 nm)
		1-BuOH	B (soft) /benzylamine/Ni(NO$_3$)$_2$ or Pd(NO$_3$)$_2$/C (500 °C)	IC (G)	n = 2 or 3: homologue hybrid structures with embedded metal nanoparticles (Ni: < 1 nm; Pd: 1–2 nm)
O46$_2$	82	1-octanol	B (soft) /benzylamine/--/C (500 °C)	IC (G)	Helical nanotubes (30-nm-thick; few μm length) with well-defined and monodisperse inner hollows (7.5 nm)
O48	84, 86	HOAc	A (soft)/self-catalyzed/ water/C (500 °C)	IC (G)	Hollow, thin tubules (inner/outer φ of 4–5/30–70 nm; a few μm length)
	86	HOAc	A/self-catalyzed + TFA/water/C (500 °C)	IC (G)	Well-defined and thinner hollow fibers (20–30-nm-thick; inner φ: 4–5 nm)
O49(H$^+$)	86	HOAc	A/self-catalyzed + TFA/water/C (500 °C)	IC (G)	Well-defined hollow nanofibers (50–70-nm-thick; inner φ: 4–5 nm)
O50	87	1-BuOH	B (soft)/self-catalyzed/ water (trace)/C (500 °C)	IC (G)	Hollow nanofibers (inner φ of 5–15 nm; wall thickness of 60–120 nm); some granular silica only if adding benzylamine
O51+**O52** (1:1)	87	1-BuOH	B (soft) /benzylamine or hydrazine/water (trace)/C (500 °C)	IC (G)	Hollow nanofibers + some granular silica; granular without catalysts
O53	89		B (soft) /benzylamine/ water (trace)/W (EtOH; without gelator elimination); A: moderate rate of sol–gel; B: low rate of sol–gel (fast cooling); C: faster rate of sol–gel (heating)	IC (G)	Hollow fibers (gelator-containing); A: 20–30-nm-thick, inner φ of 15 nm; B: inner φ of 5–15 nm; C: 40–100-nm-thick and inner φ of 15–45 nm
O56	96	EtOH	A/HBr/--/(CH_2Cl_2 removal, vacuum) + C (500 °C)	IC (P)	Hybrid (silicified gelator) helical tubules and ribbons (diam., lengths, and wall thickness of 0.5–1.5 μm, > 5 μm, and 50–150 nm, respectively); multilayered walls (4.5 nm spacing)

[a] *Synthesis conditions*: pH (A = acid; B = basic), catalyst (employed acid or basic catalyst); additives (metal salts, water, cosolvents, cogelators, . . .); washed−calcined [W(S) = washed with indicated solvent S, C (T °C) = calcined at T °C]. [b] *Template strategy*: IC (G) = in situ coassembly and sol–gel polycondensation (pathway 1; Figure 2) with organogel formation, IC (P) = in situ coassembly (and condensation) with precipitate formation, PT = organogel self-assembly (pathway 2) followed by post-transcription (pathway 3: impregnation or diffusion subsequent to organogel formation). [c] Silica morphology: ϕ (or φ) is the average diameter in the indicated units.

controlling the formation of silica nanotubes (Figures 3c and e) with different outer and inner diameters (see templating strategies in section 3.2).[41]

As it may be appreciated in Table 2 and in the selected images of Figure 3, a wide variety of silica fibrous nanostructures with high aspect ratios have been templated through organogel assemblies (with diameters ranging from the nano- to the microscale). In some cases, such as with **O13**$_{c-e}$[43] or with **O44**$_{30}$ (see Figure 3k), different morphologies form simultaneously (helical bundles, nanoribbons, and nanotubes), since the transcription may involve the formation of different intermediate metastable phases. Generally, as the result of an efficient transcription of fibrous organogels, the silica replicas present predominantly hollow or **tubular morphologies** (**exogenous templating**); see for instance Figure 3c–f,h,j–l.

However, **nonhollow** (but often mesoporous) structures may also be obtained, such as fibers or fibrous bundles (i.e., with **O1**, **O2**, **O8**, or **O13**$_{f}$), helical bundles (i.e., **O33**−**O35**), ribbons (i.e., with **O2**, **O8**, **O9**, or **O44**), or rodlike wires (i.e., with **O14**), and in some cases curved-lamellar or sheetlike morphologies are also formed. Noteworthy is that, when the employed organogel template is built with tubular (or also curved-lamellar) structures, silica transcription can take place on both the internal and external surfaces (**endogenous** and **exogenous** templating), giving rise to "rolled-paper-like", double- or multilayered tubular morphologies (i.e., with **O40**, **O41**, **O44**, **O45**, and **O56**; see, i.e., Figure 3h,j–l), or even to *"lotus-shaped"* tubular silica (**O22** or **O53**; Figure 3f). Recently, organosilica nanofibers have also been templated exclusively in the internal (helical) cavities (**endogenous templating**) of a naturally occurring polysaccharide gelator (**O32**, see section 5.1).[65]

Highly remarkable is that the **chiral morphologies** exhibited by most of the organogel templates (helical or twisted fibers, ribbons, etc.; see Table 1) may be efficiently transcribed into silica[72] (i.e., with **O4** + **O5**, **O8**, **O11**$_{c}$, **O13**, **O17**, **O18**, **O19**, **O26** + **O27**, **O33**, **O37** + **O38**, **O44**$_{30}$, and **O46**$_{2}$ derivatives) allowing the tailor synthesis of left- or right-handed (Figure 3a,b), single- (Figure 3a), double- (3b, 3i-left), or multistranded helical (twisted, or even coiled—Figure 3i, left) silica nano-objects (fibers, ribbons, tubes, or tapes), and even of silica with inner helicity[82] (**O11**$_{a}$, **O11**$_{b}$, **O13**, **O17**–**O19**, **O46**$_{2}$; see, for example, inner helices in Figure 3a,e). Noteworthy is that the transcription of chirality is not always attained by a simple or direct (one-step) replication process, but it often takes place through a more complex (multistep) **hierarchical coassembly process**, involving the in situ formation of different transient morphologies (associated with the condensing silica oligomers) with gradually increased complexity at different length scales. This is the case, for instance, of helical silicas obtained with gelators **O8** (single-strand fibers associate into double-helical or loosely coiled nanofibers; Figure 3i),[36b] **O13**$_{c-e}$ (helical nanobundles are constructed from gathered nanotubes; see diagram in Figure 5, later in section 3.2),[43] **O13**$_{f}$ (helical single strands—a few nanometers thick—self-assemble into multiple-strand fibers—50-nm-thick—which in turn associate into helical bundles—300-nm-thick—to finally give thicker helical nanofibers).[44] In some cases, **chirality can be lost** in any of the intermediate coassembly steps. When using the valine derivative **O11**$_{a}$ as a template, for instance, single helical fibers associate into nanotubes during silica sol–gel polymerization, and the gathering of these nanotubes (with inner helicity) results in nanofibers which further aggregate into nonhelical fibrous bundles.[38a]

As may also be noticed in Table 2, an accurate design of reaction conditions (type of solvent, acid or basic conditions, type of catalyst, use of cosolvent and other additives, sol–gel heating and aging conditions, and so on) becomes of paramount importance, since many different morphologies can be obtained with the same gelator template by adjusting any of these synthesis variables. The simple modification of the **gelator concentration** can be used in most cases to control the morphology or textural features. For instance, when using gelator **O25** as a template, the diameter size of the transcribed silica nanotubes was tuned by varying the gelator concentration (inner diameter of 20–25 nm and 450–600 nm for gelator concentrations of 0.1 and 3 wt %, respectively). In other cases, **many different variables** must be considered simultaneously. For instance, silica having different helical (fibrous, ribbonlike, or tubular) morphologies are formed through the use of the L-isoleucine derivative **O8** by selecting the appropriate solvents and the amount of basic catalyst (see series in Figure 3i).[36a,b] As another illustrative example, different silica morphologies (platelike, fibrous, or tubular) were templated through the use of **O3** organogels (tetra-alkyl phosphonium salts) in different solvents [EtOH, benzene, tetrahydrofuran (THF), and dimethyl sulfoxide (DMSO)] using acid (HCl or acetic acid) or base (NH_4OH or benzylamine) catalysis, and under hydrolytic or nonhydrolytic conditions.[24] The transcription of fibrous tubular morphologies was more effective in an aprotic solvent of relatively low polarity such as benzene than in the protic and polar EtOH. Moreover, the silica fibers were slightly thinner under acid-catalyzed (acetic acid) than under basic-catalyzed (benzylamine) conditions. The importance of solvent−gelator interactions may also be illustrated with gelator **O23**, leading to the transcription of tubular silica in EtOH and to hollow spheres of silica in water, or more recently with gelator **O14** (tubular, rodlike, spherical, or rolledlike silicas).[45b]

In the case of gelators bearing moieties that are sensitive to pH conditions, the adjustment of **acid or basic conditions** enables also a tuning of the resulting morphologies. The pyridine derivative **O11**$_{b}$, for instance (see series in Figure 3g), yields very thin nanofibrils (20–40-nm-thick) at more acidic pH values (ca. 3 and 4), while thicker flatlike fibers (100–250 nm), ribbonlike bundles (250–1000 μm), and finally thicker fibrous (ribbon-like) bundles are gradually formed when increasing the apparent pH (from 5 to 8).[41] In this respect, the choice of the catalyst also becomes crucial in most cases. In the case of gelator **O30**, for instance, the addition of a catalyst (benzylamine) with the ability to interact with gelator molecules decisively results in the transcription of silica nanotubes (instead of granular silica). In other cases, as occurs with gelator **O50**, the catalytic moiety (also benzylamine) is already covalently linked to

the gelator scaffold, and this enabled for the first time efficient transcription into fibrous silica in the absence of an externally added solution catalyst.

Finally, in some gelators bearing organic moieties with the ability to act as metal-binding sites (i.e., crown ether-appended cholesterols, or other gelators containing N or O donor sites), the **introduction of cationic charges** through the addition of metal salts (*such as $KClO_4$, $CdClO_4$, $AgNO_3$, or $PdNO_3$*)[74–77] becomes decisive in order to have an efficient transcription into silica (see next section) and also to control the resulting templated morphologies. In some cases, moreover, this approach can afford the transcription of **metal−SiO_2 nanocomposite materials** (with metal nanoparticles—Ni, Pd, Cs, Pd, and Ag—embedded onto the internal or external surfaces of silica nanofibers and nanotubes). For instance, the *benzo-18-crown-6*-containing cholesterol gelator **O39** (capable of binding K^+ cations) could be transcribed into hollow silica fibers only in the presence of a high concentration of K^+ ions (from $KClO_4$), while the addition of other cations (Li^+, Na^+, Rb^+, and Cs^+) led only to granular silica.[73] Similarly, the organogels of the mono-aza-18-crown-6-functionalized gelator **O40** and of the di-aza analogue **O41** were transcribed in the presence of metal (K^+ or Cs^+) ions leading to the formation of "*rolled-paper-like*" silica, although in both cases the transcription was also efficient in the absence of added metal salts.[74] In all of these cases, the presence of the metal species was not evidenced after calcination (see **O41-K^+** in Figure 3l). In contrast, the sol–gel transcription of a butanol organogel of a previously formed **O40·Ag** complex (with $AgNO_3$ in THF) resulted in the first example (Figure 3j) of formation of **metal−silica (Ag-SiO_2) nanofibrous composites** [multilayered tubular silica containing Ag metal nanoparticles (1–5 nm) into the interlayer space].[75] Similarly, in the case of the gelator derivative **O42**, the addition of metal salts (such as $AgNO_3$ and $CsClO_4$) was indispensable in order to have an efficient transcription into silica, enabling the formation of novel (hybrid) metal−silica right-handed spirals (with some additional lamellar silica in the case of $CsClO_4$).[76] The chelating properties of crown-ether moieties have also been recently exploited to transcribe Ag-SiO_2 hybrid nanotubes using the sugar-appended crown-ether gelator **O36** as a template.[69] Similarly, the incorporation of metal species into the organogel phase may also be accomplished through coordinating interactions with gelators containing amide moieties (as metal-binding sites), as is the case of gelator **$O45_n$** which contains a neutral diamine moiety. Helical **Ni-SiO_2** and **Pd-SiO_2** nanocomposite materials have been transcribed with this gelator.[81]

More recently, 1-D aggregates of a simple *ammonium tartrate* (long crystals formed through intermolecular H bonding) in an EtOH/H_2O mixture (at pH = 11 by exposure to ammonia vapors) have also been used as templates to direct the growth of facetted hollow silica tubes, and metal (Ag and Au) nanoparticles (NP) were anchored in one step (in situ coassembly) to produce hybrid (Au/Ag) NP-SiO_2 nanocomposites.[112]

3.1.B. Nonsiliceous Metal Oxide Fibrous Materials. On the other hand, **nonsilica-based metal oxide nanofibrous materials** have also been templated through the use of organogels. Relevant information about the morphologies, textures, and synthesis conditions are shown in Table 3, which summarizes the different nonsiliceous oxide- and nonoxide-based nanofibrous morphologies templated with organogels (also with some hydrogels), including relevant information about morphology and dimensions, the employed organogelator and solvent, synthesis conditions, and templating strategy. Some SEM or TEM images of a selection of these materials (Al, Ti, V, Ta, and Ti−Zr oxide-based) are shown in Figure 4.

As may be appreciated, the use of different organogel templates (**O1**, **O10**, **$O11_{d,e}$**, **O16**, **O20**, **$O44_{30}$**, **O47**, and **O49-H^+** compounds) has enabled the successful transcription of a wide variety of metal oxide materials (Al_2O_3, TiO_2, ZrO_2, ZnO, Ta_2O_5, WO_3, and V oxo-based) exhibiting different fibrous morphologies, such as fibers or (mesoporous) fibrous bundles (Al[20] and Ti[35,85] oxides), hollow tubes (Ti,[37,38b,c,40b,48,52a] Ta,[38c] Zr,[48] Zn,[48] and W[48] oxides), left-handed or right-handed tubes (Ti, Ta, and V oxides),[52b] hollow helical ribbons (Ti),[80] and double-layered (or double-walled) tubular structures (Ti,[80,83] Zr,[83] and Ta[83] oxides). Although the polymerization reactions (or precipitation) with these metals progress more rapidly and are less easy to control than in the case of silica species, in most cases, the transcription has been carried out through the use of an in situ **coassembly** process (*IC(G)* or *IC(P)*), in the presence of the appropriate solvent, a basic (amine or NH_4OH) or acidic (HCl or HOAc) catalyst, and the corresponding inorganic salts (chlorides, oxychlorides, or acetates) or metal−organic (alkoxide) precursors. In the case of titania transcription, the in situ procedure resulted, in some cases (**O20**),[52] in the formation of a precipitate (IC(P)) instead of an organogel (IC(G)). Differently, the transcription of Ti, Zr, and Ta oxides with gelator **O47** was performed, rather, through a **post-transcription** strategy (*PT*), since the metal−organic precursors (alkoxides) were added onto a preassembled (previously cooled) organogel phase, and without the addition of any external catalyst.[83] Very interestingly, the same post-transcription procedure was applied with a mixture of Zr and Ti precursors, enabling the template growth of hollow microtubules (400–450-nm-thick; inner hollow of ca. 300 nm) of **binary transition metal** (Ti + Zr) **mixed oxides**.[83]

Alternatively, in the transcription of Ti, Zr, and Zn single oxides using the gelator compound **O16** (tripodal bile acid derivative), an inorganic gel consisting of partially condensed species (catalyzed with acetic acid or with KOH) was formed as a previous step and was then subsequently mixed with the organogel hot solution, following the formation of the "physical" organogel (**IC(G)***** strategy in Table 3).[48]

The extension of this approach to the design of any other (multicationic) oxide-based system would draw tremendous interest due to the improved and diverse optical, electrical, or magnetic properties associated with transition metal mixed oxides.

3.2. Templating Mechanisms. Different templating mechanisms or pathways have been proposed to explain the

Table 3. Summary of Different Nonsiliceous Oxide- And Nonoxide-Based Nanofibrous Materials Templated with Organogels (and Also with Some hydrogel Systems), Including Relevant Information about Morphology and Dimensions, Employed organogelator and Solvent, Synthesis Conditions, Templating Strategy, and Corresponding References

material type	morphology (dimensions)[a]	organogel./solvent	synthesis conditions[b] (precursors/pH/catalyst/addit./calcine or washing)	strategy[c]	ref
Oxides					
Al_2O_3- based	Entangled fibrous bundles (200–500-nm-thick) of thinner hollow nanofibers (φ_{ex} = 15–30 nm; φ_{in} = 4–10 nm;)	**O1**/EtOH	$AlCl_3$ /(<1) /---/---/350–800 °C	IC(G)	20
	Fibrous bundles (300–500-nm-thick; more elongated and coaligned)	**O1**/EtOH	$AlCl_3$/ca. 2/$(Et)_3N$ (TEA)/---/350 °C	IC(G)	20
TiO_2	Entangled fibers (200–1200-nm-thick) of thinner nanofilaments (15–150 nm thick) based on anatase + rutile nanocrystals (15–30 nm)	**O7**/EtOH	$Ti(OiPr)_4$/acid/HCl/---/450 °C	IC(G)	35
	Nanotubes (300–600-nm-thick) Nanotubes (150–200-nm-thick) Nanotubes (30–50-nm-thick)	**O10**/EtOH **O10**/BuOH **O10**/dioxane	$Ti(OiPr)_4$/basic/ propylamine/--/W ($CHCl_3$ or BuOH) + C (500 °C)	IC(G)	37
	Morphologies depend on **O12$_3$** conc.: spherical (<10 g/L), rodlike coaxial bundles (15 g/L), bulk aggregates or bloks of aligned fibers 100-nm-thick (25 g/L), bulk particles + fibers (50 g/L); anatase-based tubes form after calcine (with 15 g/L)	**O12$_3$**/BuOH	$Ti(Obut)_4$/--/--/--/C (400 °C)	IC(G)	40b
	Nanotubes (10–20-nm-thick; inner channels: 4–7 nm; a few hundred nm in length) based on anatase	**O16**/H_2O/EtOH	$Ti(Obut)_4$/acid/CH_3COOH)/--/ W (EtOH) + C (500 °C)	IC(G)[(*)]	48
	Hollow tubes (150–600-nm-thick; inner hollow: 50–300 nm; max. length: 200 μm) based on anatase	**O20R** (PF_6^-)/EtOH	$Ti(OiPr)_4$/basic/NH_4OH/--/C (450 °C)	IC(P)	52a
	Left-handed (**O20-R**) or right-handed (**O20-S**) helical tubes (200–900-nm-thick; several μm length)	**O20-R** or **-S** (ClO_4^-)/ EtOH	$Ti(OiPr)_4$/basic/NH_4OH/--/W (CH_3CN) + C (450 °C)	IC(P)	52b
	Hollow helical ribbons and double-layered nanotubes (ca. 560-nm-thick; inner hollow: 500 nm; interlayer hollow: 8–9 nm)	**O44$_{30}$**/Hac/H_2O	$Ti(OiPr)_4$/--/bzlNH_2 (B)/--/C (500 °C)	IC(G)	80
	Thick and aggregated fibrouslike structures (ca. 100-nm-thick)	**O49**(H^+)/CH_3CO_2H (+ TFA)	$Ti(Obut)_4$/acid/HOAc + TFA/--/W or C (unclear)	IC(G)	85
ZrO_2	Nanotubes (ca. 25-nm-thick; inner φ of 4–7 nm; few hundreds of nm in length) of monoc. + tetrag. + cubic phases (+ spherelike particles)	**O16**/H_2O/Hac	$ZrOCl_2$/base + acid/NH_3+ HOAc/--/W (EtOH) + C (500 °C)	IC(G)[(*)]	48
ZnO	Nanotubes (30–60-nm-thick; inner φ of ca. 20 nm; several hundreds of nm in length) of hexagonal phase	**O16** /H_2O/EtOH/HOAc	$ZnAc_2$/base + acid/KOH + HAc/--/W (EtOH) + C (500 °C)	IC(G)[(*)]	48
WO_3	Nanotubes or bundles of nanotubes (ca. 40-nm-thick; inner φ of ca. 5 nm; a few of hundreds of nm in length) of monoclinic phase	**O16**/H_2O/HOAc	tungstic acid/acid/HAc/--/W (EtOH) + C (500 °C)	IC(G)	48
TiO_2 and Ta_2O_5	$O11_d$: Hollow nanotubes with average outer ϕ of 360 nm (TiO_2) and 365 nm (Ta_2O_5) and inner ϕ of ca. 20–150 nm; $O11_e$: Hollow nanotubes with aver. outer ϕ of 210 (TiO_2) and 240 nm (Ta_2O_5)	$O11_{d-e}$/EtOH/H_2O	$Ti(OiPr)_4$ or $Ta(OEt)_5$/basic/NH_3/--/W(CH_3CN) + C (500 °C)	IC(G)	38b,c
Ta and V oxides	Left-handed (**O20-R**) or right-handed (**O20-S**) helical tubes; sizes (with Ta): 100–600 nm thick; inner hollow: 30–180 nm; max. length: 30 μm; amorphous	**O20-R** or **-S** (ClO_4^-)/ EtOH	$Ta(OC_2H_5)_4$ or $OV[OCH(CH_3)_2]_3$/basic/NH_4OH/--/W (CH_3CN) + C (450 °C)	IC(G)	52b
TiO_2, ZrO_2, and Ta_2O_5	Double-walled tubules (560-nm-thick; inner hollow: 460 nm; interlayer hollow: 50 nm; several hundred μm in length (TiO_2 anatase phase (T < 800 °C); Ta and Zr: not characterized)	**O47**/CH_3CN + water	$Ti(OiPr)_4$, $Zr(Obu)_4$, or $Ta_2(Obu)_5$/noncatalyzed/ --/--/C (500 °C)	PT	83
mixed TiO_2/ZrO_2	Binary metal oxide microtubules (400–450-nm-thick; inner hollow: ca. 300 nm; several μm in length (crystallinity not characterized)	**O47**/CH_3CN + water	$Ti(OiPr)_4$ and $Zr(Obu)_4$ (3:1 and 5:1 wt %)/ noncatalyzed/--/--/C (500 °C)	PT	83

Table 3. Continued

material type	morphology (dimensions)[a]	organogel./solvent	synthesis conditions[b] (precursors/pH/catalyst/addit./calcine or washing)	strategy[c]	ref
Metals					
Ag	Double- (short exposure, 17 h) and multiwall (longer exposure, 30 h) nanotubes (ca. 50-nm-thick; interlayer: 3 nm)	**O6$_a$** /water−EtOH	$AgNO_3$ (aq.)/--/--/UV + daylight exposure (17–30 h)/--	PT	29
	Left- and right-handed nanohelices (width: 100–200 nm; pitch: ca. 2.8 μm) of Ag nanoparticles (1–10 nm)	**O15**/$CHCl_3$	$AgNO_3$ (aq.)/--/--/$NaBH_4$ (reducing agent)W (EtOH)	PT	46
Au	Nanoparticles (3–10 nm) confined in the hollow cavities of gelator nanotubes	**O28**/water	$HAuCl_4$ (aq.)/--/--/UV photoirradiation/--	PT	60
	Discrete nanoparticles "decorating" the surface of gelator helical tubes without (in situ) or with regular helical pattern (post-transcription)	**O56**/EtOH−water	$HAuCl_4$ (aq.)/--/--/--/--	PT/IC(G)	95
Ni, Cu	Thin metal coatings onto gelator tubules	**O6$_b$** /citric acid−citrate buffer	$NiCl_2 \cdot 6H_2O$ or $CuCl_2 \cdot 2H_2O$/6/cit. acid-citrate/reducing agents: hypophosphite (Ni), dimethylaminoborane (Cu)/---	PT	31
	Thin metal coatings onto gelator tubules	**O56**/--	---	PT	92
Calchogenides					
CdS	Pearl-necklace (50–150-nm-thick; 24 h exposure) or netlike (200–250-nm-thick; 72 h exposure) nanofibrous structure	**O29**/H_2O	$Cd(NO_3)_2$ (aq.)/--/--/EtOH (cosolvent), H_2S (S source)/ unwashed (but suspended in $CHCl_3$)	IC(G) + PT(H_2S)	61
	Necklace fibrous structures (spheres linked) forming necklace tubules (180–300-nm-thick; inner diameter of 30–80 nm) of hexag. (polycryst.) CdS	**O31**/water−EtOH (20:1 v/v)	$Cd(OAc)_2$/--/--/H_2S (S source)/W (water; without gelator removal)	IC(G) + PT(H_2S)	64
	Pearl-necklace tubular nanofibers (60-nm-thick; inner diameter of 4–6 nm) of wormlike porous CdS (cubic) nanoparticles network	**O54**/EtOH	$Cd(OAc)_2$/--/--/1-BuOH (cosolvent), H_2S (S source)/W ($CHCl_3$)	IC(G) + PT(H_2S)	90
	Coiled helices (from 25- to 100-nm-thick; helical pitch ca. 40–50 nm) of polycrystalline (4–8-nm-grained) CuS (zinc blende structure)	**O57**/2-ethylhexyl methacrylate	$Cd(NO_3)_2$/--/--/THF (Cd solvent), H_2S (S source)/W (THF)	IC(G) + PT(H_2S)	98
	Similar coiled helices (as above), but with a 60 nm pitch	**O57**/ethyl-methacrylate (suspension)	*idem.*, but templating in nongelled suspension of gelator	IC(susp.) + PT(H_2S)	
CuS	With H_2S(g) and thioacetamide sources: bending helical nanofibers (40–100-nm-thick; inner diameter of 4–6 nm) with pitches of 100–200 (H_2S) or 50 nm (thioacetamide) of hexagonal CuS	**O55**/benzene-1-BuOH	$Cu(OAc)_2$/--/--/EtOH (solvent for Cu and S sources), thioacetamide or H_2S (S sources)/ unwashed (but suspended in EtOH)	IC(G) or IC(G) + PT(H_2S)	91
	With H_2S(g): straight nanofibers (40–100-nm-thick; inner diameter of 4–6 nm); hexagonal CuS; with thioacetamide: bending helical nanofibers with pitches of 50 nm (also hexagonal CuS)	**O55**/butyl acetate	*idem*	*idem*	91
NiS	Well-formed, smooth-surfaced and thin nanotubes (35–100-nm-thick; inner diameter of 15–35 nm)	**O31**/water−EtOH (20:1 v/v)	$Ni(OAc)_2$/--/--/H_2S (S source)/W (water; without gelator removal)	IC(G) + PT(H_2S)	64
Sulphates					
$ZnSO_4$	Nanotubes (10–12-nm-thick; inner φ of ca. 4 nm; from 200 to 300 nm to several hundreds of nm in length) of orthorhombic phase	**O16** /H_2O/HOAc	$ZnSO_4$ (H_2O + NH_3)/basic + acid/NH_3 + CH_3COOH/--/ W(EtOH) + C (500 °C)	IC(G)	48
$BaSO_4$	Nanotubes (small aspect ratio: ca. 100-nm-thick; inner φ of ca. 9 nm; 250–350 nm in length)	**O16** /H_2O/HOAc	$BaCl_2$ (aq.)/acid/CH_3COOH/$(NH_4)_2SO_4$/W (EtOH) + C (500 °C)	IC(G)	48
Other					
$Ca_{10}(PO_4)_6(OH)_2$	Hybrid gelator nanofibers (15–20-nm-thick) mineralized (covered) with polycrystalline hydroxy-apatite, HA ($Ca_{10}(PO_4)_6(OH)_2$)	**O58**/H_2O	$CaCl_2$, Na_2HPO_4 /acid/HCl (vap)/ aqueous I_2 (oxidant)/unwashed	PT	99

[a] *Morphology dimensions*: ϕ (or φ) is the average diameter in the indicated units. [b] *Synthesis conditions:* Precursors (inorganic precursors), pH (acidic or basic), catalyst (employed acid or basic catalyst); additives (water, cosolvents, and cogelators); calcine [maximum temperature (°C) with or without previous washing] or washing (W) treatment. [c] *Templating strategy:* IC(G) = in situ coassembly with organogel formation (pathway 1, Figure 2); IC(G)$^{(*)}$ = formation of an inorganic gel with partially condensed species, followed by mixture with organogel sol and subsequent organic gel formation. IC(P) = in situ coassembly with precipitate formation; PT = organogel self-assembly (pathway 2) followed by post-transcription (pathway 3: impregnation with, or diffusion of, metal salt or gas precursors).

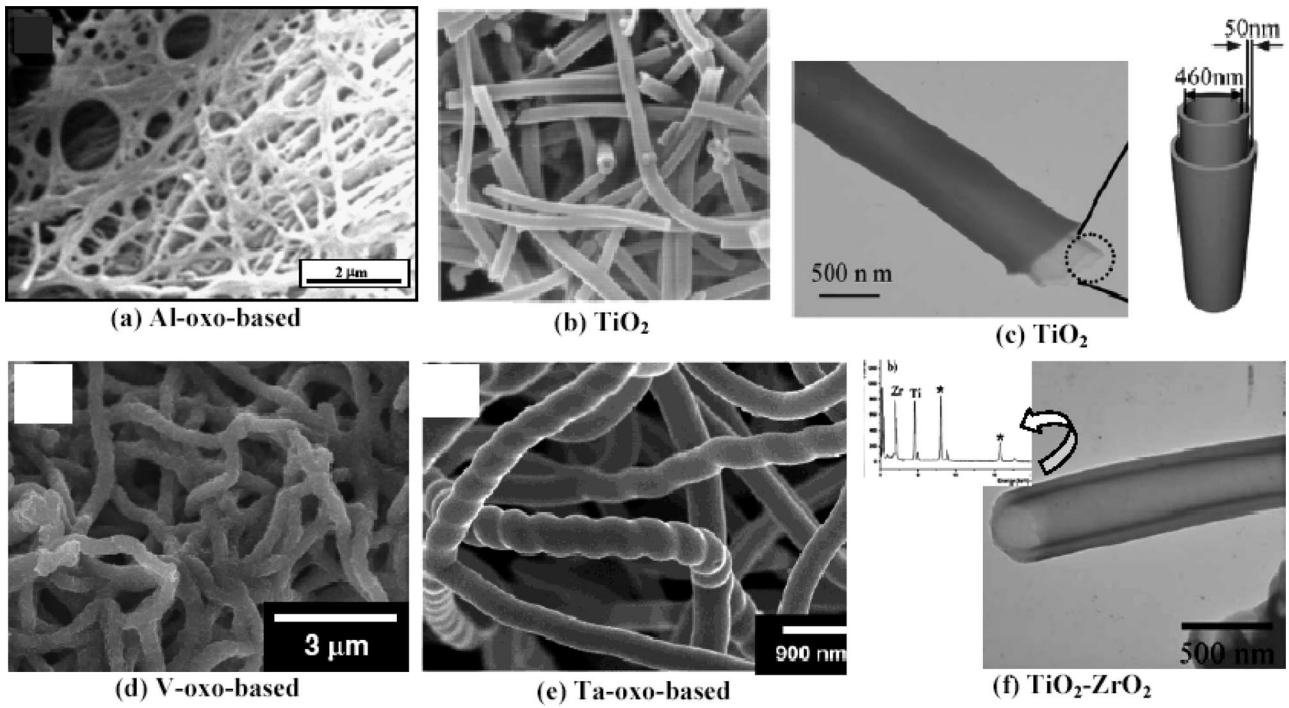

Figure 4. Selected SEM or TEM images of different organogelator-templated nonsiliceous oxide-based nanofibrous morphologies (all after calcination, except the V-oxo-based material): (**a**) **alumina-based** fibrous network templated with O1 (ref 20), (**b**) hollow tube of **TiO_2** templated with O20R/PF_6^- (ref 52a), (**c**) double-walled tube of **TiO_2** templated with O47 (ref 83), (**d** and **e**) **V-** and **Ta-oxo-based** right-handed helical nanotubes, respectively, templated with O20S/ClO_4^- (ref 52b), and (**f**) double-walled tube of **mixed TiO_2−ZrO_2** (EDAX analysis in the inset) templated with O47 (ref 83). Adapted with permission from refs 20, 52a, and 52b (Copyright 2000 and 2002 American Chemical Society) and from ref 83 (Copyright 2005 The Royal Society of Chemistry).

efficient transcription of the nanofibrous morphologies from the organogels to the inorganic replicas (see a general scheme in Figure 5).

The relevant parameters involved in the transcription through organogel templates have been most extensively studied in the case of silica-based nanofibers, and different mechanisms have been proposed in the literature,[12a–c] after the first evidence of the important role played by cationic charges in the transcription process emerged.[5] Material transcription through organogel templates must be understood as the result of a balanced equilibrium among different competitive and cooperative events, which depend on different and interrelated variables.

3.2.A. Silica Templating. In an overall analysis (see general scheme in Figure 5), the relevant aspects that should be taken into account for an efficient transcription and tailored design of silica-based replicas could be categorized at four different levels:

(I) *Selection of the Templating Strategy*. Control of the morphology by performing either an *in situ coassembly* or a *post-transcription* procedure, and also through the selection of a gelator system (gelator, solvent, and additives) that enables endogenous or exogenous templating (or both of them)

(II) *Control of Supramolecular Interactions and Synthesis Conditions*. Morphology control through a careful design of the key interactions among gelator and inorganic (or hybrid) species enabling an efficient transcription, and also by selecting the appropriate sol–gel synthesis conditions, which are interdependent

(III) *Control of the Mechanistic and/or Transcription Pathways*. Control the relative predominance and temporal sequence of silica condensation through a *surface propagation* or a *solution (or bulk) propagation* pathway, and also through the associated possible occurrence of *hierarchical* (multistep) *coassembly processes*

(IV) *Control of Post-Templating Variables.* Final morphology control by adjusting important variables after the templating or coassembly process, such as the aging conditions and the protocol followed for the drying and removal of the organogel template.

All of these variables must be considered all at once, and herein we comment upon some important aspects and provide some examples for each level.

First Level (I). As an important preliminary consideration, the transcribed morphologies may be very different by using either an "in situ coassembly" (IC) or a "post-transcription" (PT) or post-diffusion methodology.[41] In the first case (IC), the transcription takes place through a synergistic (cooperative) coassembly process (the in situ forming organogel fibrils direct the growth of nanofibrous silica, and *vice versa*, the condensing silicate species affects the way the gelator molecules and the organogel fibrils self-assemble). In the second case (PT), however, the fibrous organogel is previously self-assembled (and therefore its morphology can be separately engineered prior to the addition of the inorganic (or hybrid) precursors, being rather a more simple or direct transcription). This post-diffusion route may be useful for complex systems (i.e. multimetallic) in which the use of the "in situ" procedure can be difficult (insolubility of precursors, incompatibility between pH/catalyst conditions and the

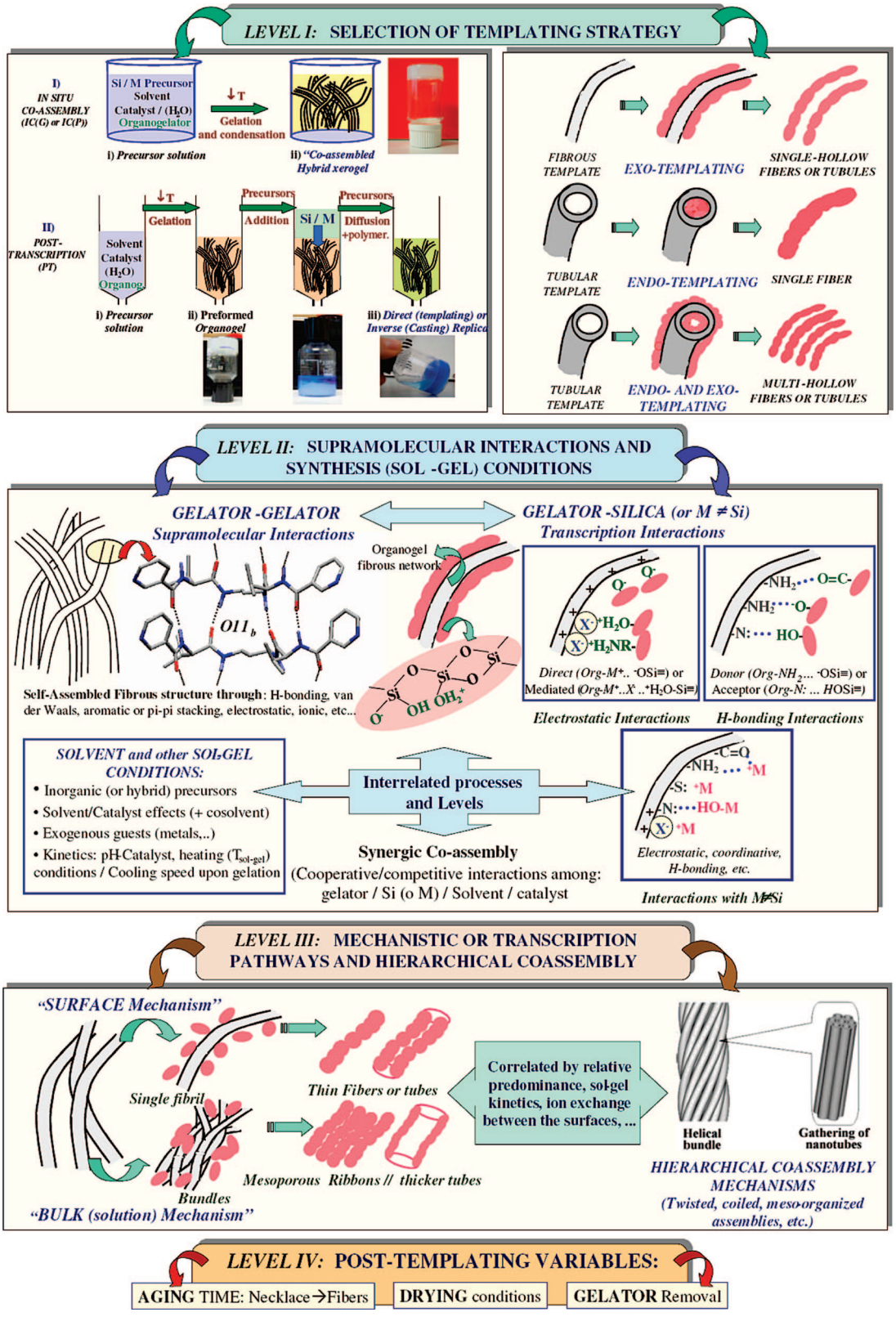

Figure 5. General scheme including the main strategies, mechanisms (transcription pathways), and processes for the template synthesis of oxide-based nanofibrous materials. Transcription can be controlled at four different levels (I → IV). The molecular structure shown in Level II (left) and the diagram shown in Level III (right) have been adapted with permission from refs 41 and 43. Copyright 2006 The Royal Society of Chemistry and 2005 The Chemical Society of Japan.

organogelation process, etc.). Also in this level, by selecting the appropriate gelator/solvent system, the morphology (and surfaces' philicity) of the self-assembled organogel (SAFIN) may enable the confinement of transcription regions on either the outer (**exogenous templating**) or inner surfaces (**endogenous templating**), or on both of them. Examples of the three possibilities have been described in previous sections (and a simplified diagram is shown in Figure 5 top-right).

Second Level (II). Once the templating strategy has been selected, the efficient transcription depends mainly of the

existence of "favorable" **supramolecular interactions** among the gelator molecules and the condensing inorganic species (silica oligomers). These interactions may be essentially electrostatic (among negatively charged silicate species—above the isoelectronic point of silica, at a pH of ca. 2—and positively charged gelators) or hydrogen-bonding interactions (between H-donating amine moieties and negatively charged silicate species). Therefore, the existence of favorable supramolecular (gelator−silicate) interactions can be engineered at the molecular level through the selection of an organogelator with the appropriate structural features (or moieties) to enable these electrostatic or H-bonding interactions. However, a careful design of the **sol–gel synthesis conditions** is also needed, since these sol–gel conditions not only affect the kinetics of the polymerization reactions (decisive on the third level) but also influence the supramolecular interactions among gelator and silicate species, and the competitive gelator/solvent and silicate/solvent interactions.

Considering first the structural features of gelators enabling transcription,[12a–c] the efficient templating of nanofibrous silica has been accomplished using organogelators containing either **cationic charges** or **H-donating groups**, or both of them. The importance of the cationic charges in silica transcription was confirmed with the first successful transcription (by Shinkai et al.)[5] through the use of mixtures of the neutral gelator **O37** with the cationic gelator **O38**.[72] In this case, the cationic charge is **covalently attached** to the gelator scaffold through the quaternary ammonium moiety (**Org**−$\mathbf{NR_2H^+\cdots{}^-O}$−**Si**≡). Transcription through covalently attached cationic charged moieties was also attained when using mixtures (with the appropriate ratios) of cationic and neutral cyclohexane diamide or bis-urea derivatives (**O18** + **O17** and **O18** + **O19**),[51] and also in the transcription of titania nanotubes with the cationic bisurea derivatives **O2O** (R or S).[52b] A further confirmation of the importance of cationic charges was obtained (by Ono and co-workers) when using benzo- or aza-crown-ether cholesteric gelators (**O39–O43**).[73–77] In these cases, as discussed in the previous section, externally added cationic charges may be incorporated in a **noncovalent manner** to the gelator scaffold through complexation by the crown moieties, and therefore these gelators enabled the transcription into silica in the presence of some metal salts (**Org**·$\mathbf{M^+\cdots{}^-O}$−**Si**≡). Moreover, in some cases (gelators **O41**−**O43**), the transcription was also possible in the absence of added metal species, since the **protonated N atoms** were also found to be efficient transcription directors. The existence of protonable amine moieties may behave therefore as "latent" covalently bonded cationic centers, enabling the transcription of silica under appropriate acidic conditions, as was also observed with the gelator **O44**.

On the other hand, transcription through **H-bonding interactions** was first observed with the cholesteric diamine gelator $\mathbf{O45}_n$.[81] This result could explain why some of the aza-crown gelators (such as **O41** or **O44**) could also be efficiently transcribed into silica in the absence of metal species and under stronger basic conditions (using Et_4NOH as a catalyst). Under these conditions, the amine centers are not protonated, and therefore H-bonding interactions are the single mechanism enabling transcription (**Org**−$\mathbf{NRH\cdots{}^-O}$−**Si**≡). Therefore, in the different amine-containing gelator derivatives (i.e., in gelators **O6**−**O16**, the cholesterol derivatives previously mentioned, and also in the sugar-based derivatives **O21**−**O24** or the azo form of **O25**), the transcription is enabled mainly through H-bonding interactions, and also through electrostatic interactions when the N atoms are protonated.

Regarding the importance of sol–gel conditions (solvent, catalyst, acid or basic conditions, counterions, additives or exogenous guests, etc.), we comment herein upon only a few examples. Other aspects will be commented upon later in the level III section. As previously mentioned, the **acid- or base-catalyzed** conditions strongly determine the type of supramolecular interactions which are operative. Under very acidic conditions (pH < ca. 2), the silica is protonated, and therefore, the electrostatic interactions with cationic gelators are impeded, unless the mediation or bridging effect of anionic counterions is provided (see the particular effect of templating aminopropyl-silica under strong acidic conditions with gelator **O2** in section 5.1). Under moderate acidic conditions, the silica will be negatively charged while the amine moieties can be partially protonated, enabling transcription mainly via electrostatic forces, but also (depending on pH and the pK_a of the amine moiety) through H-bonding interactions. Under more basic conditions, the amine moieties are no longer protonated, and therefore the transcription is operative only through the H-bonding mechanism.

The selection of the appropriate solvent also becomes crucial in order to modulate the gelator−silica interactions, since these interactions may be affected by competitive silica−solvent and gelator−solvent interactions. An illustrative example can be found in the recent study of Weiss et al. about the transcription of nanofibrous silica through the use of gelator **O3** (phosphonium salts) as a template.[24] In a protic solvent such as EtOH, its ability to form H bonds with silicate species attenuates the silicate−template electrostatic interactions, thus resulting in a less efficient templating of silica (platelike silica is obtained). In contrast, in an aprotic solvent of relatively low polarity such as benzene, the templating was more efficient, leading to fibrous silica. In the same study, the importance of the **counterions** was also proven (using benzene organogels): a higher amount of untemplated (granular) silica was obtained with the harder F^- and ClO_4^- anions (since the phosphonium cations of the gelator molecules are hard Lewis acids, their interactions with the harder F^- and ClO_4^- anions are more favored than with the softer Cl^-, Br^-, or I^- anions, and thus the interaction of silicates with the P^+ centers is more attenuated).

Third Level (III). Upon selection of the gelator and the sol–gel conditions for silica transcription, the supramolecular interactions among gelator, silica, and solvent molecules become established, as do the kinetics of the silica condensation reactions. At this level, there exists a competition between the condensation of silica species in the bulk liquid (*solution mechanism*) and that onto the surface of organogel fibers (*surface mechanism*), which ultimately determines the efficiency of the templating process. In order to attain an

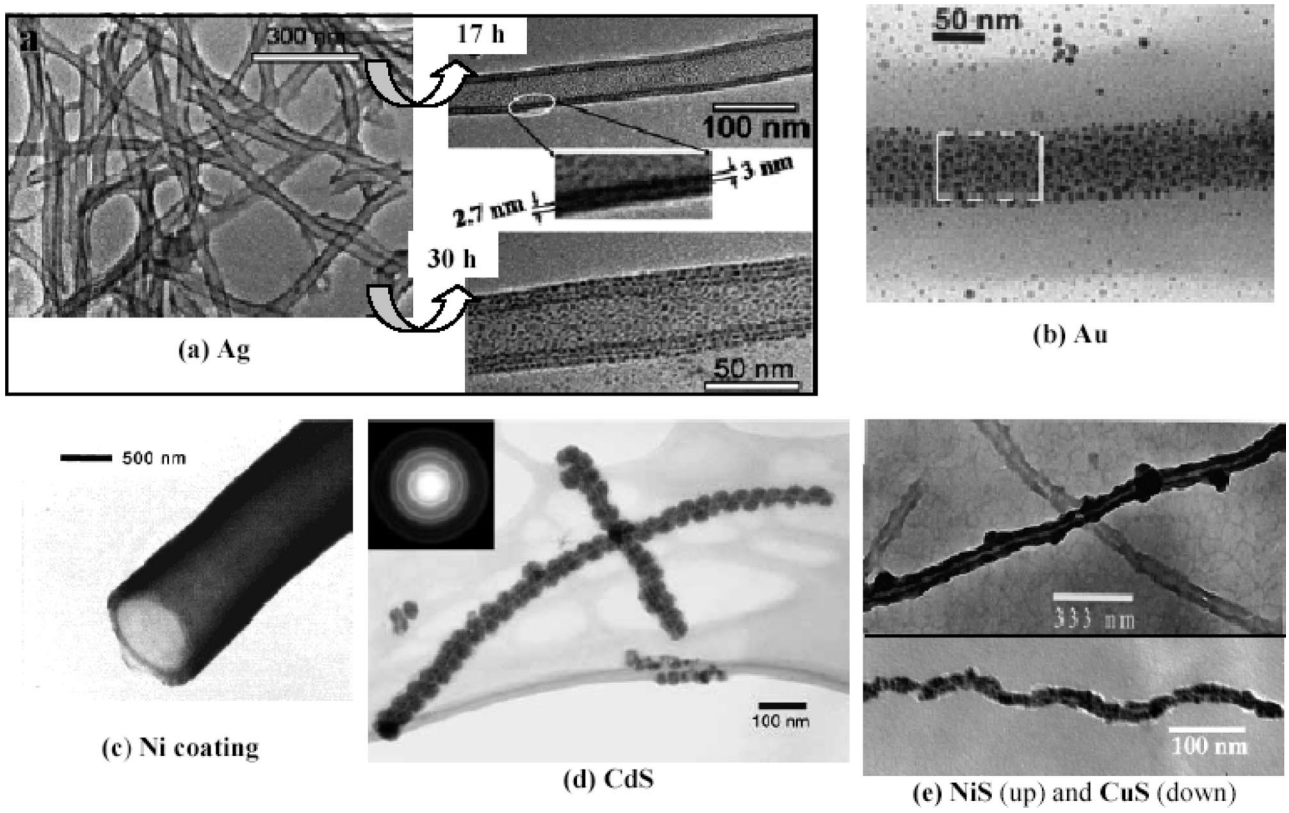

Figure 6. SEM or TEM images of a selection of non-oxide-based nanofibrous morphologies templated through organogels (or hydrogels). *Metals*: (**a**) double- and multiwalled nanotubes of **Ag** prepared with the bolaamphiphile **O6a** (EDGA) after different exposure times (17 and 30 h), respectively (see magnification images right, ref 29), (**b**) confined **Au** nanoparticles into nanotubes of gelator **O28** (ref 60), and (**c**) **Ni** thin coating onto nanotubes of gelator $\mathbf{O6_b}$ (ref 31). *Semiconductor chalcogenides*: (**d**) coiled helix of **CdS** prepared with **O57**/EHMA (ref 98) and (e) **NiS** nanotubes (top; ref 64) and **CuS** bending helical hollow nanofibers (bottom; ref 91) templated with **O31** and **O55** gelator templates, respectively. Reproduced (or adapted) with permission from refs 29, 31, and 91 (Copyright 2000, 2004, and 2006 American Chemical Society), ref 60 (Copyright 2004 The Royal Society of Chemistry), ref 98 (Copyright 2002 Wiley-VCH Verlag GmbH & Co. KgaA), and ref 64 (Copyright 2006 American Scientific Publishers, http://www.aspbs.com).

efficient transcription of silica, the surface mechanism must occur preferentially with respect to the solution mechanism, and this depends simultaneously on the strength of gelator−silica supramolecular interactions, on the kinetics of silica sol–gel condensation, and on the silica−solvent interactions (solvent effects). In the following, the interdependence of these factors will be illustrated with some selected examples.

First, the relative predominance of both (surface and solution) mechanisms is highly dependent on the catalyst conditions. For instance, the combination of gelator **O30** with benzylamine (a conventional basic catalyst for silica condensation) provides a good example of how the **gelator−catalyst** interactions may provide an efficient transcription-enabling mechanism.[63] In effect, the highly probable interactions between benzylamine and the *p*-nitrobenzylidene moieties of **O30** molecules (through $\pi-\pi$ stacking and additional hydrophobic interactions) resulted in the predominant condensation of silica on the surface of gelator fibers (due to the H-bonding interactions of silicates with the incorporated benzylamine moieties), resulting in the formation of tubular silica. However, with **O30**, conventional granular silica was obtained with other structurally incompatible catalysts (such as hydrazine).

The important role during silica transcription played by the competition between these two pathways was first reported by van Bommel and Shinkai when using the cholesteric gelator **O50**, as a template.[87] In this study, the benzylamine moiety covalently linked to the gelator scaffold of compound **O50** enabled for the first time efficient transcription into fibrous silica in the absence of an externally added solution catalyst. This was the confirmation of the existence of the so-called **surface mechanism** or surface transcription pathway, which enables the growth of silica exclusively on the fiber surface, mimicking the silica biomineralization processes occurring for instance in the silicification of marine sponges.[134] Transcription with mixtures of the related **O51** and **O52** was only possible in the presence of benzylamine as an external catalyst. In those cases where the surface pathway predominates with respect to the solution mechanism, thinner nano-objects may be obtained, since silica transcription can be initiated onto nonaggregated single fibrils. For instance, when using the cholesterol gelator $\mathbf{O46_2}$ as a template,[82] the size of the inner (helical) hollows suggests that the helical packing structure of cholesterol gelator $\mathbf{O46_2}$ is directly reflected in the silica structure (very efficient transcription), and thus, the incipient organogel fibers are encapsulated in these silica tubes.

Very recently, Weiss and Huang further described the importance of both *templating mechanisms* in a study about the transcription of fibrous organogels of *1-12-hydroxystearic acid* (*HAS*) and its sodium salt (*HAS-S*) into inorganic oxides (mainly silica, but also Fe_2O_3-based nano-objects).[113] They found that, when the sol–gel polymerization reactions of silica are preferentially initiated (and held) near the surfaces

of the gelator template fibrils (in the case of organogels of HAS/benzene, without catalyst, and of HAS-S/THF, noncatalyzed or with a weak basic catalyst such as benzylamine), silica can grow onto single strands of the template, resulting in the formation of nanofibrous objects with thinner (tens of nanometers) cross-sections. However, if the condensation of silicate species is initiated to a higher extent in the liquid bulk (HAS-S organogels in ethanol—without added catalyst—or in THF with a stronger basic catalyst, such as NH_4OH), these preformed nontemplated species are too large to differentiate individual fibrils, and thus they further condense onto fibrous bundles (rather than onto single fibrils) giving rise to considerably thicker fiberlike objects (with "necklace" features).

The importance of the **kinetics of sol–gel condensation** reactions may also be confirmed by the different morphologies that result by simply varying the temperature conditions during the in situ sol–gel condensation or during the organogelation process (slow or fast cooling). In the case of transcription with gelator **O33**, for instance, the transcription yielded nonhelical fibers or left-handed helical silica by performing the sol–gel coassembly process under heating (80 °C) or room temperature conditions, respectively. Similarly, different silica structures were obtained by adjusting the temperature during the sol–gel polycondensation of silica in the presence of $\mathbf{O44_{30}}$ as a template:b in the absence of heating, only double-layered tubular silica formed, whereas if the sol–gel condensation was performed with prolonged (2 days) heating, the resulting silica had a vesicular structure. In the case of **O48**, to obtain these thin tubules (with an inner diameter of 4–5 nm corresponding to the molecular length of **O48**) and avoid aggregation into larger bundles, the sol–gel transcription was performed under moderate heating conditions.[85] Also, interestingly, when using the gelator **O53**,[89] the inner diameters of the hollow silica could be controlled (5–15, 15, or 15–45 nm) by adjusting the rate of sol–gel condensation (heating or cooling conditions) after catalyst addition.

To conclude with this level, as also shown in Figure 5, the balance between these two competing pathways (the relative predominance and temporal sequence of surface and solution mechanisms) may also in some cases determine (along with other kinetic or supramolecular factors) the possible occurrence of multistep *hierarchical coassembly* processes (with formation of different metastable coassembled phases at different lengthscales). The importance of these hierarchical processes was already illustrated (section 3.1) in the case of transcription of different chiral morphologies through the use of the amino acid derivatives **O8**, $\mathbf{O13}_{c-e}$, and $\mathbf{O13}_f$, and an illustrative diagram[43] is shown in Figure 5—bottom, right—as an example).

Fourth Level (IV). Finally, transcribed morphologies can also become ultimately affected due to other important post-transcription variables after the templating or coassembly process, such as the aging conditions and the protocol followed for the drying and removal of the organogel template. In the same study by Weiss et al. previously mentioned (with phosphonium salts, **O3**),[24] for instance, it was found that the shape, size, and yield of the silica objects are strongly affected by the periods of gel aging. Thus, the templated silica fibers are considerable thicker, and more straight and flat with longer periods (aging) for the sol–gel polymerization (aging during 5–30 days) before the drying and removal of the organogelator.

3.2.B. Templating of Nonsiliceous Metal Oxide Fibrous Materials. In the case of **nonsiliceous oxides**, the transcription of fibrous morphologies through the use of organogel or hydrogel templates presents greater difficulty due to the much faster condensation speed of the more electropositive metal species, which results in the rapid formation of precipitates. The mechanisms for transcription of these nonsiliceous oxides have not been studied in as much detail as in the case of silica nano-objects. However, in most of the reported synthesis, the transcription mechanisms are assumed to take place through similar interactions as those found in silica (electrostatic or H-bonding). For instance, Hanabusa et al. proposed an electrostatic templating mechanism for the transcription of titania using the *L-lysine* derivative **O10**.[37] The anionic titania oligomers formed in the sol–gel condensation were attracted to the charged nanofibers arising from the reaction of the carboxy groups of the gelator with the propylamine used as a basic catalyst. In the case of using the cationic gelators $\mathbf{O11_{c,d}}$[38c] and **O20** (R or S),[52] the transcription of Ti, Ta, and V oxides under basic conditions is also assumed to take place mainly through electrostatic interactions (among anionic oligomers and the cationic quaternary ammonium salts).[52]

The transcription mechanism in the templated growth of alumina-based nanofibers through the use of the anthracenic gelator **O1** could have proceeded also through electrostatic interactions, although the possibility that the fibrous structure originated from replication of the phase-separated solvent cannot be discarded.[20] On the other hand, Shinkai et al. have assigned the efficient transcription of Ti, Ta, and Zr oxides through the use of the diamine-containing cholesterol **O47** to the intermolecular hydrogen-bonding interaction between the OH group of the hydrolyzed alkoxides and the amino group of **O47**.[83] In the hydrogel-template approach reported by Rao and co-workers for the transcription of Ti, Zr, W, and Zn oxides (through the use of **O16** hydrogels),[48] other metal precursors different from alkoxides were used. The organogel formation was performed in this case after the partial condensation of inorganic species, and an efficient transcription of metal oxide nanotubes was observed, although the templating mechanism was not discussed.

4. Nonoxide-Based Nanofibrous Materials

The versatility of the organogelator-template approach is confirmed by its successful application to also prepare many other nonoxide-based inorganic materials, such as elemental metals (Ag, Au, Ni, and Cu), semiconductor calchogenides (CdS, CuS, and NiS), metal sulfates ($ZnSO_4$ and $BaSO_4$), and other more complex inorganic phases (such as hydroxyapatite). The different prepared materials, morphologies, and preparation conditions are also summarized in Table 3, and the morphologies of some selected materials (SEM/TEM images) may be seen in Figure 6.

In the case of **metals**, a post-transcription strategy has been mostly employed. Accordingly, the precursor metal salts (i.e., $AgNO_3$ and $HAuCl_4$,) are first mixed with dispersions of preassembled organogels or hydrogels, and then the adsorbed metal species are *in situ* reduced by adding reducing agents (i.e., $NaBH_4$) or by UV photoirradiation. In the case of **Ag**, the use as a template of a preassembled fibrous xerogel of **O15** (containing hydrophilic sulfonic and amide moieties) enabled the growth of both right- and left-handed **Ag** nanohelices.[46] Also through post-transcription procedures, formation of **Au** nanoparticles was confined in the hollow cavities (endotemplating) of the sugar-based gelator **O28** (see Figure 6b)[60] or served to coat the surface (exotemplating) of preassembled helical tubes of **O56**.[95] In this latter case, the regular helical pattern of gold nanoparticles was not attained when using an *in situ* coassembly process. Similarly, thin metal coatings of **Ni** and **Cu** were also formed onto preassembled tubules of the same gelator (**O56**).[92] Also noteworthy is that the preassembled micelar rodlike aggregates of bisamides **O6a** and **O6b** have enabled the post-transcription of double- and multiple-wall Ag nanotubes (see Figure 6a)[29] or the formation of Ni and Cu metal nanowires (interesting for nanoelectronics),[31] respectively (see Figure 6c).

In the case of **semiconducting chalcogenides**, different nanofibrous objects of **CdS** (pearl-necklace nanofibers, tubular morphologies, or coiled helices), **CuS** (bending helical or straight nanofibers), and **NiS** (well-formed, thin nanotubes) have been templated with gelator compounds **O29**,[29] **O31**,[64] **O54**,[90] **O55**,[91] and **O57**.[98] The transcription strategy is based on the in situ coassembly of the organogel (or hydrogel) phases in the presence of the Cd, Cu, or Ni salts (**IC (G)**), followed by the postdiffusion (**PT**) of H_2S (g). In the case of **O29**,[29] for instance, CdS particles are precipitated by penetrating with H_2S (gas), and the preformed CdS nanoparticles act then as a growing point for the continuous growth of CdS nanoparticles along the hydrophilic head of the fiber. Interestingly, if Cu^{2+} or Ag^{+} salts were added to the organogel solution, then a precipitate would form instead of gelation occurring, because of the stronger coordination between Cu^{2+} or Ag^{+} and the N atom of Schiff base units and S atom of thiourea of **O29** molecules, with respect to Cd^{2+}. In the case of gelator **O54**, pearl-necklace tubular nanofibers of CdS were obtained,[90] whereas the transcription of the gelator compound **O57** enabled the formation of coiled helices of CdS (see Figure 6d), with a different helical pitch depending on the gelled solvent.[98]

Similarly, the application of the same transcription methodology (IC(G) + PT) with the gelator compound **O31** (glucose nucleobase) enabled the formation of **CdS** "nanonecklaces" and **NiS** with well-defined and thin tubular structures (i.e., see NiS in Figure 6e).[64] In this case, the transcription into different morphologies was explained by the different adsorption affinities between Cd^{2+} and Ni^{2+} ions and the hydrophilic Schiff base carried by glucose groups. Finally, through the use of organogel templates of the 3-oxopentane derivative **O55** (having two different binding sites for Cu^{2+} ions, it has been possible to transcribe **CuS** nanofibers (see detail in Figure 6e) from two different S sources: H_2S (two-step IC(G) + PT methodology) and thioacetamide (in situ IC(G) methodology). Remarkably, the helical pitch can be tuned by controlling the **binding sites**, which depends on the **solvent effects** (the two different gelated solvents lead to different interaction sites between Cu^{2+} ions and the binding sites of the gel fibers).[91]

On the other hand, nanotubes of **Zn and Ba sulfates** have also been transcribed from acidic hydrogels of the gelator compound **O16**.[48] In the former, the hydrogel was in situ coassembled (IC(G) procedure) in the presence of a basic solution (ammonia) of $ZnSO_4$. In the latter, the organogel was formed in the presence of $BaCl_2$, and a solution of ammonium sulfate was subsequently added to precipitate the $BaSO_4$ onto the hydrogel fibers.

Finally, the tremendous potential of this approach to prepare any other complex inorganic phase is illustrated by the use of the cylindrical micelar-like self-assemblies of the complex amphiphilic derivative **O58** as a template to transcribe **hydroxyapatite** (HA; $Ca_{10}(PO_4)_6(OH)_2$).[99] The efficient transcription is obtained through the strong interactions between Ca ions and the phosphorylated serine part of **O58**.

5. Hybrid Nanofibrous Materials Templated with LMOGs

Herein we review some important classes of hybrid, organic–inorganic nanofibrous materials (mainly—but not only—silica-based) that have been so far prepared through the use of the "organogelator-template approach". We have so far described the transcription of purely inorganic materials through the use of organogel templates and by means of either an in situ coassembly (IC, pathway 1) or a post-transcription (PT, pathways 2 + 3) synthesis methodology (see Figure 2). The subsequent extraction of the organogelator template (washing and/or calcination procedures; pathway 5) leads to the formation of the corresponding fibrous (tubular etc.) purely inorganic replica (*material C*). In both cases, however, before the process of organogelator removal, a hybrid **gelator−mineral nanocomposite** is formed (*material B*), which can exhibit by itself many interesting properties, as discussed in section 2.3.

In this respect, we have shown how the organogelation properties of many gelator compounds can be modified and controlled with added metal salts, and in some cases, their in situ self-assembly (in the presence of a variety of metal ions, IC route) has led to the formation of many *metal−gelator hybrid systems*, with potential applications in multiple fields. For instance, hybrid fibrous xerogels of **O21** (in EtOH) with a homogeneous dispersion of the metal salt (i.e., $CoCl_2$) into the gel fibers (containing amino groups as binding sites) have been obtained. Alternatively, the metals can also be postloaded into a preformed, self-assembled organogel (diffusion, impregnation, etc.) through electrostatic, hydrophilic, or coordinating interactions (post-transcription strategy, or PT route), leading to the same type of nanofibrous **gelator−mineral nanocomposite**. Some examples are the Au–gelator composite materials prepared with **O28** and **O56** gelators (previously discussed)[60,95,114] or the Pd-loaded hybrid gels obtained with the *para* derivative of $\mathbf{O11_b}$ (catalytic gels).[39] Similarly, hybrid nanofibrous materials

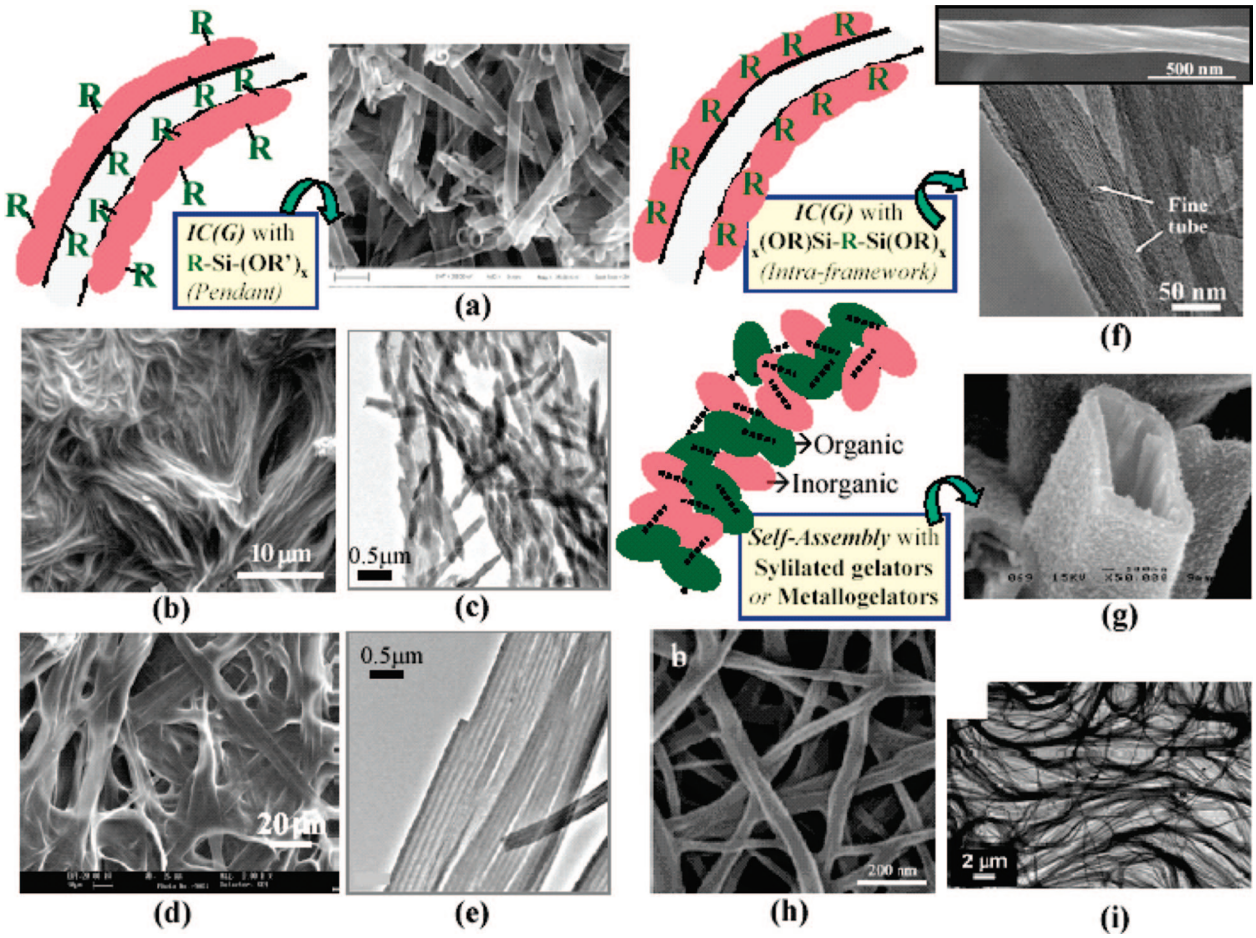

Figure 7. Selected SEM or TEM images of different organogelator-templated hybrid nanofibrous materials. *In situ coassembled organosilicas with pendant organic functions*: (**a**) anthracene dye-organosilica (**O40**, ref 78), (**b** and **c**) SEM and TEM or phenyl-organosilica (**O2**, ref 19), (**d**) methacrylate-organosilica (**O2**, private communication), and (**e**) aminopropyl-organosilica (**O2**, ref 19). *In situ coassembled organosilicas with intraframework organic functions*: (**f**) phenylene-organosilica (helical bundles and ultrafine mesoporous nanofibers; **O13f**, ref 44). *Self-assembled sylilated organogels:* (**g**) **SO1** cyclohexane diureido-based (ref 116) and (**h**) **SO4** bisamidoureido-based (at low concentration; ref 119). *Self-assembled metallo-organogel:* (**i**) **MO7.Cu** (porphyrine-based + Cu; ref 122b). Reproduced with permission from refs 44, 78, 119, and 122b (Copyright 2004, 2005, and 2006 American Chemical Society), ref 19 (Copyright 2003 The Royal Society of Chemistry), and ref 116 (Copyright 2003 Wiley-VCH Verlag GmbH & Co. KgaA).

could also be easily prepared through "simple" postfunctionalization with organic moieties of inorganic nanofibrous materials previously templated with organogels.

In the following lines, we only report on the synthesis of two important classes of hybrid (organic–inorganic) functional nanofibrous materials (see selected SEM or TEM images in Figure 7) through the use of organic or hybrid organogelators as templates: (i) *hybrid organosilicas* formed through *in situ coassembly and sol–gel polycondensation* of hybrid (sylilated) precursors and (ii) *hybrid organogels* in situ self-assembled (when using hybrid, organic–inorganic "self-templating" gelators). A selection of the latter (self-templating gelator systems) is shown in Figure 8. We include also a brief discussion of some mechanistic aspects (particular to the templating of hybrid organosilicas). Table 4 summarizes the different hybrid (organic–inorganic) nanofibrous (1-D) materials templated with organogelators (also self-assembled hybrid gelators), including relevant information about morphology and dimensions, the type of organogelator (and/or main organic moiety) and solvent, synthesis and strategy conditions, and their corresponding references.

5.1. Nanofibrous Organosilicas Templated through Organogel Templates. The growth of hybrid organosilicas supporting different functional moieties has been successfully directed through the use of templating strategies with organogel assemblies. By in situ performing the sol–gel condensation reactions of organo-trialkoxysilanes or organosilsesquioxanes during the assembly of the organogel phase (in situ coassembly procedure, IC), it has been possible to prepare nanofibrous organosilica replicas having pendant (5.1.A) or intraframework (5.1.B) organic functions (see Table 4, and selected images in Figure 7a–e,f, respectively).

5.1.A. Nanofibrous Organosilicas with Pendant Organic Functionalities. As the first precedent, organogels of **O1** and **O2** were used as templates for preparing fibrous and ribbonlike morphologies of organically modified silicas supporting accessible and functional organic moieties such as phenyl and protonated amine (**O1** and **O2**),[18,19] mercaptopropyl (**O2**),[21] and more recently also methacrylate, ethylendiamine, and dinitrophenylamine functions (only with **O2**, *private communication*). In the case of using the more amphiphilic phenazine derivative (**O2**) as a template, the

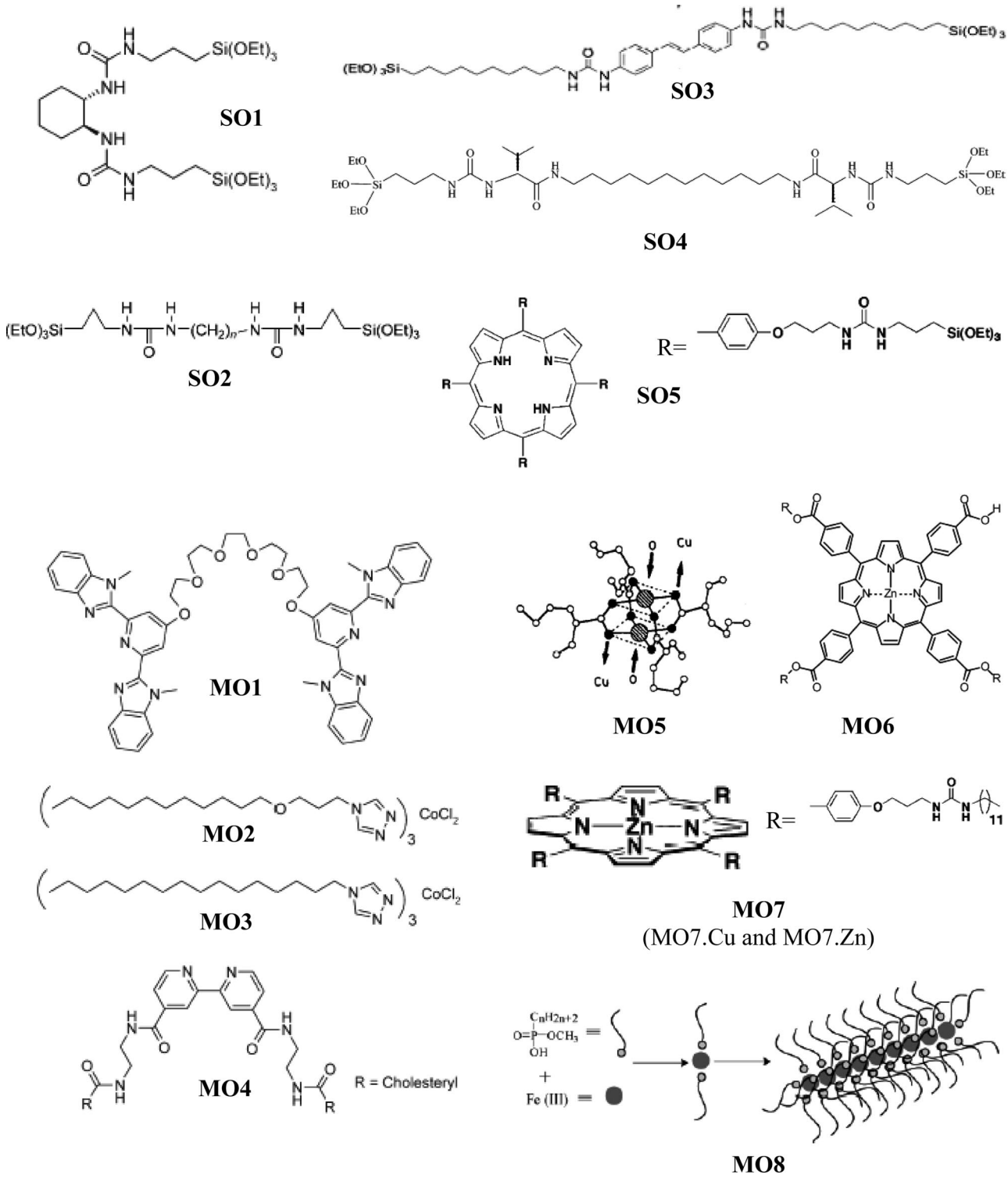

Figure 8. Some selected hybrid (organic–inorganic) organogelator systems leading to self-assembled nanofibrous networks: sylilated gelators (**SO1**−**SO5**) and metallogelators (**MO1**−**MO8**). Adapted with permission from ref 10 (Copyright 2005 The Royal Society of Chemistry) and from refs 122, 126b, 127b, and 129 (Copyright 1992, 2003, 2005, and 2006 American Chemical Society).

hybrid organosilicas (supporting the phenyl, amino, mercapto, methacrylate, diamino, and dinitrophenylamino moieties) were synthesized by templating the cocondensation between tetraethyl orthosilicate (TEOS) and the corresponding organotrialkoxysilanes (PTES, APTES, MPTMS, MAPTMS, *en*PTMS, and DNPAPTES, respectively), mainly under acid-catalyzed conditions.

The templating of fibrous morphologies was successful in all cases, irrespective of the different hydrophobic or hydrophilic character of the employed organotrialkoxysilanes, and the morphologies were preserved after removal of the organogel template. Noteworthy is that the templated hybrid organosilica-containing phenyl moieties (the most hydrophobic) consisted of highly intertwined fibrous bundles (see

Table 4. Summary of Different Hybrid (Organic–Inorganic) Nanofibrous (1-D) Morphologies Templated with organogelators (also Self-Assembled Hybrid Gelators), Including Relevant Information about Morphology, Dimensions, and Processing Conditions (Gelator Template, Solvent, Catalyst, etc.)

hybrid material	templating strategy [a]	main organic moiety (R)	morphology (dimensions)[b]	gelator	synthesis conditions[c]: solvent/pH(Catal.)/addit./(gelator removal: W or C)	ref. [d]
Organosilicas:						
R-SiO_2 (pendant)	IC(G) (TEOS + R-Si$(OR)_3$	phenyl (Ph)	Entangled fibers/fibrous bundles (φ = 200–300 nm to 1–5 μm)	**O1**	EtOH/ca. 3 (HCl)/-- (C, 350 °C)	18, 19
			Entangled fibers (φ = 100–300 nm) and fibrous bundles (up to 10–15 μm)	**O2**	CH_3CN/*ca.* 2 (TFA)/-- (C, 350 °C)	19
		amine (Am)	Straight and coaligned fibers (φ = ca. 200 nm)	**O1**	CH_3CN/ca. 2–3 (HCl)/-- (washed, CH_3CN)	18, 19
			Straight, multichanneled (ca. 10 nm) ribbons (φ = 2–15 μm) of coaligned fibrils (φ = 100–200 nm)	**O2**	CH_3CN/ca. 1 (HCl + TFA)/-- (washed, CH_3CN)	19
		mercapto (Mp)	Entangled fibrous bundles (φ = 2–15 μm) of densely packed coaligned fibrils (φ = 100–200 nm)	**O2**	CH_3CN/ca. 2 (TFA)/-- (washed, CH_3CN)	21
		methacrylate (Mac)	Straight (intertwined) ribbons (φ = 2–20 μm) of coaligned fibrils (φ = 100–200 nm)	**O2**	CH_3CN/ca. 2 (TFA)/-- (washed, CH_3CN)	PC
		ethylen-diamine (Dam)	Straight and elongated fibers (5–10-μm-thick and 100–150 μm in length) surface-coated with silica nanoballs	**O2**	CH_3CN/ca. 10 (autocat.)/-- (washed, CH_3CN)	PC
		dinitrophenyl-amine (Dpam)	Intertwined fibrous bundles (5–10-μm-thick)	**O2**	CH_3CN/ca. 3–4 (HCl)/-- (washed, CH_3CN)	PC
		coumarin or anthracene dyes	Hollow tubes (400–500-nm-thick; wall thickness: ca. 40 nm)	**O40**	1-butanol/B ($bzlNH_2$)/-- (washed, THF/EtOH)	78
	IC(P) R-Si$(OR)_3$	propylene	Short condensation times (5 d): 1-D array of nanoparticles (φ = 10–15 nm); longer times (20 d): hybrid silica nanofibers (25-nm-thick) surrounded by gelator	**O32**	water: DMSO (95:5 v/v)/--/--/unwashed	65
O_xSi-R-SiO_x (intraframework)	IC(G) organo-silsesqui-oxanes	phenylene	Aligned right-handed helical bundles ($\varphi \approx$ 300 nm) and random ultrafine nanofibers ($\varphi \approx$ 50 nm), with mesoporous channels (2.3 nm) parallel to fiber axis	**O13$_f$**	water/A (HCl)/-- (washed, HCl/MetOH; stable up to 500 °C)	44
		methylene and ethane	Straight fibrous bundles (ca. 200–400 nm thick)	**O13$_f$**	water/A (HCl)/-- (washed, HCl/MetOH)	44
		ethene and 1,3-phenylene	Right-handed (twisted) helical mesoporous bundles ($\varphi \approx$ 150–300 nm)	**O13$_f$**	water/A (HCl)/-- (washed, HCl/MetOH)	44
		octane	Huge ball-like aggregates of nanofibers	**O13$_f$**	water/A (HCl)/-- (washed, HCl/MetOH)	44
Hybrid LMOGs:		*Gelator family or main group*:				
(A) sylilated organogels	SA(IC)	cyclohexane diureido	Helical (left- or right-handed) fibrous bundles (300–1000-nm-thick) of thin fibrils (1–5 nm)	**SO1**	water/A (HCl)/--/W (water and EtOH)	115
			Hollow tubular structures (0.5–2-μm-thick; inner hollow: 0.3–1.6 μm; up to 15 μm in length) with many parallel lined-up fibrils (15–25 nm)	**SO1**	water/EtOH (5:2 v/v)/B (NaOH)/--/ W (H_2O, EtOH, acetone)	116
	SA(IC)	alkylidene bisureas	Lamellar structures (thin plates 1–2 μm large, 3–5-μm-long, and 50–100-nm-thick)	**SO2$_n$** (n = 9–12)	water/A (HCl) /--/ W (H_2O, EtOH, acetone)	117
	SA(PC)	diamino-stilbene bisurea	Ribbonlike morphologies (5-μm-wide) stacked into compact sheets	**SO3**	toluene or THF/A (HCl + H_2O vapors)/--/--	118
	SA(PC)	bis-amido-ureido	Low concentration (10 mg/L): straight (nonhelical) fibrous bundles (20–100-nm-thick); Higher concentration (50 mg/L): twisted (left- or right-handed) helical nanofibers (hundreds of nm to several μm)	**SO4**	dioxane or dioxane−water (1:1 v/v)/A (HCl (aq.)/--/W (H_2O, MetOH, acetone)	119
	SA(PC)	phorphirine derivative	2D sheetlike morphology [with fine stripped structure (2 nm)]	**SO5**	benzene/A [TFA (aq.)]/--/W (benz. + $CHCl_3$/EtOH + EtOH)	121, 122
			3D network of multistriped fibrous bundles with uniform sizes (18–22-nm-thick; up to 15 μm in length)	**SO5.Cu**	anisole/A (HCl (aq.)/--/W (H_2O, MetOH, acetone)	122
(B) metallogelators:	SA	benzimidazolyl derivative	With La or Eu + Co or Zn: not characterized	**MO1**	$CHCl_3$−CH_3CN/--/Lan$(NO_3)_3$ + M$(ClO_4)_2$/--	124
	SA	4-alkylated 1,2,4 triazoles	(**MO2**)$_3CoCl_2$: fibrous networks (5–30 nm width); (**MO3**)$_3CoCl_2$: crystalline nanoaggregates (500–1500-nm-long and 30–50 nm in width)	**MO2.Cu**, **MO3.Cu**	$CHCl_3$/--/ $CoCl_2$ (complexes **MO2** or **MO3** in metOH)/--	125
	SA	bipyridine cholesteric	**MO4** (only): network of fibers (13–100-nm-thick), with left-handed helical motif; (**MO4**)$_2$Cu: fibrous bundles (40–100-nm-thick)	**MO4**, **MO4.Cu**	1-butyronitrile/--Cu$(MeCN)_4PF_6$/--	8a
	SA	*tetra*-carboxylates	**MO5**(Cu): not characterized	**MO5.Cu**	methylcyclohexane/--/--/--	126b
	SA	phorphyrine-based	**MO6.Zn**: rodlike assemblies (3–6 nm in diameter; lengths: 50–1500 nm)	**MO6. Zn**	cyclohexane/--/--/--	127
			2D sheetlike morphology (with fine stripped structure (2 nm)	**MO7**	benzene/--/--/W	121, 122
			Multistriped fibrous bundles (similar to **SO5.Cu**)	**MO7.Cu**	anisole/--/--/W	122
			With 0/0.5/1 equiv. of piperazine: spherical/fibrous network (100–200-nm-thick) /2-D sheetlike	**MO7.Zn**	benzene/--/piperazine (diamine)/--	128
	SA	phosphonates	Cylindrical fibers (ca. 1.5 nm)	**MO8.Fe**	*n*-octane/--/MO-86 (Fe precursor)/--	129
	SA	amide, pyridyl-based	3-D network of beltlike fibers	**MO9.Ag**	toluene/--/$AgSO_3CF_3$ (EtOH)/--	130

[a] *Templating strategy*: IC(G) = in situ coassembly and cocondensation with organogel formation; IC(P) = in situ coassembly and cocondensation with precipitate formation; SA = self-assembly of hybrid (organic–inorganic) organogel; SA(IC) = self-assembly of hybrid (organic–inorganic) organogel with in situ sol–gel condensation of inorganic polymerizable species; SA(PC) = self-assembly of hybrid (organic–inorganic) organogel with subsequent postcondensation of inorganic polymerizable species. [b] *Morphology dimensions*: ϕ (or φ) is the average diameter in the indicated units. [c] *Synthesis conditions*: Precursors (inorganic precursors) pH (A = acid; B = basic), catalyst (employed acid or basic catalyst); additives (water, cosolvents, cogelators); gelator removal (W or C) (W(S) = washed with indicated solvent S, C (T °C) = calcined at T °C). [d] *References*: PC = private communication.

Figures 7b–c), ca. 5–20-μm-thick, resulting from the aggregation of much thinner fibrils, whereas the protonated amine sample (highly hydrophilic) was formed (see Figure 7e) by a mesh of straighter and elongated fibrous ribbons (ca. 5–10-μm-thick) also arising from the aggregation of much thinner, and this time perfectly coaligned, fibrils. In the case of mercapto and methacrylate samples (with intermediate hydrophobic or hydrophilic character), both types of morphologies (intertwined fibrous bundles and entangled ribbons) were observed, with a predominance of ribbonlike regions (the methacrylate-functionalized silica is shown in Figure 7d).

Nanofibrous organosilicas with higher organic loadings were also obtained in the case of functionalization with ethylenediamine and the fluorescent dinitrophenyl-aminopropyl (80 mol % per Si) moieties (*private communication*). In the former (although an external catalyst was not added), the faster silica condensation reactions resulted in the formation of thicker and more elongated nanofibers, surface-coated with silica spheres. Some granular silica was also formed in the case of the organic-dye functionalized silica.

Also interestingly, the accessibility of the organic moieties and functionality of the final materials was also confirmed by performing different postfunctionalization reactions (imine formation, grafting of gold nanoparticles—example of material E in Figure 2—methacrylate polymerization, and Cu adsorption experiments) or measurements (surface-plasmon resonance associated to gold nanoparticles and preserved fluorescence properties in the organic-dye functionalized organosilica).

From a mechanistic point of view, the efficient transcription of the different organosilicas may arise from different supramolecular forces, such as H bonding (between silanols, carboxylate or amine groups present in organosilanes, and hydrophilic N and O positions of organogelator molecules), and propably also through electrostatic coupling (charge-mediated process between protonated silanols (I^+) and protonated amine groups of organosilanes (IN^+), counterions (X^-), and protonated organogelator fibrils (ON^+): $I^+-X^--N^+O$ and $IN^+-X^--N^+O$ mechanisms). The aggregation into thicker fibrous bundles may also arise from organosilica−organosilica or silica−solvent interactions that result in the condensation of silica in the spaces left (solution condensation pathway) among the fibrils.

Similarly, luminescent organosilica nanotubes loaded with functional dyes (coumarin and anthracene) have been recently prepared using fibrous organogels of **O40** (in 1-butanol) as templates (anthracene−silica is shown in Figure 7a, and coumarin−silica is the selected material C shown in Figure 2). These materials could find application as optical sensors and luminescence diodes.[78]

On the other hand, through the use of an **endogenous templating** strategy with compound **O32** (SPG), it has been possible to template the growth of organosilica nanofibers confined to the inner one-dimensional cavity of **O32** nanohelices (though a true organogel template is not formed).[65] Indeed, SPG adopts a triple helix (t-SPG) in nature that can be dissociated into a single chain (s-SPG) by dissolving it in DMSO and reverted again to the original triple helix by exchanging DMSO for water. Therefore, when performing the renaturing process (from s-SPG to t-SPG), adding an aqueous solution of trimethoxypropylsilane (TMPS) to a solution of s-SPG in DMSO, the in situ sol–gel polycondensation was confined to the inner one-dimensional cavity of SPG to afford either a one-dimensional array of organosilica nanoparticles or well-formed hybrid organosilica nanofibers at prolonged condensation times. However, this transcription process implies first solubilization in water and then precipitation of the organosilica during the dialysis treatment, without formation of a true hydrogel template.

5.1.B. Nanofibrous Organosilicas with Intraframework Organic Moieties. Recently, the sol–gel condensation reactions (acid catalyzed) of different organosilesquioxanes have been in situ templated through the coassembly of fibrous (helical) hydrogels of the *L-phenylalanine* derivative $\mathbf{O13}_f$ (10PyBr).[44] Differently from the previous approach, the use of organosilsesquioxanes as Si precursors instead of organotrialkoxysilanes enables the incorporation of the organic functions within the walls of the organosiloxane network (intraframework). The template transcription enabled the synthesis of hybrid silica nanofibers (functionalized with methylene, ethane, ethene, octane, phenylene, and 1,3-phenylene moieties). Interestingly, the helicity was preserved in the case of functionalization with phenylene (see SEM/TEM details in Figure 7f), 1,3-phenylene, and ethene moieties (right-handed—twisted—helical bundles were formed), while nonhelical straight fibrous bundles formed with methylene and ethane moieties, and huge ball-like aggregates of nanofibers, were obtained in the case of octane.

5.2. Self-Assembled Hybrid (Organic–Inorganic) Organogels with Nanofibrous Networks. In this approach, the inorganic species becomes incorporated into gelator-like structures, either covalently attached (case of *sylilated hybrid organogels* **SO1**−**SO5**) or through covalent dative (coordinative metal–ligand) interactions (metallic organogelators or **metallogelators**, i.e., **MO1**−**MO9**). Therefore, this approach is rather based on a self-assembly process (the sol–gel polymerization of covalently attached sylilated species or the metal−gelator ligand exchange interactions become indispensable for the 1-D stacking of gelator molecules) and does not involve a true templating.[142]

Sylilated hybrid gelators (see examples in Figure 8) were first reported by Moreau et al., who obtained chiral organosilicas directly through sol–gel polymerization, without formation of a true organogel. They were prepared using sylilated enantiomers [(R,R) or (S,S)] of the *trans-1,2-diaminocyclohane (diureido)* derivative **SO1**.[115] When the polymerization was conducted in ethanol/water mixtures, a better defined tubular organosilica was obtained (see Figure 7g),[116] as a result of the H-bonding interactions between urea moieties, combined with aromatic $\pi-\pi$ or hydrophobic interactions. Similarly, although the *sylilated alkylidene diureido* derivatives $\mathbf{SO2}_n$ (with $n = 9$–12) can gelate toluene, their polymerization in nongellated water (acid-catalyzed with HCl) only resulted in the formation of lamellar silica (plates about 50–100-nm-thick), instead of fibrous 1-D morphologies (amorphous when catalyzed by fluorides).[117] Interestingly, Moreau et al. also conducted the condensation

of another sylilated derivative (*diaminostilbene diureido* derivative **SO3**, with fluorescent properties) previously self-assembled (in toluene or THF) by the postdiffusion of HCl and water vapors (referred to as the organogel (OG)-hybrid gel (HG) process; SA (PC) strategy in Table 4), obtaining ribbonlike monolithic silica.[118] The prefomed ribbonlike morphologies become organized (stacked) into compact sheets or lamellae after the gel-vapor condensation.

Interestingly, by exploiting the same concept, Hanabusa et al. prepared first straight or twisted helical (left- and right-handed) fibrous nanobundles of hybrid organosilica by postcondensation of a preformed hybrid xerogel (in a dioxane/water mixture) of the *bis-amido-ureido* derivative **SO4** (*L*- and *D*-*valine* derivatives),[119] in which the silsesquioxane contains an alkylene segment with 12 carbons ($n = 12$). The helicity was unexpectedly transcribed into the hybrid organosilica by an increase of the gelator concentration (only straight nanofibers formed at low concentrations; see Figure 7h). More recently,[120] this templating approach has been extended to include other related *L*- and *D*-*valine* derivatives (**SO4**$_n$) containing odd ($n = 7$ and 9) or even ($n = 6$, 8, and 10) alkylene segments, resulting in the formation of left- and right-handed helices (the helicity showing an odd–even effect depending on the number of C units).

Also noteworthy is that Hanabusa's group has recently analyzed the gelation properties and the resulting 2-D or 1-D fibrous morphologies of a series of porphyrin-based gelators. Interestingly, the introduction of triethoxysilyl moieties in the phorphirin-based derivative **MO7** (see later in the discussion of metallogelators) results in the formation of the **hybrid sylilated porphyrin SO5**, which presents an improved gelation ability when complexed with Cu, **SO5·Cu** (SO5 only gelates benzene). In contrast to **MO7** and **SO5**, which both give rise to 2D sheetlike xerogels,[121] the self-assembly of their Cu complexes **MO7·Cu** (see later) and **SO5·Cu** (in anisole solvent) results in the formation of 1-D fibrous morphologies, which are maintained (in the second case) after the subsequent sol–gel polycondensation of the covalently attached silicate species.[122] In order to obtain the fibrous superstructure, it is indispensable to self-assemble (preorganize) the xerogel before conducting the sol–gel condensation reactions [SA (PC) strategy], which in turn results in the immobilization and mechanical reinforcement (14-fold increased elasticity) of the hybrid organosilica and also in an improved thermostability (the critical gelation temperature of **SO5·Cu** after polymerization is enhanced up to 160 °C).

More recently, **alkylsylilated nucleoside-based (guanosine)** hybrid gelators have also shown excellent gelation ability in alkane (nonpolar) solvents, but their self-assembly (involving the formation of guanosine−guanosine base pair complementary interactions) results in the formation of two-dimensional supramolecular structures instead of fibrous morphologies.[123]

On the other hand, hybrid self-assembled organogels with interesting properties have been prepared through the use of gelators containing metal-coordinated atoms (hereafter, **metallogelators**). There are different families or metallogelators, depending on the main gelator scaffold possessing the coordinating sites (N, O, or S). Some of these metallogelators may be considered as a **second generation of LMOGs**, since through molecular design they may be sensitive to external stimuli leading to *stimuli-responsive hybrid organogelator systems* (the aggregation modes and sol–gel transition can be controlled for instance as a response to photo or redox stimuli,[8] or by changing the coordination state of the metal species), resulting in advanced functional nanostructured materials (thermochromic, fluorescent, conductive, and so on).

Some of these smart functional gels have been recently reviewed (i.e., gelators **MO1** to **MO4**).[10] For instace, the *2,6-bis(benzimidazolyl)-4-hydroxypyridine* (BIP-OH) derivative of *pentaethylene glycol* (**MO1**) is able to gelate $CHCl_3$/CH_3CN mixtures in the presence of lanthanoid and transition metal ions. Indeed, their supramolecular hybrid organogels prepared in the presence of a combination of metal ions such as Co/La, Co/Eu, Zn/La, and Zn/Eu exhibit thermo-, chemo-, and mechanoresponses, as well as light-emitting properties (especially, the gel containing Zn/Eu was photoluminiscent), although their morphologies were not characterized.[124] Very interestingly, the lipophilic cobalt(II) complexes of 4-alkylated 1,2,4-triazoles (**MO2** and **MO3**) are two rare examples of **organogelation induced by heating** (heat-set organogels), and their supramolecular gels in chloroform exhibit an interesting **thermochromic behavior** (the bluish color of the gel-like assembly at room temperature becomes a liquid upon cooling and eventually turns into a pink solution at 0 °C, the color change being induced by a change in the coordination state of the Co complex from octahedral to tetraedral upon gelation).[125] A similar reversible chromatic change and sol–gel phase transition is also observed upon cooling (thermochromic phase transition) the Cu(I) complex [**(MO4)$_2$.Cu**] of metallogelator **MO4** (a 2,2′-bipyridine derivative bearing two cholesteryl moieties). This thermocromic sol−gel transition has been attributed to some distortion in the tetrahedral coordination mode of Cu(I) during the molecular packing in the gel fibrils. Also noteworthy is that the gelation ability and thermochromic properties of this complex depend on the oxidation state of copper (I or II) and therefore can be tuned by a redox process, becoming a hybrid organogel responsive to oxidative/reductive stimuli.[8a]

In addition, mononuclear and binuclear complexes of alkoxyphenylenes and alkanoates may gelate hydrocarbon solvents.[126] For instance, the binuclear Cu(II) tetracarboxylate **MO5** ($Cu_2(O_2C\text{-}R)_4$, with R = 2-ethylhexanoate) is able to form viscous blue jellies in methylcyclohexane, and the transient elastic 3-D network consists of molecular threads.[126b]

Of special relevance is the family of **porphyrine-based** hybrid metallogelators (**MO6** and **MO7**). First, it was found that the Zn(II) complex of a long-chain triester of *meso-tetrakis*[*p*-carboxyl]phenyl porphyrine, herein metallogelator **MO6** (**MO6·Zn**: *zinc(II) 5-(p-carboxyphenyl)-10,15,20-tris[((p-hexadecyloxy) carbonyl)phenyl] porphinate*), was capable of forming rodlike fibrous aggregates in some apolar organic solvents (hydrocarbons), such as cyclohexane.[127] The fibrous aggregates arise from the 1-D self-aggregation of

gelator molecules into tetrameric rodlike assemblies,[127b] resulting in highly tixotropic organogels.[127c]

Similarly, Shinkai et al. recently reported on the gelation properties and resulting self-assembled hybrid structures of the Cu(II) and Zn(II) complexes of another porphyrine-based gelator bearing four peripheral urea groups, **MO7** (5,10,15,20-*tetrakis*-[4-[3-(3-*N*-dodecylureido)propoxy]phenyl]-porphine Zn(II) or Cu(II)).[122,128] Without complexed metals, gelator **MO7** is an efficient organogelator of organic solvents and self-assembles into 2D sheetlike structures.[121] Interestingly, its Cu(II) complex (**MO7·Cu**) is also a very efficient gelator and gives rise to 1-D fibrous morphologies (see Figure 7i),[122] whereas its Zn(II) complex (**MO7·Zn**) is only capable of gelating (at higher concentrations) two of the studied sovents (anisole and 1,4 dioxane),[122] although its gelation efficiency may be significantly improved by the addition of some amines as piperazine.[128] Also remarkably, the self-assembly of the **MO7·Zn** complex in the presence of 0.5 equiv of piperazine leads to the formation of thixotropic organogels, and the morphology and aggregation modes (J- or H-like) of the resulting xerogels (i.e., in benzene) may also be controlled by varying the ratio of piperazine versus **MO7·Zn** (spherical at 0 equiv, 1-D fibrous at 0.5 equiv, and 2-D sheetlike at 1.0 equiv).[128]

Very interestingly, solutions of several organic molecules may also aggregate into elongated objects ressembling inverted giant wormlike micelles that become gels when complexed with Al(III) or Fe(III) and other metals.[129] For instance, complexation of the **phosphonate** moieties of some phosphorus-containing amphiphilies (phosphonic acid monoester, phosphonic acid, or phosphoric acid monoester) and the Fe(III) ions of added ferric salts is accompanied by their in situ isothermal polymerization leading to the formation of self-assembled **hybrid (isothermal) hydrogels** consisting of fibrillar networks (i.e., the monophosphonate ester **MO8**).[129] Thus, these are examples of two-component "latent" gelators, where the in situ molecular interactions between the phosphorus-containing "latent" gelator and Fe(III) ions lead to linear aggregation in the form of giant inverted micelar rods (diameter of ca. 1.5 nm; see, e.g., the diagramatic representation of Fe(III) complexed *n*-alkyl monophosphonate ester, herein **MO8**, in Figure 8).[129]

More recently, a silver-coordinated supramolecular organogel (**MO9·Ag**, not shown in Figure 8) based on a pyridyl-containing amide-based gelator (**MO9**: *3,4,5-tris(hexadecyloxy)-N-(pyridin-4-yl) benzamide*) has been designed, which exhibits an interesting *multiresponsive behavior* (a rapid chemical response to some anions, gases, and also pH changes);[130] only the binary coordinated metal ion $[Ag^{+}(MO9)_2]$ leads to the formation of a 3-D gel structure, consisting of a network of beltlike fibers (composed of ordered lamellar arrangements of the coordinated complex).

The formation of a novel luminiscent form of gold(I) phenylthiolate via self-assembly (in alkylnitrile/alcohol mixtures) and decomposition of isonitrile gold(I) phenylthiolate complexes has been also reported, although the self-assembled aggregates are precipitated instead of forming a true organogel.[131]

Finally, as another recently exploited smart (and striking) alternative, the self-assembly of an exclusively organic naphtalenic dipeptide derivative, [not shown: *(S)-2-((S)-2-(2-(naphtalen-6-yl)acetamido)-3-phenyl-propanamido)-3-phenylpropanoic acid*] has been in situ reinforced by surface-modified metal oxide magnetic nanoparticles (magnetite).[132] The self-assembly process results therefore in the formation of a supramolecular **hybrid nanofibrous hydrogel containing magnetic nanoparticles** and exhibiting **magneto-rheological properties** (gel−sol transition upon application of an external magnetic field). This gelator compound is able to self-assemble, forming fibrous hydrogels (3-D network of fibrous bundles, with nanofiber diameters around 18–45 nm and lengths longer than micrometers).[133] Thus, the "in situ" addition of Fe_3O_4 nanoparticles surface-modified (L-Fe_3O_4 conjugate) with a dipeptide compound (L-phenylalanine derivative) to an aqueous solution of this gelator induces the formation of a hybrid nanofibrous hydrogel (nanofiber diameters around 20–30 nm), homogeneously coated with Fe_3O_4 nanoparticles. As described by the authors, the L-phenylalanine dipeptide has the ability to bind the magnetite nanoparticles and also to interact with organogelator molecules through noncovalent (H-bonding) interactions. Therefore, the self-asembly of gelator molecules affords the primary chains, and the noncovalent interactions allow the incorporation of L-Fe_3O_4 into the chains to give the secondary, hybrid nanofibers. This hierarchical arrangement allows the localization of the magnetic nanoparticles in a small volume fraction, resulting in the magneto-responsive properties.

6. Concluding Remarks

Hierarchical constructions on a scale ranging from nanometers, to micrometers, to millimeters are characteristic of biological structures and serve to address the physical and chemical demands occurring at these different length scales.[134–137] Indeed, natural materials are highly elaborated systems assimilating high-level miniaturization, integrated inorganic and organic components, and hierarchical control. The design of functional materials having hierarchical structures with controlled anisotropic morphologies will allow the development of innovative advanced materials with promising applications in many fields (among them, biomaterials and implants, therapeutic multifunctional biocarriers, nanophotonic and nanobiophotonic materials, magnetic devices, catalysts, photovoltaic and fuell cells, smart textiles and membranes, etc.) Hierarchical structures can be obtained by recently developed micromolding methods in which macrotemplates are coupled directly with the sol–gel-micellar reaction media.[138,139] The most commonly used submicronic or micronic templates are latex beads or silica nanoparticles, large polymers, microemulsion droplets, and bacterial threads. Many developments which follow integrative chemistry routes combining soft matter and soft chemistry[139,140] are of paramount importance because they will permit control shape, porosity, and selective functionalization.

In the past few years, new strategies to construct hierarchical structures with controlled anisotropic morphologies by associating organogels as templates and sol–gel chemistry have appeared. The type of gelators and solvent used, the

size and morphology of the fibrous organogel replicas, and the main synthesis conditions and experimental methodologies employed are directly controlling the structure, texture, and functionality of the resulting fibrous materials. The three main synthesis pathways to form organogels and the resulting inorganic or hybrid nanofibrous replicas are based on *in situ coassembly*, *post-transcription*, and *direct self-assembly* (when using inorganically functionalized organogelators). The key aspects that should be taken into account for an efficient transcription and to control the morphologies of the transcribed inorganic replicas can be categorized at three different but interdependent levels: the type of organogelator−solvent interactions, the kinetics of the sol–gel polymerization reaction, and the quality of the hybrid interface between the sol–gel-derived polymers and the organogel blueprint. The main postulated mechanisms that are used to describe the mode of action or interaction of the template with the inorganic species during the coassembly or transcription process are mainly electrostatic—charge-matching or charge-transfer processes—and H-bonding interactions.

Following these strategies, it is feasible today to prepare different fibrous or tubular inorganic materials (mainly metal-oxide-based systems, but also some metals, semiconductor chalcogenides, and other simple or more complex inorganic salts) through the use of organogelator templates.

We should emphasize the possible extension of these approaches to other interesting single oxide (i.e., magnetic iron or cobalt oxides) or hybrid systems and also to the preparation of nanofibers and nanotubes or more complex multimetallic oxide-based systems (such as transition metal mixed oxides, perovskites, spinelles, etc.), thus opening a land of opportunities to design nanofibers and nanotubes of any inorganic or hybrid phase. The combination of organogelator templates and electrospinning processes[141] will likely allow the production of fibrous materials with hierarchical structures in shorter processing times. In the future, applications in the field of filters, textiles, catalysts, coating reinforcement, and other medical applications such as tissue engineering and wound healing might be expected.

However, this field of research is in its infancy because the understanding of the physical chemistry of its complex background is still far below the knowledge already accomplished with surfactant-based micellar assemblies and lyotropic liquid crystals. Consequently, among some important challenging issues we should first highlight the crucial need to gain a more complete knowledge of the various and complex interaction processes taking place simultaneously and governing the transcription processes. This achievement could help us have better control and enable the tailored design of sizes and morphologies of the obtained nanofibrous replicas.

Acknowledgment. M.L. is grateful to the "Generalitat Valenciana" from Spain for financial support (GV04B-697 and GV05/089 projects).

References

(1) (a) Bodenhöfer, K.; Hierlemann, A.; Seemann, J.; Gauglitz, G.; Koppenhoefer, B.; Göpel, W. *Nature* **1997**, *387*, 577. (b) Hu, J.; Odom, T. W.; Lieber, C.M. *Acc. Chem. Res.* **1999**, *32*, 435. (c) Lieber, C. M. *Sol. State Chem.* **1998**, *107*, 607. (d) Hodgkinson, I.; Wu, Q. H. *Adv. Mater.* **2001**, *13*, 889. (e) Patzke, G. R.; Krumeich, F.; Nesper, R. *Angew. Chem., Int. Ed.* **2002**, *41*, 2446. (f) Soai, K.; Osanai, S.; Kadowaki, K.; Yonekubo, S.; Shibata, T.; Sato, I. J. *Am. Chem. Soc.* **1999**, *121*, 11235.
(2) (a) Rao, C. N. R.; Nath, M. *Dalton Trans.* **2003**, 1. (b) Rao, C. N. R.; Deepak, F. L.; Gundiah, G.; Govindaraj, A. *Prog. Solid State Chem.* **2003**, *31*, 5.
(3) (a) Xiong, Y.; Mayers, B. T.; Xia, Y. *Chem. Commun.* **2005**, 5013. (b) Xia, Y.; Yang, P. *Adv. Mater.* **2003**, *15*, 351. (c) Xia, Y.; Yang, P.; Sun, Y.; Wu, Y.; Mayers, B. T.; Gates, B.; Yinn, Y.; Kim, F.; Yan, H. *Adv. Mater.* **2003**, *15*, 353.
(4) Shimizu, T.; Masuda, M.; Minamikawa, H. *Chem. Rev.* **2005**, *105*, 1401.
(5) Ono, Y.; Nakashima, K.; Sano, M.; Kanekiyo, Y.; Inoue, K.; Hojo, J.; Shinkai, S. *Chem. Commun.* **1998**, 1477.
(6) (a) Estroff, L. A.; Hamilton, A. D. *Chem. Rev.* **2004**, *104*, 1201. (b) Gronwald, O.; Snip, E.; Shinkai, S. *Curr. Opin. Colloid Interface Sci.* **2002**, *7*, 148. (c) Gronwald, O.; Shinkai, S. *Chem.—Eur. J.* **2001**, *7*, 4328. (d) Van Esch, J. H.; Feringa, B. L. *Angew. Chem., Int. Ed.* **2000**, *39*, 2263. (e) Abdallah, D.; Weiss, R. G. *Adv. Mater.* **2000**, *17*, 1237. (f) Wang, R.; Geiger, C.; Chen, L.; Swanson, B.; Witten, D. G. J. *Am. Chem. Soc.* **2000**, *122*, 2399. (g) Terech, P.; Weiss, R. G. *Chem. Rev.* **1997**, *97*, 3133.
(7) (a) Special series *Top. Curr. Chem.*, 2005, *256*; (Fages, F. *Low Molecular Mass Gelators: Design, Self-Assembly, Function*; Springer-Verlag: New York, 2005). (b) Weiss, R. G.; Terech, P. *Molecular Gels: Materials with self-assembled Fibrillar Networks*; Springer: New York, 2006.
(8) (a) Sugiyasu, K.; Fujita, N.; Shinkai, S. J. *Synth. Org. Chem. Jpn.* **2005**, *63*, 359. (b) An interesting an recent example of a blue-emitting hydrogel, with a pH-responsive, gelation-induced fluorescence emission: Kim, T. H.; Seo, J.; Lee, S. J.; Kim, J.; Jung, J. H. *Chem. Mater.* **2007** [Online Nov. 17, 2007] DOI: 10.1021/cm071391k.
(9) (a) Kawano, S.-I.; Fujita, N.; Shinkai, S. *J. Am. Chem. Soc.* **2004**, *126*, 8592. (b) Mallia, V. A.; Tamaoki, N. *Chem. Soc. Rev.* **2004**, *33*, 76. (c) Ayabe, M.; Kishida, T.; Fujita, N.; Sada, K.; Shinkai, S. *Org. Biomol. Chem.* **2003**, *1*, 2744. (d) Eastoe, J.; Sánchez-Dominguez, M.; Wyatt, P.; Heenan, R. K. *Chem. Commun.* **2004**.
(10) Sangeetha, N. M.; Maitra, U. *Chem. Soc. Rev.* **2005**, *34*, 821.
(11) (a) Miravet, J. F.; Escuder, B. *Org. Lett.* **2005**, *7*, 4791. (b) Miravet, J. F.; Escuder, B. *Tetrahedron* **2007**, *63*, 7321.
(12) (a) Friggeri, A.; van Bommel, K. J. C.; Shinkai, S. In *Molecular Gels: Materials with self-assembled Fibrillar Networks*; Weiss, R. G., Terech, P., Eds.; Springer: New York, 2006; pp. 857–893. (b) Jung, J.-H.; Shinkai, S. *Top. Curr. Chem.* **2004**, *248*, 223. (c) van Bommel, K. J. C.; Friggeri, A.; Shinkai, S. *Angew. Chem., Int. Ed.* **2003**, *42*, 980. (d) See also ref 10.
(13) LMOGs may also be used as templating agents of organics, i.e., for the polymerization of organic monomers. For instance, Shinkai et al. have recently directed the polymerization of organic monomers (like aniline, pyrrole, ethylendioxythiophene, etc.) through electrostatic interactions with cationic (protonated cyclohexane diamines) or anionic (sulphonated synthetic lipids) assemblies of LMOGs as templates; see, e.g., (a) Hatano, T.; Bae, A.-H.; Takeuchi, M.; Fujita, N.; Kaneko, K.; Ihara, H.; Takafuji, M.; Shinkai, S. *Chem.—Eur. J.* **2004**, *10*, 5067. (b) Li, C.; Hatano, T.; Takeuchi, M.; Shinkai, S. *Chem. Commun.* **2004**, 2350.
(14) Fuhrhop, J.-H.; Helfrich, W. *Chem. Rev.* **1993**, *93*, 1565.
(15) (a) Pozzo, J.-L.; Clavier, G. M.; Colomes, M.; Bouas-Laurent, H. *Tetrahedron* **1997**, *53*, 6377. (b) Pozzo, J.-L.; Desvergne, J.-P-; Clavier, G. M.; Bouas-Laurent, H.; Jones, P. G.; Perlstein, J. *J. Chem. Soc., Perkin Trans.* **2001**, *2*, 824.
(16) (a) Brotin, T.; Untermöhlen, R.; Fages, F.; Bouas-Laurent, H.; Desvergne, J. P. *J. Chem. Soc., Chem. Commun.* **1991**, *416*. (b) Terech, P.; Desvergne, J. P.; Bouas-Laurent, H. J. *Colloid Interface Sci.* **1997**, *174*, 258. (c) Desvergne, J. P.; Brotin, T.; Meerschaut, D.; Clavier, G.; Placin, F.; Pozzo, J.-L.; Bouas-Laurent, H. *New J. Chem.* **2004**, *28*, 234.
(17) Clavier, G. M.; Pozzo, J.-L.; Bouas-Laurent, H.; Liere, C.; Roux, C.; Sanchez, C. J. *Mater. Chem.* **2000**, *10*, 1725.
(18) Llusar, M.; Roux, C.; Pozzo, J.-L.; Sanchez, C. J. *Mater. Chem.* **2003**, *13*, 442.
(19) Llusar, M.; Monrós, G.; Roux, C.; Pozzo, J.-L.; Sanchez, C. J. *Mater. Chem.* **2003**, *13*, 2505.
(20) Llusar, M.; Pidol, L.; Roux, C.; Pozzo, J.-L.; Sanchez, C. *Chem. Mater.* **2002**, *14*, 5124.
(21) Llusar, M.; Monrós, G.; Pozzo, J.-L.; Roux, C.; Sanchez, C. Z. *Anorg. Allg. Chem.* **2005**, *631*, 2215.
(22) Lu, L.; Weiss, R. G. *Chem. Commun.* **1996**, 2029.
(23) Abdallah, D. J.; Weiss, R. G. *Chem. Mater.* **2000**, *12*, 406.
(24) Huang, X.; Weiss, R. G. *Langmuir* **2006**, *22*, 8542.
(25) Oda, R.; Huc, I.; Candau, S. J. *Angew. Chem., Int. Ed.* **1998**, *37*, 2689.
(26) Oda, R.; Huc, I.; Schutz, M.; Candau, S. J.; MacKintosh, F. C. *Nature* **1999**, *399*, 566.
(27) Sugiyasu, K.; Tamaru, S.-I.; Takeuchi, M.; Berthier, D.; Huc, I.; Oda, R.; Shinkai, S. *Chem. Comunn.* **2002**, 1212.
(28) Tomioka, K.; Sumiyoshi, T.; Narui, S.; Nagaoka, Y.; Iida, A.; Miwa, Y.; Taga, T.; Nakano, M.; Handa, T. J. *Am. Chem. Soc.* **2001**, *123*, 11817.
(29) Gao, P.; Zhan, C. L.; Liu, M. H. *Langmuir* **2006**, *22*, 775.
(30) (a) Kogiso, M.; Ohnishi, S.; Yase, K.; Masuda, M.; Shimizu, T. *Langmuir* **1998**, *14*, 4978. (b) Matsui, H.; Gologan, B. J. *Phys. Chem. B* **2000**, *104*, 3383.

(31) Matsui, H.; Pan, S.; Gologan, B.; Jonas, S.H. J. *Phys. Chem. B* **2000**, *104*, 9576.
(32) Hanabusa, K.; Tange, J.; Taguchi, Y.; Koyama, T.; Shirai, H. *J. Chem. Soc., Chem. Commun.* **1993**, 390.
(33) (a) Hanabusa, K.; Tanaka, R.; Suzuki, M.; Kimura, M.; Shirai, H. *Adv. Mater.* **1997**, *9*, 1095. (b) Hanabusa, K.; Hiratsuka, K.; Kimura, M.; Shirai, H. *Chem. Mater.* **1999**, *11*, 649. (c) Suzuki, M.; Owa, S.; Yumoto, M.; Kimura, M.; Shirai, H.; Hanabusa, K. *Tetrahedron Lett.* **2004**, *45*, 5399. (d) Suzuki, M.; Owa, S.; Kimura, M.; Kurose, A.; Shirai, H.; Hanabusa, K. *Tetrahedron Lett.* **2005**, *46*, 303. (e) Suzuki, M.; Sato, T.; Kurose, A.; Shirai, H.; Hanabusa, K. *Tetrahedron Lett.* **2005**, *46*, 2741.
(34) (a) Suzuki, M.; Yumoto, M.; Kimura, M.; Shirai, H.; Hanabusa, K. *Chem. Commun.* **2002**, *884*. (b) Suzuki, M.; Yumoto, M.; Kimura, M.; Shirai, H.; Hanabusa, K. *Chem.—Eur. J.* **2003**, *9*, 348. (c) Suzuki, M.; Nanbu, M.; Yumoto, M.; Shirai, H.; Hanabusa, K. *New J. Chem.* **2005**, *29*, 1439.
(35) Kobayashi, S.; Hanabusa, K.; Suzuki, M.; Kimura, M.; Shirai, H. *Chem. Lett.* **1999**, *1077*.
(36) (a) Yang, Y.; Suzuki, M.; Owa, S.; Shirai, H.; Hanabusa, K. *Chem. Commun.* **2005**, *4462*. (b) Yang, Y.; Suzuki, M.; Owa, S.; Shirai, H.; Hanabusa, K. *J. Mater. Chem.* **2006**, *16*, 1644.
(37) Suzuki, M.; Nakajima, Y.; Shirai, H.; Hanabusa, K. *Chem. Commun.* **2006**, 377.
(38) (a) Yang, Y.; Suzuki, M.; Shirai, H.; Kurose, A.; Hanabusa, K. *Chem. Commun.* **2005**, *4462* 2032. (b) Hanabusa, K; et al. *Sen'i Gakkaishi* (*J. Soc. Fiber Sci. Technol.*, in Japanese) **2006**, *62*, 278. (c) Hanabusa, K.; Numazawa, T.; Kobayashi, S.; Suzuki, M.; Shirai, H. *Macromol. Symp.* **2006**, *235*, 52.
(39) Miravet, J.-F.; Escuder, B. *Chem. Commun.* **2005**, 5796.
(40) (a) Escuder, B.; Martí, S.; Miravet, J.-F. *Langmuir* **2005**, *21*, 6776. (b) Mantion, A.; Taubert, A. *Macromol. Biosci.* **2007**, *7*, 208.
(41) Roy, G.; Miravet, J.-F.; Escuder, B.; Sanchez, C.; Llusar, M. *J. Mater. Chem.* **2006**, *16*, 1817.
(42) Yang, Y.; Suzuki, M.; Kimura, M.; Shirai, H.; Hanabusa, K. *Chem. Commun.* **2004**, *1332*.
(43) Yang, Y.; Fukui, H.; Suzuki, M.; Shirai, H.; Hanabusa, K. *Bull. Chem. Soc. Jpn.* **2005**, *78*, 2069.
(44) Yang, Y.; Suzuki, M.; Fukui, H.; Shirai, H.; Hanabusa, K. *Chem. Mater.* **2006**, *18*, 1324.
(45) (a) Xueling, C.; Wang, L.; Yang, Y.; Yang, X.; Xu, H. *Mater. Chem. Phys.* **2006**, *9*, 61. (b) Chang, X.; Li, H.; Yang, Y.; Yang, X.; M., Y. *J. Sol-Gel Sci. Technol.* **2007**, *43*, 15.
(46) Zhan, C.; Wang, J.; Yuan, J.; Gong, H.; Liu, Y.; Liu, M. *Langmuir* **2003**, *19*, 9440.
(47) Maitra, U.; Mukhopadhyay, S.; Sarkar, A.; Rao, P.; Indi, S. S. *Angew. Chem., Int. Ed.* **2001**, *40*, 2281.
(48) Gundiah, G.; Mukhopadhyay, S.; Govind, U.; Tumkurkar, U. G.; Govindaraj, A.; Maitra, U.; Rao, C. N. R. *J. Mater. Chem.* **2003**, *13*, 2118.
(49) Hanabusa, K.; Yamada, M.; Kimura, M.; Shirai, H. *Angew. Chem., Int. Ed.* **1996**, *108*, 2086.
(50) (a) Murata, K.; Auki, M.; Suzuki, T.; Harada, T.; Kawabata, H.; Komori, T.; Ohseto, F.; Ueda, K.; Shinkai, S. *J. Am. Chem. Soc.* **1994**, *116*, 6664. (b) Yoza, K.; Ono, Y.; Yoshihara, K.; Akao, T.; Shinmori, H.; Takeuchi, M.; Shinkai, S.; Reinhoudt, D. N. *Chem. Commun.* **1998**, *907*.
(51) (a) Jung, J. H.; Ono, Y.; Hanabusa, K.; Shinkai, S. J. *Am. Chem. Soc.* **2000**, *122*, 5008. (b) Jung, J. H.; Ono, Y.; Shinkai, S. *Chem.—Eur. J.* **2000**, *6*, 4552.
(52) (a) Kobayashi, S.; Hanabusa, K.; Hamasaki, N.; Kimura, M.; Shirai, H. *Chem. Mater.* **2000**, *12*, 1523. (b) Kobayashi, S.; Hamasaki, N.; Suzuki, M.; Kimura, M.; Shirai, H.; Hanabusa, K. *J. Am. Chem. Soc.* **2002**, *124*, 6550.
(53) (a) Amanokura, N.; Kanekiyo, Y.; Shinkai, S.; Reinhoudt, D. N. *J. Chem. Soc., Perkin Trans. 2* **1999**, 1995. (b) Jung, J. H.; Amaike, M.; Nakashima, K.; Shinkai, S. *J. Chem. Soc., Perkin Trans. 2* **2001**, 1938.
(54) Jung, J. H.; Amaike, M.; Shinkai, S. *Chem. Commun.* **2000**, 2343.
(55) Jung, J. H.; Amaike, M.; Shinkai, S. *Trans. Mater. Res. Soc. Jpn.* **2001**, *26*, 527.
(56) Amaike, M.; Kobayashi, H.; Shinkai, S. *Chem. Lett.* **2001**, 620.
(57) Jung, J. H.; Shinkai, S.; Shimizu, T. *Nano Lett.* **2002**, *2*, 17.
(58) Jung, J. H.; John, G.; Masuda, M.; Yoshida, K.; Shinkai, S.; Shimizu, T. *Langmuir* **2001**, *17*, 7229.
(59) Jung, J. H.; Yoshida, K.; Shimizu, T. *Langmuir* **2002**, *18*, 8724.
(60) Yang, B.; Kamiya, S.; Yoshida, K.; Shimizu, T. *Chem. Commun.* **2004**, 500.
(61) Bao, C.; Lu, R.; Jing, M.; Xue, P.; Tan, C.; Zhao, Y.; Liu, G. *J. Nanosci. Nanotechnol.* **2004**, *4*, 1045.
(62) Gronwald, O.; Shinkai, S. *J. Chem. Soc., Perkin Trans. 2* **2001**, 1933.
(63) Friggeri, A.; Gronwald, O.; van Bommel, K. J. C.; Shinkai, S.; Reinhoudt, D. N. *Chem. Commun.* **2001**, 2434.
(64) Bao, C.; Lu, R.; Xue, P.; Jin, M.; Tan, C.; Liu, G.; Zhao, Y. *J. Nanosci. Nanotechnol.* **2006**, *6*, 807.
(65) Numata, M.; Li, C.; Bae, A. H.; Kaneko, K.; Sakurai, K.; Shinkai, S. *Chem. Commun.* **2005**, 4655.
(66) Tamaru, S.-I.; Nakamura, M.; Takeuchi, M.; Shinkai, S. *Org. Lett.* **2001**, *3*, 3631.
(67) Kawano, S.-I.; Tamaru, S.-I.; Fujita, N.; Shinkai, S. *Chem.—Eur. J.* **2004**, *10*, 343.
(68) Tamaru, S.-I.; Takeuchi, M.; Sano, M.; Shinkai, S. *Angew. Chem., Int. Ed.* **2002**, *41*, 853.
(69) Jung, J. H.; Rim, J. A.; Cho, E. J.; Lee, S. J.; Jeong, I. Y.; Kameda, N.; Masuda, M.; Shimizu, T. *Tetrahedron* **2007**, *63*, 7449.
(70) A review on the gelation of liquids by cholesterol derivatives may be found in ref d. More detailed and comprehensive overviews—monographic chapters—of the gelating and structural properties of cholesterol-based gelators can be found in ref 7.
(71) (a) Murata, K.; Aoki, M; Suzuki, T.; Harada, T.; Kawabata, H.; Komori, T.; Ohseto, F.; Ueda, K.; Shinkai, S. *J. Am. Chem. Soc.* **1994**, *116*, 6664. (b) Murata, K. Ph.D. Thesis, Graduate School of Engineering, Kyushu University, Fukuoka, Japan, 1997.
(72) (a) Ono, Y.; Nakashima, K.; Sano, M.; Hojo, J.; Shinkai, S. *Chem. Lett.* **1999**, *1119*. (b) Ono, Y.; Nakashima, K.; Sano, M.; Hojo, J.; Shinkai, S. *J. Mater. Chem.* **2001**, *2412*.
(73) Ono, Y.; Kanekiyo, Y.; Inoue, K.; Hojo, J.; Shinkai, S. *Chem. Lett.* **1999**, 23.
(74) Jung, J. H.; Ono, Y.; Shinkai, S. *Langmuir* **2000**, *16*, 1643.
(75) Jung, J. H.; Ono, Y.; Shinkai, S. *J. Chem. Soc., Perkin Trans. 2* **1999**, 1289.
(76) Jung, J. H.; Ono, Y.; Shinkai, S. *Angew. Chem., Int. Ed.* **2000**, *39*, 1862.
(77) Jung, J. H.; Ono, Y.; Sakurai, K.; Sano, M.; Shinkai, S. *J. Am. Chem Soc.* **2000**, *122*, 8648.
(78) Han, W. S.; Kang, Y.; Lee, S. J.; Lee, H.; Do, Y.; Lee, Y.-A.; Jung, J. H. *J. Phys. Chem. B* **2005**, *109*, 20661.
(79) (a) Jung, J. H.; Kobayashi, H.; Masuda, M.; Shimizu, T.; Shinkai, S. *J. Am. Chem. Soc.* **2001**, *123*, 8785. (b) Jung, J. H.; Lee, S. H.; Yoo, J. S.; Yoshida, K.; Shimizu, T.; Shinkai, S. *Chem.—Eur. J.* **2003**, *9*, 5307.
(80) Jung, J. H.; Kobayashi, H.; van Bommel, K. J. C.; Shinkai, S.; Shimizu, T. *Chem. Mater.* **2002**, *14*, 1445.
(81) (a) Jung, J. H.; Ono, Y.; Shinkai, S. *Chem. Lett.* **2000**, 636. (b) Jung, J. H.; Shinkai, S. *Chem. Soc., Perkin Trans. 2* **2000**, 2393.
(82) Jung, J. H.; Shinkai, S.; Shimizu, T. *Chem. Mater.* **2003**, *15*, 2141.
(83) Jung, J. H.; Shimizu, T.; Shinkai, S. J. *Mater. Chem.* **2005**, *15*, 3979.
(84) Jung, J. H.; Nakashima, K.; Shinkai, S. *Nano Lett.* **2001**, *1*, 145.
(85) Sugiyasu, K.; Fujita, N.; Takeuchi, M.; Yamada, S.; Shinkai, S. *Org. Biomol. Chem.* **2003**, 985.
(86) Sugiyasu, K.; Fujita, N.; Shinkai, S. *J. Mater. Chem.* **2005**, *15*, 2747.
(87) van Bommel, K. J. C.; Shinkai, S. *Langmuir* **2002**, *18*, 4544.
(88) Malik, S.; Kawano, S. I.; Fujita, N.; Shinkai, S. *Tetrahedron* **2007**, *63*, 7326.
(89) Xue, P.; Lu, R.; Li, D.; Jin, M.; Bao, C.; Zhao, Y.; Wang, Z. *Chem. Mater.* **2004**, *16*, 3702.
(90) Xue, P.; Lu, R.; Huang, Y.; Jin, M.; Tan, C.; Bao, C.; Wang, Z.; Zhao, Y. *Langmuir* **2004**, *20*, 6470.
(91) Xue, P.; Lu, R.; Li, D.; Jin, M.; Tan, C.; Bao, C.; Wang, Z.; Zhao, Y. *Langmuir* **2004**, *20*, 11234.
(92) Schnur, J. M.; Price, R.; Schoen, P.; Yager, P.; Calvert, J. M.; Georger, J.; Singh, A. *Thin Solid Films* **1987**, *152*, 181.
(93) Baral, S.; Schoen, P. *Chem. Mater.* **1993**, *5*, 145.
(94) Chappel, J. S.; Yager, P. J. *Mater. Sci. Lett.* **1992**, *11*, 633.
(95) Burkett, S. L.; Mann, S. *Chem. Commun.* **1996**, 321.
(96) Seddon, A. M.; Patel, H. M.; Burkett, S. L.; Mann, S. *Angew. Chem., Int. Ed.* **2002**, *41*, 2988.
(97) Zuvarev, E. R.; Pralle, M. U.; Sone, E. D.; Stupp, S. I. *J. Am. Chem. Soc.* **2001**, *123*, 4105.
(98) Sone, E. D.; Zubarev, E. R.; Stupp, S. I. *Angew. Chem., Int. Ed.* **2002**, *41*, 1705.
(99) Hartgerink, J. D.; Beniash, E.; Stupp, S. I. *Science* **2001**, *294*, 1684.
(100) Zhu, G.; Dordick, J. S. *Langmuir* **2006**, *18*, 5988.
(101) Hirst, A. R.; Smith, D. K. *Chem.—Eur. J.* **2005**, *11*, 5496.
(102) Friggeri, A.; Grownwald, O.; van Bommel, K. J. C.; Shinkai, S.; Reinhoudt, D. N. *J. Am. Chem. Soc.* **2002**, *124*, 10754.
(103) (a) Wang, R.; Geiger, C.; Chen, L.; Swanson, B.; Whitten, D. G. *J. Am. Chem. Soc.* **2000**, *122*, 2399. (b) Sakurai, K.; Jeong, Y.; Koumoto, K.; Friggeri, A.; Gronwald, O.; Sakurai, S.; Okamoto, S.; Inoue, K.; Shinkai, S. *Langmuir* **2003**, *19*, 8211.
(104) (a) Liu, X. Y.; Sawant, P. D. *Appl. Phys. Lett.* **2001**, *79*, 3518. (b) Liu, X. Y. In ref a.
(105) Lescanne, M.; Colin, A.; Mondain-Monval, O.; Fages, F.; Pozzo, J.-L. *Langmuir* **2003**, *19*, 2013.
(106) Tan, G.; John, V. T.; McPherson, G. L. *Langmuir* **2006**, *22*, 7416.
(107) Lescanne, M.; Colin, A.; Mondain-Monval, O.; Heuzé, K.; Fages, F.; Pozzo, J.-L. *Langmuir* **2002**, *18*, 7151.
(108) (a) Suzuki, M.; Nakajima, Y.; Yumoto, M.; Kimura, M.; Shirai, H.; Hanabusa, K. *Org. Biomol. Chem.* **2004**, *2*, 1155. (b) Suzuki, M.; Nakajima, Y.; Yumoto, M.; Kimura, M.; Shirai, H.; Hanabusa, K. *Langmuir* **2003**, *19*, 8622.
(109) Sanchez, C.; Julián, B.; Belleville, P.; Popall, M. *J. Mater. Chem.* **2005**, *15*, 3559.
(110) Sada, K.; Takeuchi, M.; Fujita, N.; Numata, M.; Shinkai, S. *Chem. Soc. Rev.* **2007**, *36*, 415.
(111) Love, C. S.; Chechik, V.; Smith, D. K.; Wilson, K.; Ashworth, I.; Brennan, C. *Chem Commun.* **2005**, 1971.
(112) Chaundhary, Y. S.; Ghatak, J.; Bhatta, U. M.; Khushalani, D. *J. Mater. Chem.* **2006**, *16*, 3619.
(113) Huang, X.; Weiss, R. G. *Tetrahedron* **2007**, *63*, 7375.
(114) in a rather different but related approach, hexagonal patterns of au nanorods have been recently grown onto coassembled poly(n-isopropylacrylamide) microgel particles: kumar, v. r. r.; samal, a. k.; sreeprasad, t. s.; pradeep, t. *langmuir* **2007**, *23*, 8667. in this case, thus, the strategy consisted of

the assembly of polymer microgel particles previously coated with gold nanoparticles (surface-modified with ctab surfactant).
(115) Moreau, J. J. E.; Vellutini, L.; Man, M. W. C.; Bied, C. *J. Am. Chem. Soc.* **2001**, *123*, 1509.
(116) Moreau, J. J. E.; Vellutini, L.; Man, M. W. C.; Bied, C. *Chem.—Eur. J.* **2003**, *9*, 1594.
(117) (a) Moreau, J. J. E.; Vellutini, L.; Man, M. W. C.; Bied, C.; Bantignies, J. L. *J. Am. Chem. Soc.* **2001**, *123*, 7957. (b) Moreau, J. J. E.; Vellutini, L.; Man, M. W. C.; Bied, C.; Dieudonné, P.; Bantignies, J. L.; Sauvajol, J. L. *Chem.—Eur. J.* **2005**, *11*, 1527.
(118) Dautel, O. J.; Lère-Porte, J.-P.; Moreau, J. J. E.; Man, M. W. C. *Chem. Commun.* **2003**, 2662.
(119) Yang, Y.; Nakazawa, M.; Suzuki, M.; Kimura, M.; Shirai, H.; Hanabusa, K. *Chem. Mater.* **2004**, *16*, 3791.
(120) Yang, Y.; Nakazawa, M.; Suzuki, M.; Shirai, S.; Hanabusa, K. *J. Mater. Chem.* **2007**, *17*, 2936.
(121) Kishida, T.; Fujita, N.; Sada, K.; Shinkai, S. *Chem. Lett.* **2004**, *33*, 1002.
(122) (a) Kishida, T.; Fujita, N.; Sada, K.; Shinkai, S. *J. Am. Chem. Soc.* **2005**, *127*, 7298. (b) Kishida, T.; Fujita, N.; Sada, K.; Shinkai, S. *Langmuir* **2005**, *21*, 9432.
(123) Yoshikawa, I.; Yanagi, S.; Yamaji, Y.; Araki, K. *Tetrahedron* **2007**, *63*, 7474.
(124) Beck, J. B.; Rowan, S. J. *J. Am. Chem. Soc.* **2003**, *1258*, 13922.
(125) Kuroiwa, K.; Shibata, T.; Takada, A.; Nemoto, N.; Kimizuka, N. *J. Am. Chem. Soc.* **2004**, *126*, 2016.
(126) (a) Terech, P.; Chachaty, C.; Gaillard, J.; Godquin-Giroud, A. M. *J. Phys. Fr.* **1987**, *48*, 663. (b) Terech, P.; Schaffhauser, V.; Maldivi, P.; Guenet, J. M. *Langmuir* **1992**, *8*, 2104. (c) Terech, P.; Schaffhauser, V.; Maldivi, P.; Guenet, J. M. *Europhys. Lett.* **1992**, *17*, 515.
(127) (a) Terech, P.; Gebel, G.; Ramasseul, R. *Langmuir* **1996**, *12*, 4321. (b) Terech, P.; Scherer, C.; Demé, B.; Ramasseul, R. *Langmuir* **2003**, *19*, 10641. (c) Terech, P.; Scherer, C.; Lindner, P.; Ramasseul, R. *Langmuir* **2003**, *19*, 10648.
(128) Kishida, T.; Fujita, N.; Hirata, O.; Shinkai, S. *Org. Biomol. Chem.* **2006**, *4*, 1902.
(129) George, M.; Funkhouser, G. P.; Terech, P.; Weiss, R. G. *Langmuir* **2006**, *22*, 7885.
(130) Liu, Q. T.; Wang, Y. L.; Li, W.; Wu, L. X. *Langmuir* **2007**, *23*, 8217.
(131) Bachman, R. E.; Bodolosky-Bettis, S. A.; Glennon, S. C.; Sirchio, S. A. *J. Am. Chem. Soc.* **2000**, *122*, 7146.
(132) Yang, Z.; Gu, H.; Du, J.; Gao, J.; Zhang, B.; Zhang, X.; Xu, B. *Tetrahedron* **2007**, *63*, 7349.
(133) Yang, Z. M.; Liang, G. L.; Wang, L.; Xu, B. *J. Am. Chem. Soc.* **2006**, *128*, 3038.
(134) Sun, Q.; Vrieling, E. G.; van Saten, R. A.; Sommerdijk, N. A. J. M. *Curr. Opin. Solid State Mater. Sci.* **2004**, *8*, 111.
(135) Bauerlein, E. *Angew. Chem., Int. Ed.* **2003**, *42*, 614.
(136) Sanchez, C.; Arribart, H.; Giraud, G. M. M. *Nat. Mater.* **2005**, *4*, 277.
(137) Mann, S.; Burkett, S. L.; Davis, S. A.; Fowler, C. E.; Mendelson, N. H.; Sims, S. D.; Walsh, D.; Whilton, N. T. *Chem. Mater.* **1997**, *9*, 2300.
(138) (a) Trau, M.; Yao, N.; Kim, E.; Xia, Y.; Whitesides, G. M.; Aksay, I. A. *Nature* **1997**, *390*, 674. (b) Yang, P. D.; Deng, T.; Zhao, D. Y.; Feng, P. Y.; Pine, D.; Chmelka, B. F.; Whitesides, G. M.; Stucky, G. D. *Science* **1998**, *282*, 2244.
(139) Soler-Illia, G. J. d. A. A.; Sanchez, C.; Lebeau, B.; Patarin, *J. Chem. Rev.* **2002**, *102*, 4093.
(140) Backov, R. *Soft Matter* **2006**, *2*, 452.
(141) Greiner, A.; Wendorff, J. H. *Angew. Chem., Int. Ed.* **2007**, *46*, 5670.
(142) Similarly, some *organometallic* compounds (bearing direct transition-metal-to-carbon bonds) can also lead to fibrous hybrid organogels (i.e., the pentacarbonyl chromate hybrid gelator synthesized by Bühler et al.), but they are not reported herein. Bühler; et al. *Angew. Chem., Int. Ed.* **2003**, *42*, 2494.

CM702141E